Spring 2013

Comparison of square root of time approach and statistical approach to minimize subjectivity in the determination of minimum in-situ stress

Soumitra Bhaskar Nande

Department:

COMPARISON OF SQUARE ROOT OF TIME APPROACH AND STATISTICAL APPROACH TO MINIMIZE SUBJECTIVITY IN THE DETERMINATION OF MINIMUM IN-SITU STRESS

By

SOUMITRA BHASKAR NANDE

A THESIS

Presented to the Faculty of the Graduate School of the

MISSOURI UNIVERSITY OF SCIENCE AND TECHNOLOGY

In Partial Fulfillment of the Requirements for the Degree

MASTER OF SCIENCE IN PETROLEUM ENGINEERING

2013

Approved by

Dr. Shari Dunn-Norman, Advisor

Dr. V. Samaranayake

Larry K. Britt

Dr. Ralph Flori

ABSTRACT

A formation's minimum in-situ stress is an important parameter to determine for hydraulic fracturing. While minimum in-situ stress, and its orientation, can be measured from triaxial tests on core, it is more common to measure it as closure stress, by performing pressure testing of wells in the field. Closure stress is considered equal to, or a good approximation of the minimum in-situ stress for most cases.

The analytical methods applied to such pressure testing include the square root of time plot, G function plot and the G-dP/dG plot. These plots require the engineer to fit tangent lines to the data, and the intersection of the tangent lines defines closure stress. The answer obtained is somewhat subjective, and a range of values of closure stress may result depending on how the tangents are fitted to the data.

In 1989, Lee and Haimson described a statistical method for determining closure stress in water wells. Their work demonstrated the application of a non-linear regression technique for determining an upper and lower bound for closure stress.

This work applies the non-linear regression method to both a water well and a gas well, and compares closure stress found with a statistical analysis to the values determined from square root of time plots.

Results from this analysis show that for a water well domain, there is close agreement between closure stress derived from the square root of time plot and the value determined from statistical analysis. A slightly larger difference occurs between these values in the gas well example, indicating that a statistical analysis of closure stress may be of greater significance in analyzing oil/gas wells.

ACKNOWLEDGMENTS

This thesis would not have been possible without the guidance and the help of several individuals who in one way or another contributed and extended their valuable assistance in the preparation and completion of this study.

I would like to express my deep and sincere gratitude to my advisor, Dr. Shari Dunn-Norman. Her wide knowledge and her logical way of thinking have been of great value for me. Her understanding, encouraging and personal guidance have provided a good basis for the present thesis.

I am deeply grateful to Dr. Samaranayake who introduced me to SAS and who helped me with writing a program in SAS and performing statistical analysis on a data. This work would not have been possible without his support.

I wish to express my warm and sincere thanks to Professor Larry K. Britt, for providing the data, for a valuable advice and for friendly help. I also wish to thank City Utilities for providing the data and for making this work possible.

My sincere thanks to my committee members, Dr. Ralph Flori, Dr. Samaranayake and Professor Britt, for their constant support.

I owe my loving thanks to my family Aai, Baba and Dada, and my love Amruta. Without their love, support and encouragement, this work was never possible. Thanks are also due to my friends in Rolla and back in India. Thank You for always being there with me.

Last but not the least, to the one above all of us, the omnipresent God, for answering my prayers for giving me the strength to plod on despite my constitution wanting to give up and throw in the towel, thank you so much Dear Lord.

TABLE OF CONTENTS

LIST OF ILLUSTRATIONS

Figure Page

LIST OF TABLES

Table Page

NOMENCLATURE

Equation 3.1

ΔA = Area of the plane (in^2)

ΔF = Resultant force (lbs)

σ = Normal stress (psi)

Equation 3.2 to 3.6

σ_1 = Principle stress component (psi)

σ_2 = Principle stress component (psi)

σ_n = Normal stress acting on a plane at an angle θ (psi)

σ_x = Normal stress acting in X direction (psi)

σ_y = Normal stress acting in Y direction (psi)

τ = Shear stress acting on plane at an angle θ with OX (psi)

τ_{xy} = Shear stress acting in X-Y plane (psi)

θ = Angle of a plane on which normal stress σ_n acts (radians)

Equation 3.7

C_0 = Cohesion factor for rock material

σ_n = Normal stress acting on any physical plane (psi)

τ = Shear stress acting on any physical plane (psi)

μ = Coefficient of internal friction

ϕ = Angle of internal friction (radians)

Equation 3.8

g = Acceleration due to gravity (ft/sec^2)

h = Depth of the reservoir (ft)

σ_v = Vertical stress acting on rock plane (psi)

ρ = Density of the reservoir rock (pcf)

Equation 3.9

P = Pore pressure (psi)

α = Poroelastic constant

σ_2 = Intermediate principle stress (psi)

σ_3 = Minimum principle stress (psi)

σ_v = Vertical stress (psi)

ϑ = Poisson's ratio

Equation 6.1

d_1 = Pressure decay parameter

d_2 = Pressure decay parameter

P_{al} = Asymptotic pressure/ Reservoir pressure (psi)

P_{pi} = Modeled pressure (psi)

t = Time since pumps have been shut down (minutes)

t_L = Time since fractures have been closed (minutes)

Equation 6.2

RMS = Residual Mean Square of an error (psi)

n = Number of observation

P_i = Actual pressure (psi)

P_{pi} = Modeled pressure (psi)

Equation 6.3

P_c = Closure pressure (psi)

P_c^{et} = Upper bound for the expected value of closure stress (psi)

P_c^{lt} = Lower bound for expected value of closure stress (psi)

1. INTRODUCTION

Since its introduction in 1947, hydraulic fracturing has had a significant impact on well productivity and has become the primary means of increasing production. Over one million oil and gas wells have been stimulated in the United States to date. Hydraulic fracturing, combined with horizontal drilling, is the key technology enabling development of unconventional reservoirs.

Hydraulic fracturing consists of initiating a fracture in the formation by pumping fracturing fluid above the breakdown pressure of the formation, then propagating the fracture by injecting fracturing fluid and proppant. When the treatment ends, pump pressure is released, and the fluid in the fracture leaks off to the formation. The formation gradually closes on the proppant, which acts to keep the fracture open. The created fracture serves as a conductive pathway for the formation fluids to enter the well bore.

Minimum in-situ stress is an important parameter as far as hydraulic fracturing is considered. Minimum in-situ stress affects the pressures at which subsurface fractures occur, and the orientation of the minimum in-situ stress affects fracture morphology. Stress contrasts between adjacent formations control fracture height growth. Hence, accurate determination of the minimum stress is very important in hydraulic fracturing design.

If rock core samples are available, triaxial core testing may be conducted to measure the magnitude and orientation of the principal stress. Either an analastic strain

recovery (ASR) technique or a differential strain curve method can be used. Both of these are destructive testing methods and can only be used where core is available.

Minimum in-situ stress can also be determined from field methods, in particular pressure testing. Pump in-fall off pressure testing is easier to apply and less expensive than core analysis. Commonly applied pressure testing methods include step-rate tests with shut in, micro frac or mini frac testing. Frequently, two or more of these tests may be combined to verify the values obtained by pressure testing.

Closure stress, defined as the minimum fluid pressure inside the fracture required to hold the fracture open, is equal to the minimum in-situ stress in most cases. Closure stress is identified from the fall-off period following a pump-in, and is sometimes visible as a point where the pressure fall off data changes slope. In most cases the closure stress is not obvious from visual inspection of the recorded pressure fall-off data, and must be determined with analytical methods.

Pressure transient methods are used to analyze the pressure versus time data obtained from the pump in-fall off tests. These are square root of time plot, G-function plot, G-dP/dG plot. In these methods a tangent is drawn to fall off period every time there is a change in trend of decline. Change of slope indicates change in linear flow behavior and taken to indicate that fracture is closing.

The difficulty with the analytical methods is that the closure pressure identified may not be unique. It is possible to have the intersection of tangents over a range of values. In some cases, there may be a hundred psi or more difference in the answers obtained from different individual's analyses.

Regression analysis can be used to narrow down the range of uncertainty, and identify the highest and lowest best values of the closure stress. A Non Linear Regression Analysis (NLRA) has been identified and applied in this work. This method uses an exponential pressure decay model to isolate the open fracture segment and provide a small range over which a closure stress can be obtained.

This study presents a comparison of conventional analytical methods for determining the closure stress with the NLRA. This study utilizes pressure testing data from a water well and a gas well for comparison, demonstrating when regression is most useful. City Utility project exploratory well # 1 is a water well at CU power plant located in southwestern Missouri drilled for possible CO_2 sequestration. Lammote and Reagan sandstones are pressure tested, for closure pressure, using water as the principal fluid. The Canadian gas well # 2 is a new producing well in an existing major gas field and the aim is to place optimum fracture stimulation treatment. The data contains an in-situ stress test and a minifrac test which will be analyzed for closure pressure.

The regression method provided in this thesis may also be applied to other key parameters of pressure analysis for hydraulic fracturing, such as fracture extension pressure, instantaneous shut in pressure, and breakdown pressure. This thesis focuses on closure stress because this is a key design parameter in hydraulic fracturing.

2. LITERATURE REVIEW

Many researchers have proposed methods to determine closure stress using pressure fall off analysis. Many authors have suggested a variety of methods for the determination of closure stress using different techniques.

Sigfried and Simmons (1978), Simmons and Richter (1976), Ren and Roegiers (1983) conducted Differential Strain Curve Analysis (DSCA) on a core sample to determine the magnitude of in-situ stresses. Van dam et al (2000) also conducted laboratory experiments to determine the magnitude and direction of in-situ stresses. A.S. Abou-Sayed presented a special laboratory technique to determine minimum in-situ stress and in-situ stress contrast in absence of direct, field measured in-situ stress data. Holt et al (2001) applied a discrete particle model to simulate coring and core reloading of a cemented granular material formed under 3D state of stress.

Warpinski and Smith (1989) presented a good review of rock mechanics and fracture geometry in which they state that in-situ stresses are clearly single most important parameter controlling hydraulic fracturing. Different authors such as DeBree et al (1978), Nolte K.G. (1988), Daneshy et al (1986), Warpinski et al (1985) proposed various field testing procedures and novel analysis techniques that attempt to discern the time (pressure) of fracture closure. There have been innovative approaches to determine the closure stresses. Gu and Leung (1993) developed a 3-D numerical simulator model for fracture closure analysis. They analyzed simulator generated pressure decline curves for different cases such as high leak off, short fracture closure time and checked the applicability of pressure versus square root time plot, pressure versus G function plot to

these cases. Lin and Ray (1994) developed a mathematical model to determine principle stress direction and minimum in-situ stress magnitude. They calculated these parameters using fracture width calculations and conventional microfilm technique. Branagan and Holzhausen (1994) proposed a technique called Hydraulic Impedance Testing (HIT) for determining the magnitude of fracture closure. Wright et al (1996) developed a flow pulse technique which uses difference in pressure response observed when pumping flow pulses, of short duration but high rate, into either an open fracture or closed fracture. Upchurch et al (1999) proposed a pressure pulse technique for determination of fracture closure pressure.

Some authors note that the post closure analysis methods do not always give accurate determination of closure stress and that there is a necessity of other techniques which can provide reliable estimation of closure stress when these techniques fail. Weng et al (2002) have clearly stated that there is need to conduct "objective" pressure test to correctly and consistently determine the fracture closure pressure, required for correctly and consistently characterizing the fracture behavior. Branagan and Holzhausen (1994) have stated that mechanical fracture closure does not always create an obvious change or inflection in the fall off pressure response and more importantly does not guarantee that fracture is hydraulically closed.

Lee and Haimson (1989) suggested the use of statistical methods to calculate the various after closure parameters. They applied a regression analysis method called Non Linear Regression Analysis (NLRA) to after closure data and determined the closure pressures objectively. They used an exponential pressure decay model to fit the data that belongs to closed fracture segment of the pressure time curve and to isolate the open

fracture segment of the pressure time curve. Their work utilized pressure data from a water well. To the author's knowledge, the statistical approach has not been previously applied to oil and gas well data.

3. SUBSURFACE STRESSES

In order to implement the most efficient and cost-effective hydraulic fracturing stimulation treatment within a particular region, a thorough understanding of the in-situ stress state and rock properties is paramount (Smith et al., 1978; Warpinski et al., 1982) To understand the concept of subsurface stresses, consider Figure 3.1 which shows any randomly oriented plane of area ΔA and having a center at point P within a body on which resultant force ΔF is acting. Stress vector σ at that point can be defined as,

$$\sigma = \lim_{\Delta A \to 0} \frac{\Delta F}{\Delta A} \quad \text{..... (3.1)}$$

This quantity is defined as force per unit area. In geomechanics, by convention, compression is taken to be positive because the forces prevailing in the earth are usually compressive in nature. This resultant stress σ can be decomposed into a normal component σ_n and a shear component τ. The shear component tends to "shear" the material in the plane ΔA. It should be realized that an infinite amount of planes can be drawn through a given point varying, by the same token, the values of σ_n and τ. The stress condition, therefore, depends on the inclination. Consequently, a complete description of a stress must specify not only its magnitude, direction and sense, but also the direction of the surface upon which it acts. Quantities described by two directions, such as stresses, are known as second-order tensors. (Economides and Nolte, 2000)

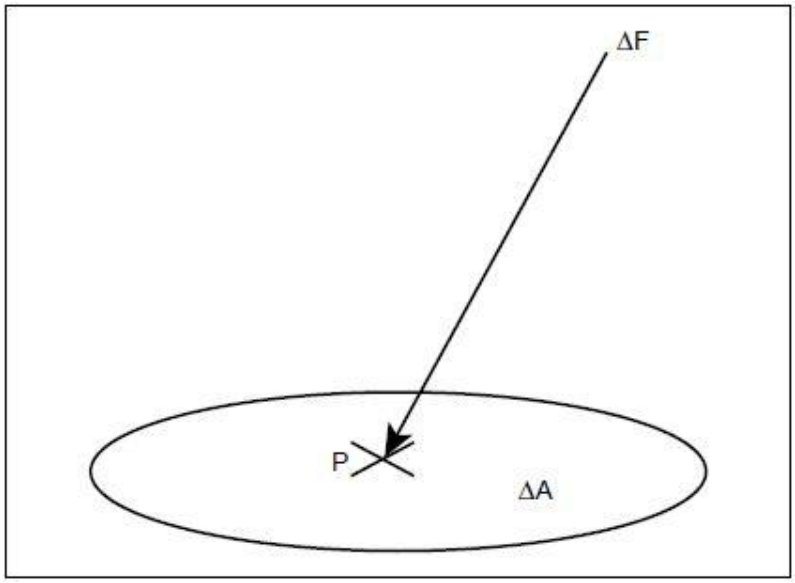

Figure 3.1.Force ΔF acting on a plane at point P having an area ΔA (Economides and Nolte, 2000)

Figure 3.2 shows different stresses in two dimensional situations. Consider thatσ_x, σ_y are normal stresses in x and y direction, τ_{yx}, τ_{xy} are shear stresses along x and y direction. If these stresses are known, stress state on any plane with normal orientation at an angle θ from OY can be derived using the following expression.

$$\sigma_n = \sigma_x \cos^2\theta + 2\tau_{xy} \sin\theta \cos\theta + \sigma_y \sin^2\theta \quad \text{..... (3.2)}$$

$$\tau = \frac{1}{2}(\sigma_y - \sigma_x) \sin 2\theta + \tau_{xy} \cos 2\theta \quad \text{..... (3.3)}$$

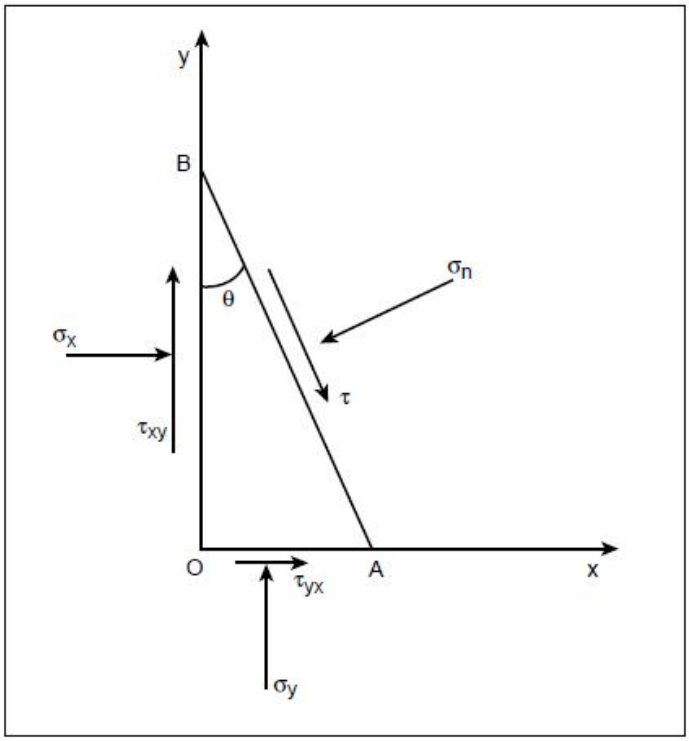

Figure 3.2.Normal and Shear stresses acting in 2-D
(Economides and Nolte, 2000)

These expressions are obtained by writing equilibrium equations of the forces along the σ_n and τ directions, respectively. The moment equilibrium implies that τ_{xy} is equal to τ_{yx}. There always exist two perpendicular orientations of ΔA for which the shear stress components vanish; these are referred to as the principal planes. The normal stresses associated with these planes are referred to as the principal stresses. In two dimensions, expressions for these principal stresses can be found by setting τ = 0 in Equation (3.3) or, because they are the minimum and maximum values of the normal stresses, by taking the derivative of Equation (3.2) with respect to the angle θ and setting

it equal to zero. Either case obtains the following expression for the value of θ for which the shear stress vanishes:

$$\theta = \frac{1}{2}\tan^{-1}\left[\frac{2\tau_{xy}}{\sigma_y - \sigma_x}\right] \quad \text{..... (3.4)}$$

And two principal stress components σ_1, σ_2 are,

$$\sigma_1 = \frac{1}{2}(\sigma_y + \sigma_x) + \left[\tau^2{}_{xy} + \frac{1}{4}(\sigma_y - \sigma_x)^2\right]^2 \quad \text{..... (3.5)}$$

$$\sigma_2 = \frac{1}{2}(\sigma_y + \sigma_x) - \left[\tau^2{}_{xy} + \frac{1}{4}(\sigma_y - \sigma_x)^2\right]^2 \quad \text{..... (3.6)}$$

If this concept is generalized to three dimensions, it can be shown that six independent components of the stress (three normal and three shear components) are needed to define the stress unambiguously. The stress vector for any direction of ΔA can generally be found by writing equilibrium of force equations in various directions. Three principal planes for which the shear stress components vanish and, therefore, the three principal stresses exist. (Economides and Nolte, 2000)

These three stresses are σ_1, which is a maximum principal stress and, σ_2,and σ_3 which are principal intermediate stress and principal minimum stress respectively. Figure 3.3 shows direction and orientation of these three stresses. Most often, the maximum principal stress is the vertical stress, often equal to the weight of the overburden, while maximum horizontal stress is the intermediate stress. In the normal faulting environment, the hydraulic fracture propagates as a vertical fracture in the direction of intermediate stress (maximum horizontal stress).

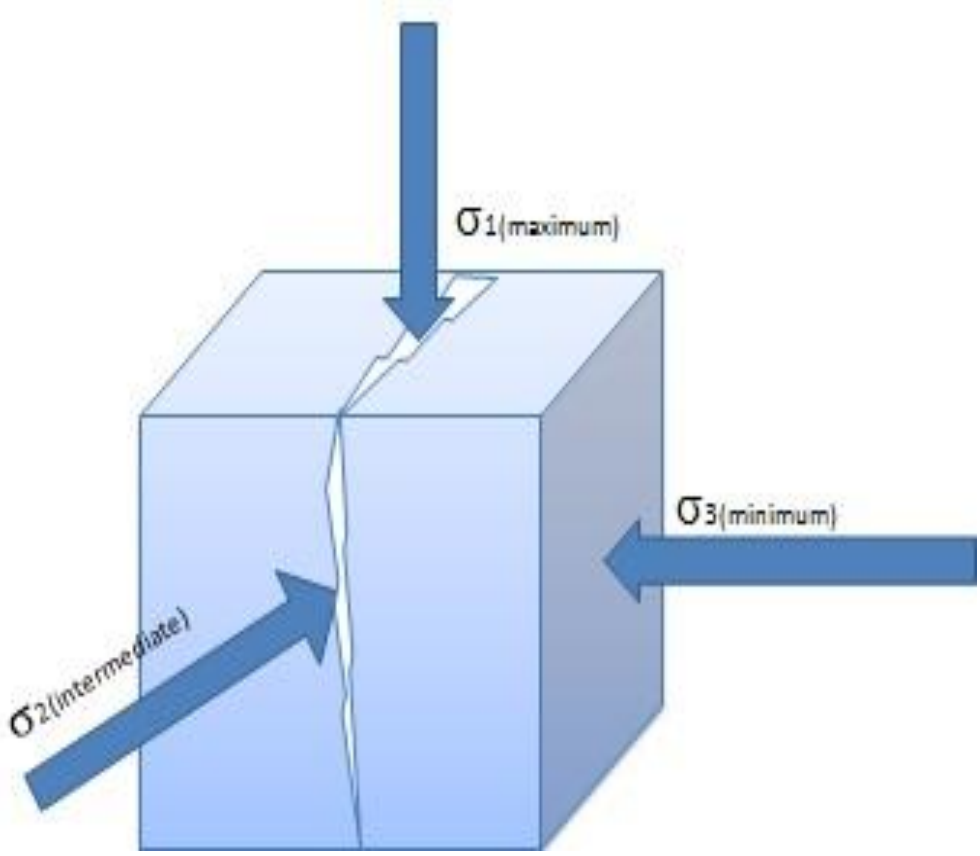

Figure 3.3.General stress state in 3-D

3.1 MOHR – COULOMB FAILURE ENVELOPE

After understanding the basics about the sub surface stresses, it is necessary to understand their critical values at which rocks tend to fail. Failure criteria provide limits to wellbore stresses and knowledge of rock strength is essential for accurate rock failure analysis and to predict wellbore instability. They are derived from laboratory tests on core samples, and can be typically divided into two broad categories: those that depend on all three principal stresses, σ_1,σ_2, σ_3 and those that neglect the effect of intermediate principal stress σ_2 on failure. Two failure criteria are based on these categories: one conventional triaxial criterion, the Mohr-Coulomb criterion, which ignores the influence of the intermediate principal stress and is thus applicable to conventional triaxial test data ($\sigma_1 > \sigma_2 = \sigma_3$), and two "triaxial" criteria, i.e. the Modified Lade and the Drucker–Prager, which consider the influence of the intermediate principal stress in polyaxial strength tests ($\sigma_1 > \sigma_2 > \sigma_3$). (Nawrocki, 2010)

The most commonly used technique is Mohr-Coulomb failure criterion. The reason for its popularity include

1. Its rock failure parameters (cohesion, angle of internal friction, uniaxial compressive strength) have physical meanings and the ranges of these parameters have been established for many rocks.
2. It defines the failure plane orientation being the $(\sigma_1 - \sigma_3)$ plane, which has always been observed in lab experiments.
3. It gives a quantitative measure of how far or how close a rock element is to shear failure under a given applied loading condition. (Tran et al, 2010)

Mohr-Coulomb criterion is a shear failure criterion that has a very clear physical meaning. It describes failure on a physical plane on which two stresses, normal σ_n and shear τ are too high for the rock to resist failure. At failure, σ_n and τ are related by:

$$|\tau| = C_0 + \mu\sigma_n \quad \text{..... (3.7)}$$

Where C_0 is the cohesion of the material and μ is the coefficient of internal friction related to the angle of internal friction ϕ of the material. Figure 3.4 shows Mohr's failure envelope developed using above equation.

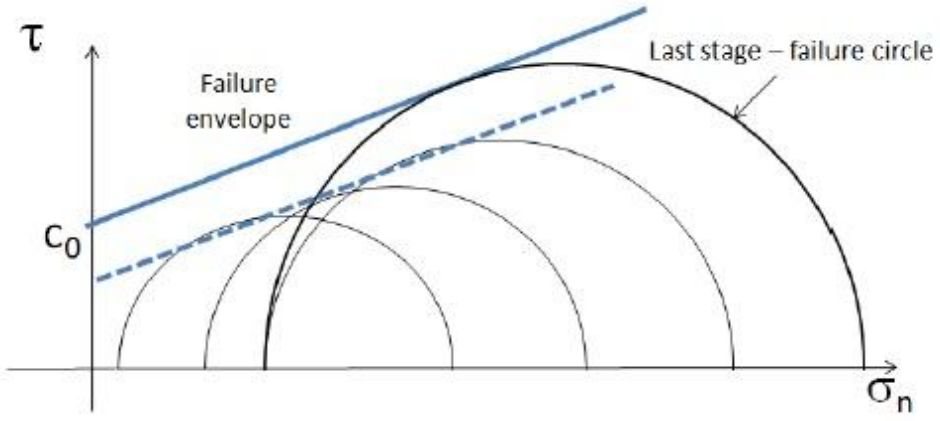

Figure 3.4.Mohr's failure envelope (Tran et al, 2010)

3.2 IN-SITU STRESS DETERMINATION

A reservoir rock, deposited in a sedimentary basin, is subjected to a certain amount of pressure from the overlying rock layers. The vertical stress magnitude, at a specific depth, H, is given by

$$\sigma_v = \int_0^H \rho h(g) dH \quad \text{..... (3.8)}$$

Here ρ is the density of the overlying rock masses and g is the acceleration due to gravity. (Economides and Nolte, 1989)

The value of this stress component can be easily obtained from the integration of a density log. If such a log is unavailable, a rule of thumb of 1.0 to 1.1 psi/ft is generally a good approximation for this vertical stress component.

The prediction of the horizontal stress is based on two fundamentally different premises. These two premises are commonly confused because, for tectonically relaxed areas, they predict approximately the same ratio of $1/3$ between the effective horizontal and vertical stresses. The first premise is that the rock is in a state of incipient faulting (Hubbert and Willis, 1957). For this condition, the state of stress is defined by the failure envelope, and is independent of the elastic properties of the rock. Poroelastic constant, α describes the efficiency of the formation fluid pressure in counteracting the total applied stress. For failure α is equal to one.

The second, and fundamentally different premise, assumes the horizontal stress depends only on the elastic behavior of the rock and is independent of the failure

envelope or any tectonic activity. In a basin not subjected to tectonic deformations, the horizontal stress components, within a specific lithology, will be the same in every direction. Because adjacent sections of a formation layer will tend to expand laterally, their net interaction is zero lateral displacement. Using stress-strain relationship it can be shown that (Hubbert and Willis, 1957)

$$\sigma_2 = \sigma_3 = \frac{\vartheta}{1-\vartheta}(\sigma_v - \alpha P) + \alpha P \quad \text{..... (3.9)}$$

Therefore, in tectonically inactive areas, the effective horizontal stress is approximately equal to one-third of the effective vertical overburden, assuming that ϑ = 0.25.The variation of Poisson's ratio between different lithologies can lead to abrupt steps in horizontal stress variations with depth.

.

3.3 IMPORTANCE OF MINIMUM IN-SITU STRESS IN TREATMENT DESIGN

The minimum in situ stress controls many aspects of the hydraulic fracturing. At very shallow depths or under unusual condition of tectonic stress and/or high reservoir pressure, the weight of the overburden may be the minimum stress and the orientation of the hydraulic fractures will be horizontal; for more normal cases, the minimum stress is generally horizontal and the maximum horizontal stress direction determines whether the vertical fracture will run north–south, east–west, etc. The phenomena can be clearly seen in Figure 3.5.

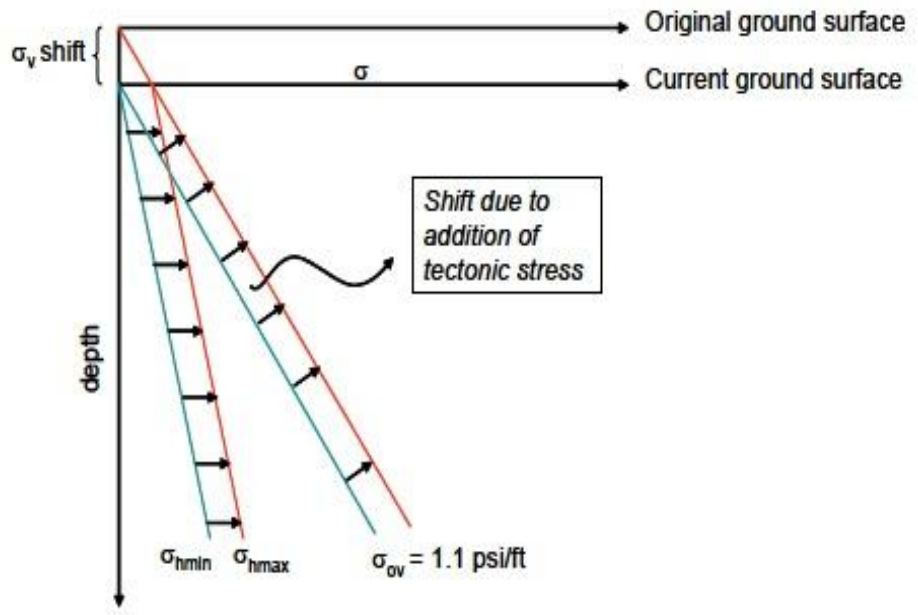

Figure.3.5.Stress gradients varying over depths (Allen and Roberts, 1989)

Through its magnitude, the stress has a large bearing on material requirements, pumping equipment, required for a treatment. Because the bottomhole pressure must exceed the in-situ stress for fracture propagation, stress controls the required pumping pressure that well tubulars must withstand and also controls the hydraulic horsepower (hhp) required for the treatment. After fracturing, high stresses tend to crush the proppant and reduce fracture conductivity; thus, the stress magnitude dominates the selection of proppant type and largely controls post fracture conductivity. (Economides and Nolte, 2000)

3.4 HYDRAULIC FRACTURING TREATMENT PRESSURE PROFILE

Figure 3.6 shows a generalized surface pressure plot for a hydraulic fracturing treatment. This section discusses the various stages of the fracture treatment during pumping and after shut-in, as shown in Figure 3.6.

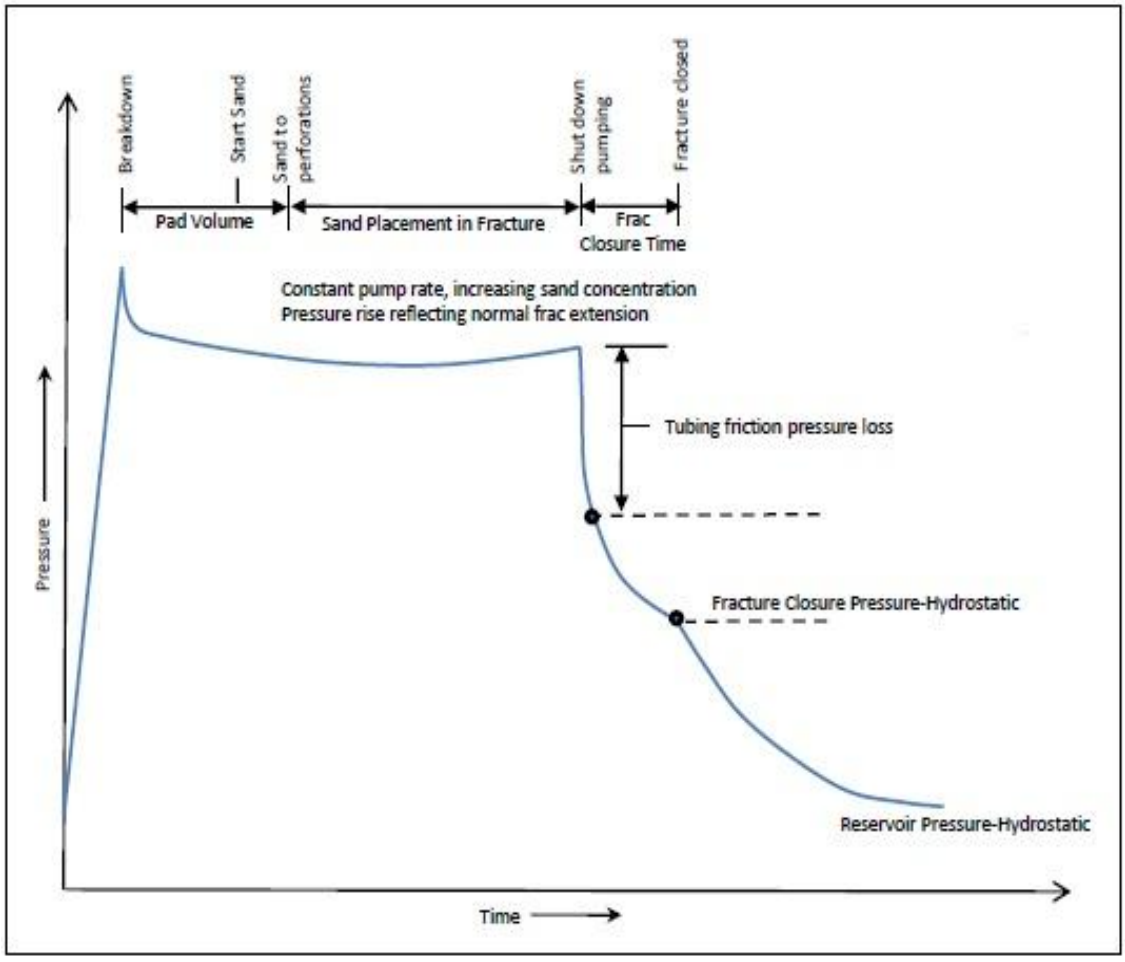

Figure 3.6.Surface pressure plot for fracturing treatment (Allen and Roberts, 1989)

When fluid is pumped down the well bore at a pressure greater than regional stresses, it results in formation break down. The fluid used for breaking down the formation is called pad fluid and the entire stage is called pad stage. Because the fluid has no space to escape, it exerts pressure on well bore walls. This results in pressure rise in the beginning of the pad stage. The occurrence of breakdown is often seen on the surface as a peak in the pressure plot. Breakdown occurs when hydraulic pressure exceeds the compressive stresses at the borehole wall. Stress concentration results when a piece of rock is removed from a rock matrix, while the regional rock matrix carries the same matrix load and thus the rock at bore hole wall faces greater compressive stresses. After the breakdown has occurred, pad fluid starts to leak off into the formation. If the injection of pad fluid is continued further, the fracture tends to grow in width as well as length, as the fluid pressure in the fracture works against the elasticity of the rock material.

After sufficient pad fluid is injected into the formation, pad stage ends and proppant stage starts. In proppant stage, slurry consisting of a fluid blended with sand or bauxite and some additives is injected down hole at a pressure sufficient to hold fracture open. Here sand acts as a proppant. Slurry is injected into the formation with increasing proppant concentration. Slurry stage is designed in such a way that, it will reach the fracture tip as soon as all the pad fluid has leaked off in to the formation. Slurry gets dehydrated gradually by leaking slurry fluid to the formation, as it moves forward through the fracture and the stages are designed to have a uniform sand concentration along the fracture at the end of pumping. Formation pore pressure gradually increases during the treatment as more and more fluid is lost to the formation. This gradual increase in pressure, referred to as an extension pressure can be seen during slurry stage in Figure

3.6. If the injection pressure is kept above extension pressure, fracture will tend to grow in length and width. If the pressure inside the fracture is below extension pressure, but above closure pressure, fracture will be held open but it will not propagate. Proppant placement results in increase in fracture half length, width and height.

Pumps are shut down as soon as final stage of proppant is pumped down hole. When pumping has stopped, there is a sudden in pressure versus time plot. The pumping pressure at the instant of pump shut down is called an instantaneous shut-in pressure (ISIP). Because fracture cannot close instantly upon pump shut-down, ISIP is generally taken as an upper bound on the value for closure stress. (Jones and Britt, 2009) A Sudden drop in pressure after pump shut down is a result of the fact that tubing friction losses occur inside the tubing.

The pressure fall off after the ISIP, follows a gradual decline. The decline continues until there is a break or an inflection point. This inflection point indicates a change in linear flow behavior and is taken to indicate fracture closing. Generally this value is taken to be value for closure stress.

Net pressure is the difference between fracture closure pressure and fracture extension pressure. Net fracture pressure acts against the elasticity, or Young's modulus, of the rock to open the fracture wider. During the fracture job, the net fracture pressure can be used as an indicator of fracture extension. The Nolte – Smith plot is a log-log representation of net pressure versus time or volume pumped which provides information regarding fracture geometry and fracture propagation during a designing phase as well as during actual treatment.

Accurate determination of closure stress is important because it is required in calculation of net treating pressure. (Figure 3.6) Erroneous calculation of the closure stress results in miscalculation of net pressure which leads to misinterpretation of critical fracture design parameters such as fracture height, width, half length and fracture geometry.

Additionally proppant conductivity depends largely upon the closure stress. Different proppants show varying response as the closure stress increases. Fracture roughness increases as the closure stress increases. Although fracture roughness is neglected in many hydraulic fracturing models, there are situations where fracture roughness is an important parameter. (van Dam et al. 1999)

There are different tests to calculate the closure stress. These tests will be discussed in the next section.

4. HYDRAULIC FRACTURING PRESSURE TESTS AND THEIR ANALYSES

4.1 HYDRAULIC FRACTURING PRESSURE TESTS

It is well established practice in oil and gas industry to determine different fracturing parameters using different field pressure tests. These tests are carried out to determine fracture closure pressure, fracture extension pressure, fluid leak off coefficient, fracture geometry, efficiency, height and different elastic properties measured in-situ. (Thompson and Church, 1993) These tests include;

1. Pump in/ flowback tests
2. Pump in/ decline tests
3. Step rate test

Figure 4.1 shows a pressure and flow rate behavior for an idealized pump in/ flowback test. Briefly, this procedure uses consists of injecting a volume of fluid at a sufficient rate to initiate or open a fracture in the formation. After the injection, the well is backflowed at an appropriate constant rate (e.g., through a surface choke) that varies for different formations. In the desired range of flowback rates (e.g., one-quarter of the injection rate), a plot of pressure vs. flowback time will exhibit a characteristic reversal of curvature (i.e., increasing rate of decline) when the fracture closes. (Nolte and Smith, 1981)

Figure 4.2 shows the influence of different flowback rates on a pump in flowback test. Figure 4.3 shows a pump in/flowback test where closure stress is clearly evident from the change of inflection during flowback.

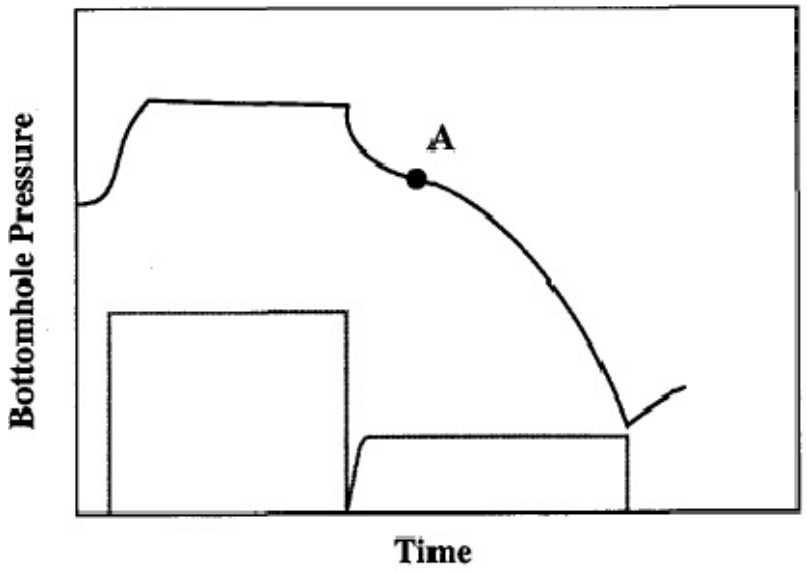

Figure 4.1.Idealized pump in/flowback test (Soliman and Daneshi, 1991)

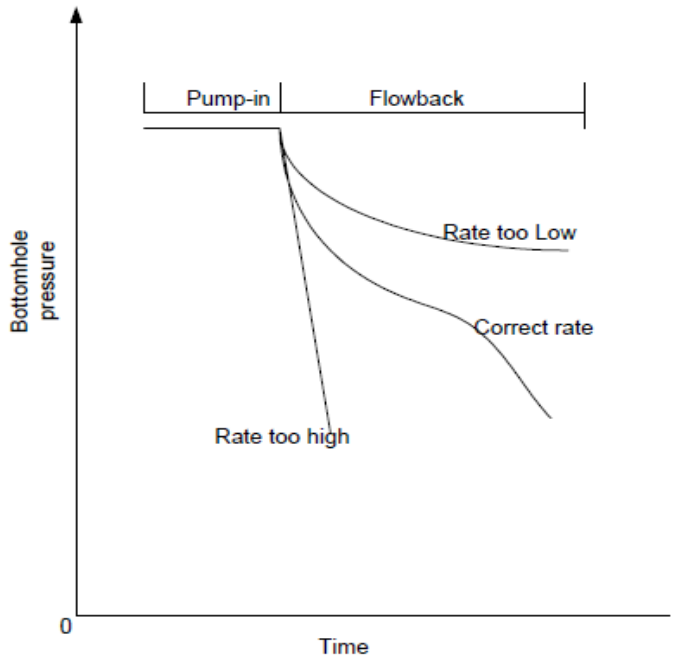

Figure 4.2.Pump in/flowback test showing effects of different rates (Nolte, 1988)

The increasing rate of pressure decline, for the post closure period, results from fluid flow through the pinched fracture width (i.e., induced fluid choking) in the near-wellbore region induced by fluid flowback. The characteristic “lazy-S” signature exhibited by the pressure during the flowback period is in contrast to the multiple inflections commonly observed with the shut-in decline test. Therefore, the flowback test provides a more objective indication of closure relative to the decline test. (Economides and Nolte, 1989) however they are difficult to conduct because they are sensitive to how flowback is conducted. (Figure 4.2)

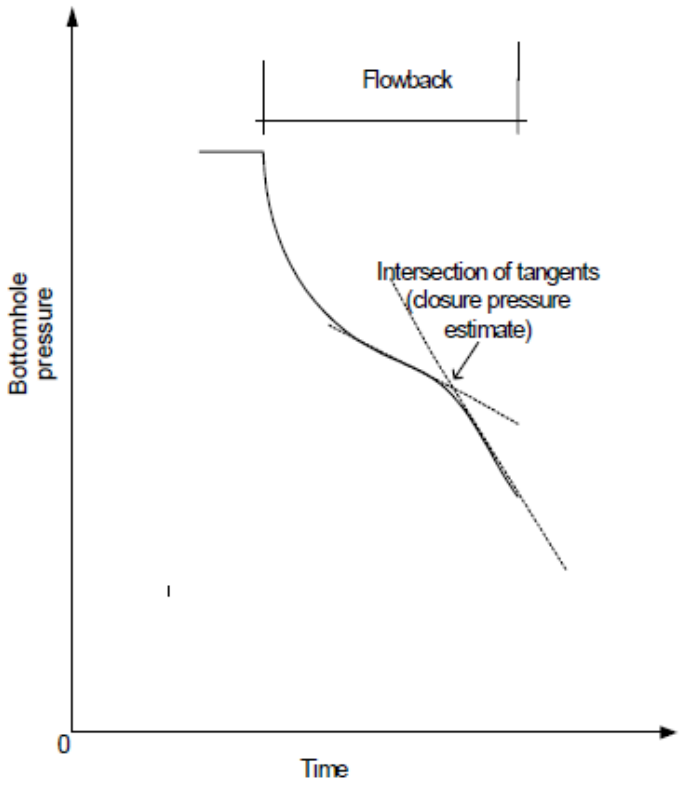

Figure 4.3.Pump in/flowback test (Nolte, 1988)

Pump in decline pressure testing is commonly employed. In these tests a volume of fluid is pumped into the formation at a constant rate and the well then shut in. Figure 4.4 shows pressure response for a typical pump in decline test. One example of pump in test is a microfrac test. This test is usually conducted by perforating small interval (1 to 2 ft) in either permeable formation or in bounding shales to develop an in situ stress profile with depth.

Small volume (0.5 to 1 bbl) of completion fluid is injected at $^1/_8$ to $^1/_4$ bbl/min. By injecting such a small volume it is accepted that ISIP is a good approximation for closure stress. For a better approximation of a closure stress, this test must be repeated several times. Generally multiple tests tend to reduce any influence of wellbore and rock strength because fracture is no longer being extended, but only reopened. ISIP is always an upper bound on closure stress because fracture cannot close instantly as soon as pumping is stopped. Therefore picking an ISIP value and making use of this value should be done with care. A change in slope indicates that the fracture is closing. (Jones and Britt, 2009) Figure 4.5 shows determination of closure stress from a decline part of the pressure response shown in Figure 4.4. As can be seen from Figure 4.5, change of slope (inflection point) is taken as the closure pressure. There are different possibilities as to how pressure will respond after the fracture has been closed.

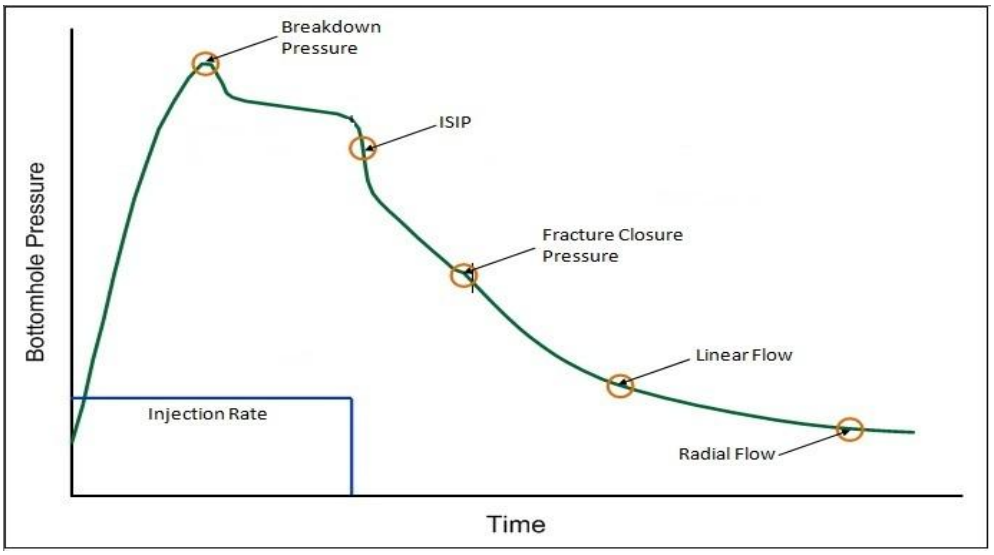

Figure 4.4.A typical pump in/decline test (Warpinski et al, 1985)

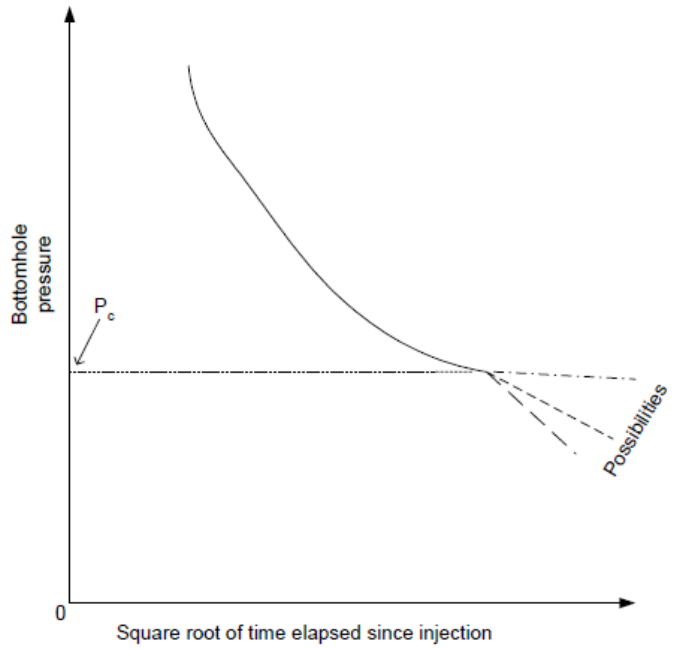

Figure 4.5.Change of slope representing closure stress value for pump in/decline test (Nolte, 1988)

A step rate test (SRT) is always conducted to determine fracture extension pressure. Fluid is pumped at constant incrementally increasing rates, and the final injection pressure recorded for each rate is plotted vs. pump rate as shown in Figure 4.6. A typical test may include injection rates ranging from 0.25 to10 bbl/min. The stabilized final pressure for each step rate is plotted vs. pump rate, and the breakpoint is observed as fracture extension pressure (Figure 4.7). For best results, each rate should be maintained for a fixed period of time (typically 1 to 2 minutes). Also because of very slow rates at the beginning of the test, proper pumping equipment is required. If bottomhole pressure gauges are not used, a reliable SRT can be performed by shutting down well after each rate step and obtaining an ISIP.

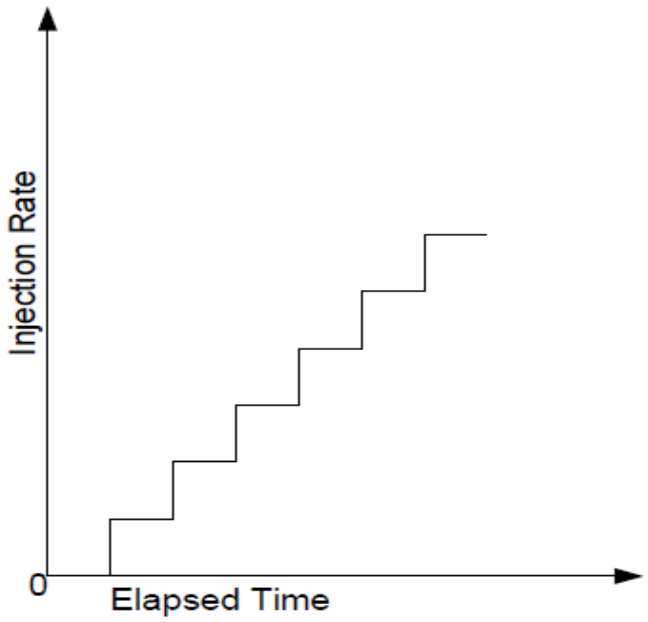

Figure 4.6.Rate v/s time plot for a typical step rate (Nolte, 1988)

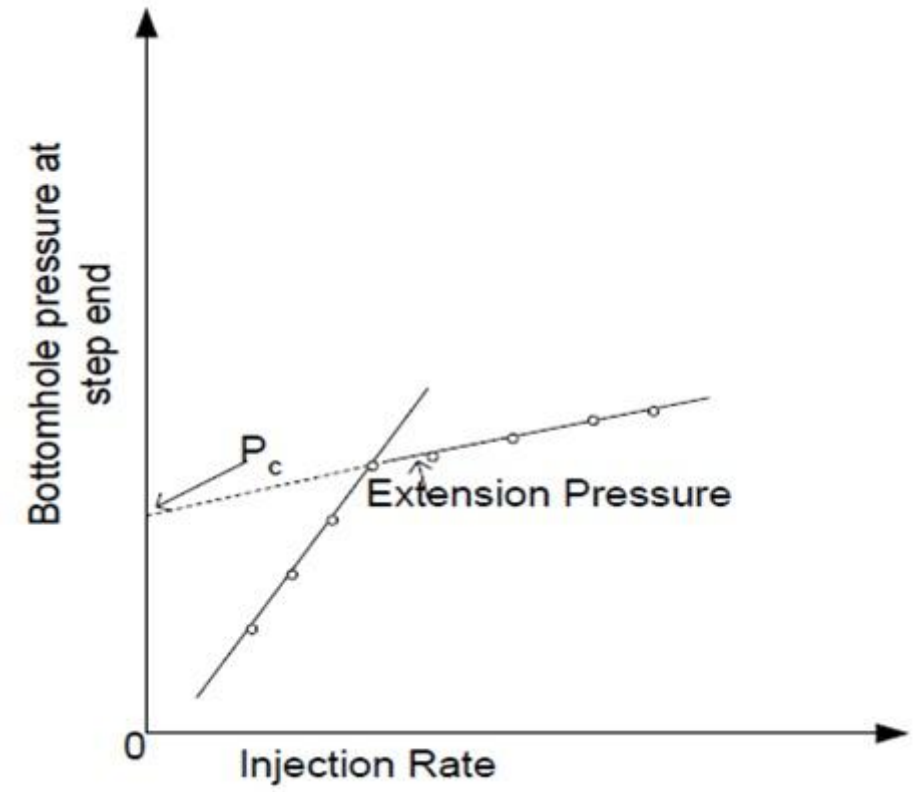

Figure 4.7.Pressure versus flow rate plot showing extension pressure

Hydraulic fracturing in water wells is not common. Although not many water wells are hydraulically fractured, records show that some have been fractured over the past many years. These wells are not fractured so as to place a conductive pathway for the recovery of formation fluid, but are fractured so as to test the formation integrity. These wells are generally fracture tested to determine stress state of the underlying rocks or to measure hydraulic conductivity.

Two different sets of tests are performed on water wells to estimate stress parameters. These tests are a hydrofrac test and a hydro jack test. (ASTM, D 4645 – 87)

The term hydraulic jacking describes an injection test carried out at several fixed injection rates, the highest of which is sufficient to open the fracture. Figure 4.8 shows a typical hydrofrac and hydro jack test. Ideally hydraulic jacking should have sufficient number of pressure steps to define both the laminar rigid fracture regime and the fracture deformation regime. Hydraulic jacking is similar to step rate testing in oil wells.

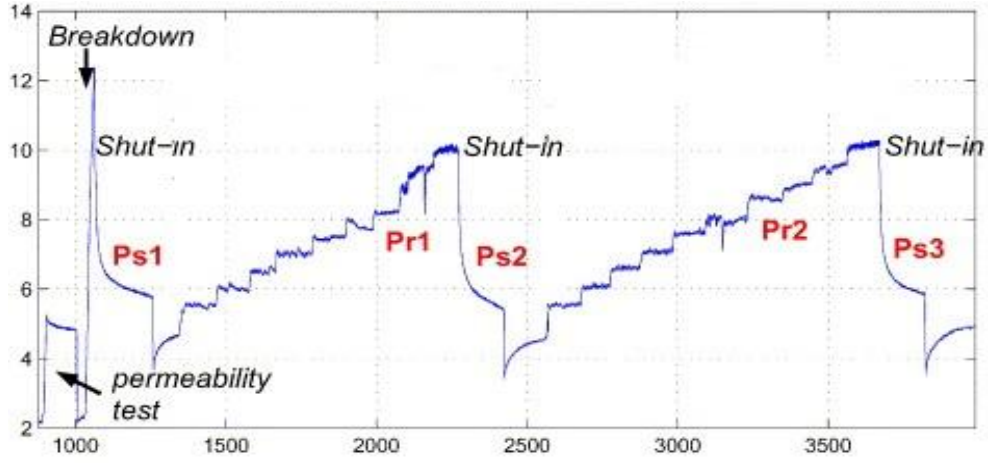

Figure 4.8.A hydrofrac and hydrojack test (ASTM, D 4645 – 87)

After each hydraulic jacking test is done, pressures are allowed to reduce down to a reservoir pressure.

Hydrofracking test is similar to pump in decline test in oil wells. The decline part is analyzed for closure pressure. Hydrofracking test is performed at least two to three times to minimize the effects of rock elasticity. With every repetition of hydrofacking

test, if closure pressure value is repeated, then it is taken as the final value. In Figure 4.8, hydrofracking test can seen after the initial permeability test. The closure pressure value P_{s1} is determined using the hydrofrac test.

Unlike oil domain, hydraulic fracturing in water wells is done using only water. There are no proppant stages. The main intention to fracture the formation is to test formation with respect to in situ stress state of stress and formation toughness and integrity. In situ stresses can be measured directly by flatjack methods or indirectly using strain rosette system, provided the location is at surface or in close proximity to an opening. The flat jack method consists of making a slot in an exposed surface and restoring measurement points to their initial position by applying pressures through flat jacks. Pressures required are in correspondence with the normal stresses acting on the slot surface. (C. Souza Martins, L. Ribiero E. Sousa, 1987). At distances less than 100 ft (30 m) or less from the access point, in situ stresses can be measured by a variety of borehole methods incorporating instruments such as borehole deformation gauge, the ‘door-stopper’ or the inclusion stressmeter. However stress field must often be determined at considerably greater distances. Hence water wells are typically tested with hydrofrac and hydrojack test.

4.2 FRACTURING PRESSURE ANALYSIS USING ANALYTICAL TECHNIQUES

The pressure data obtained after the conducting the fracturing treatment is analyzed to obtain critical fracturing parameters. Various graphical techniques are more commonly used to analyze the data. Some of these include,

1. Pressure versus square root of time analysis
2. G-Function plot analysis
3. G-dP/dG plot analysis

The Pressure versus square root of time plot is obtained by plotting bottomhole pressure on Y- axis and square root of time on X- axis. The time here corresponds to time since the pumps have been shut down. In this plot, a tangent is fitted to the early fall-off period, and then to the later time after the fracture closes. Change slope indicates fracture is closing. Therefore the intersection of the two lines approximates the formation closure stress. Along with fracture closure pressure, square root of time plot also gives important insights about exact closure time, fracture fluid efficiency and instantaneous shut in pressure (ISIP). Figure 4.9 shows an example of pressure versus square root of time plot. Here tangents are drawn whenever there is change in trend of curve and intersection of tangents is taken as closure pressure value.

G- Function plot is somewhat superior to square root of time plot. G-Function plot uses more precise relationship between pressure versus time compared to square root of time plot. In G-Function plot, shown in Figure 4.10, derivative of G-Function is plotted against the time. When derivative of G-Function is plotted against the time, it provides an important information about fracture extension after shut-in, closure pressure and pressure dependant leak-off. (Castillo, 1987) The G-Function plot finds its best application in case of high permeability reservoirs where decline after pump shut off is fast and it is difficult to observe sharp breaks in decline.

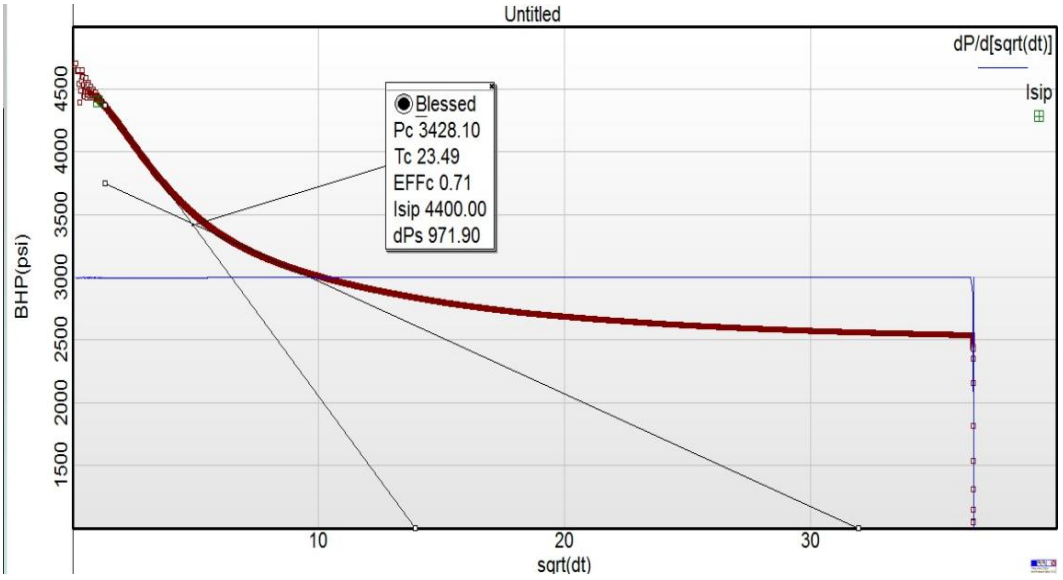

Figure 4.9.An example of square root of time plot analysis

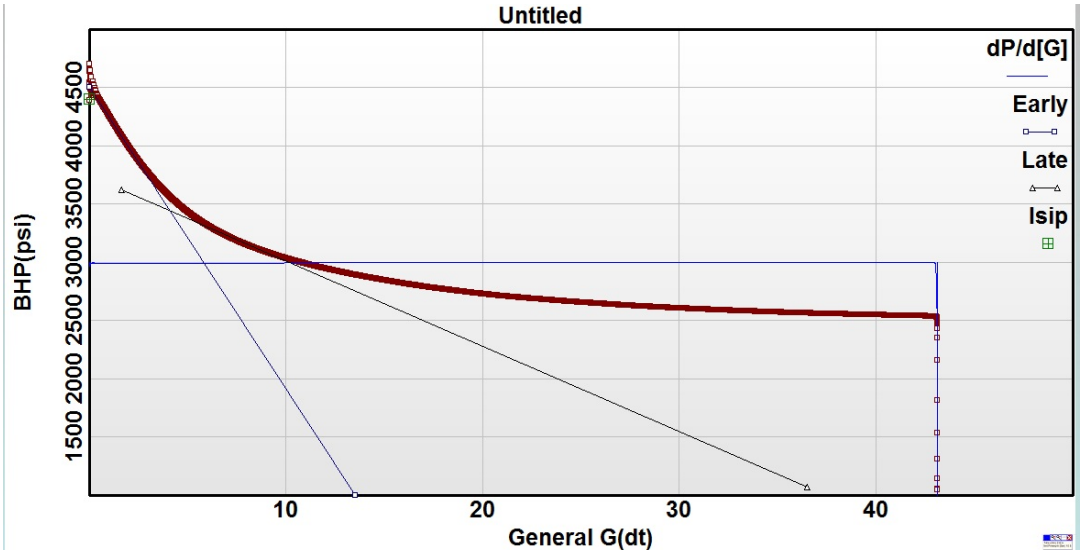

Figure 4.10.An example of G-function plot analysis

G-dP/dG plot is generated by taking the derivative of pressure with respect to G-Function (dp/dg) and plotting dp/dg as a function of the G-Function.(Baree and Mukherjee, 1996) This method provides an accurate determination of magnitude of pressure dependant leak off. As shown in Figure 4.11, second derivative pressure response would exhibit a straight line and would be above or below the ideal line for non ideal decline behavior like pressure dependent leakoff or height recession respectively.

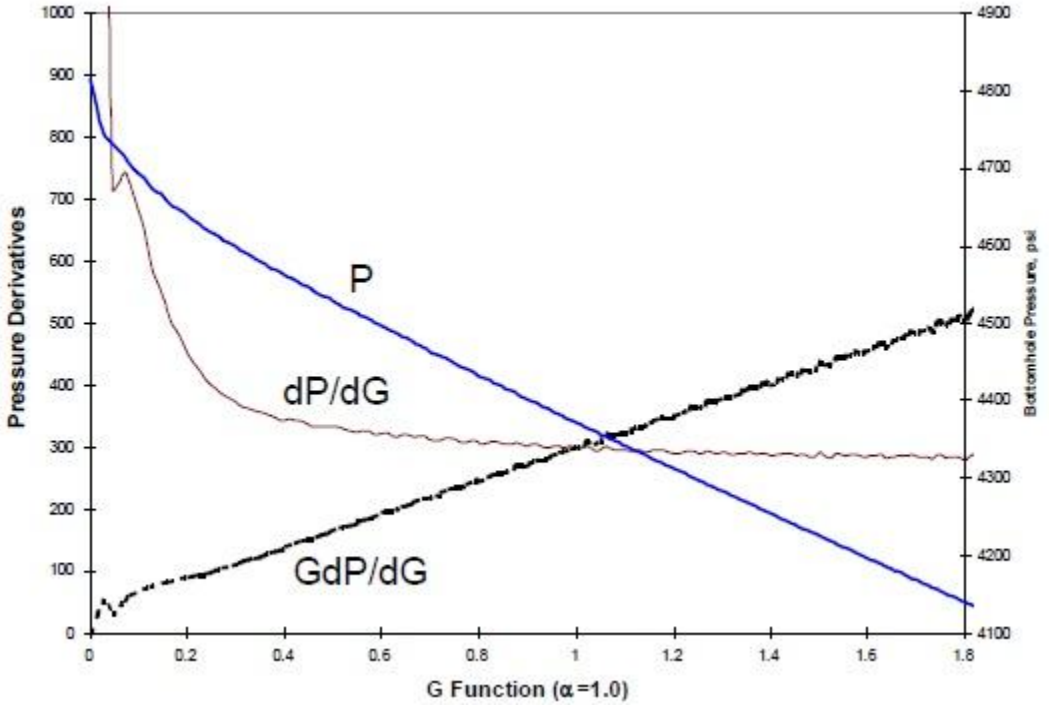

Figure 4.11.An example of G-dP/dG plot analysis (Baree and Mukherjee, 1996)

4.3 SUBJECTIVITY ISSUES WITH ANALYTICAL METHODS

The analytical methods described in the previous section are widely used for the determination of important fracturing parameters. However there may be a difficulty in using these techniques because they are subjective to individual's interpretation. Here closure stress is taken as the reference parameter to describe the subjectivity issues with these techniques.

Consider Figure 4.12 which shows the square root of time plot for some pressure fall-off data. The square root of time plot analysis was performed to obtain the closure stress value. Tangents were drawn to the curve as shown in figure 4.12. The closure stress obtained from this analysis was approximately 3428 psi.

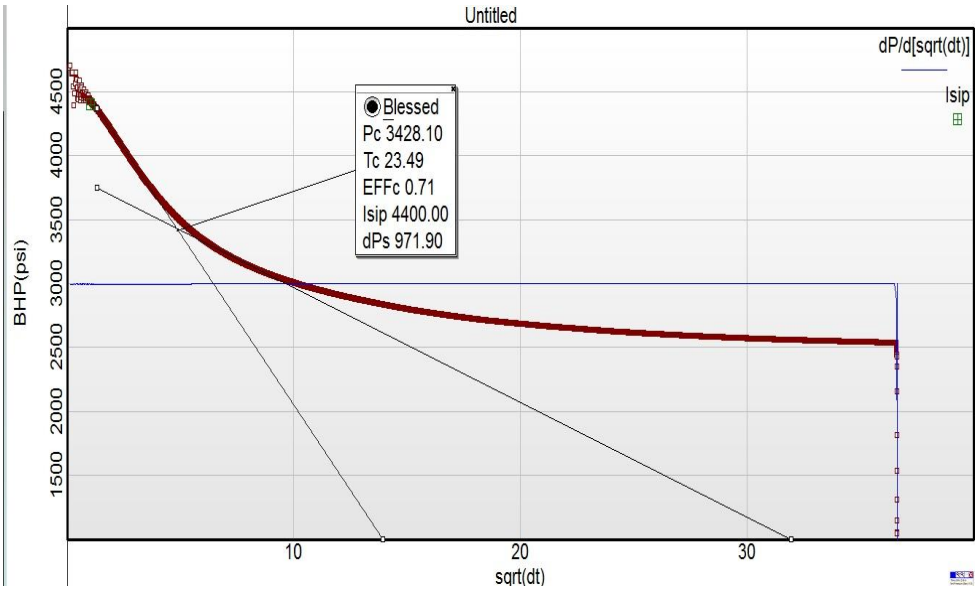

Figure 4.12.Square root of time plot analysis showing Pc of 3428 psi

Now, the same set of data was analyzed second time using the same technique of square root of time plot analysis. The only difference was that the tangents were fitted differently compared to previous analysis, placing one tangent more along the late time data. Figure 4.13 summarizes results for this analysis. In this case, closure stress obtained for the same set of data was around 2847 psi, which was more than 500 psi smaller than the previous analysis.

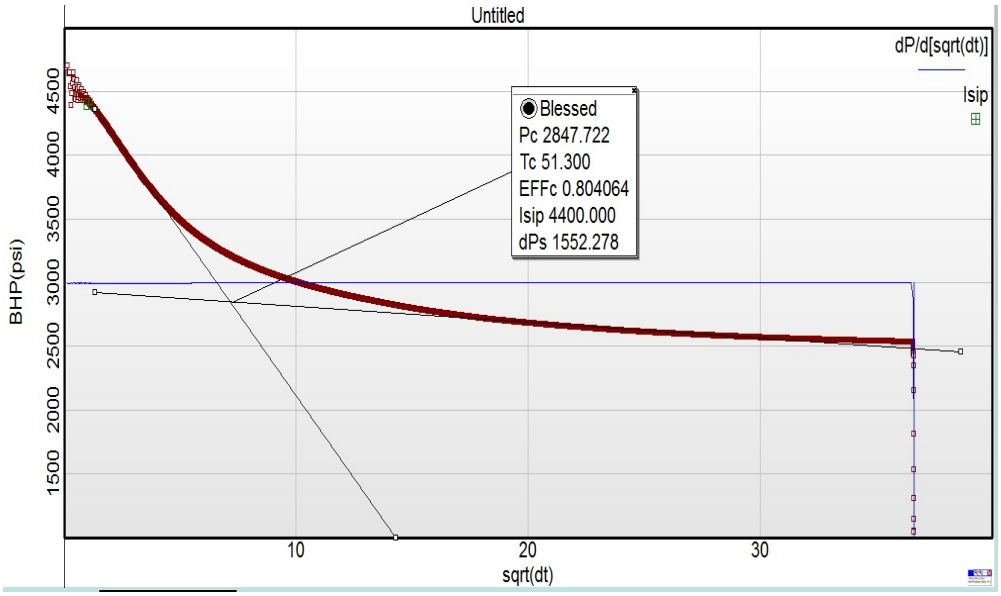

Figure 4.13.Square root of time plot analysis showing Pc of 2847 psi

As with the previous example one may also fit tangents with greater emphasis on early time data. Figure 4.14 shows results obtained from this analysis. Here, for the same

decline, closure stress value obtained was around 3003 psi which was 400 psi smaller than the first analysis and about 150 psi greater than the second analysis.

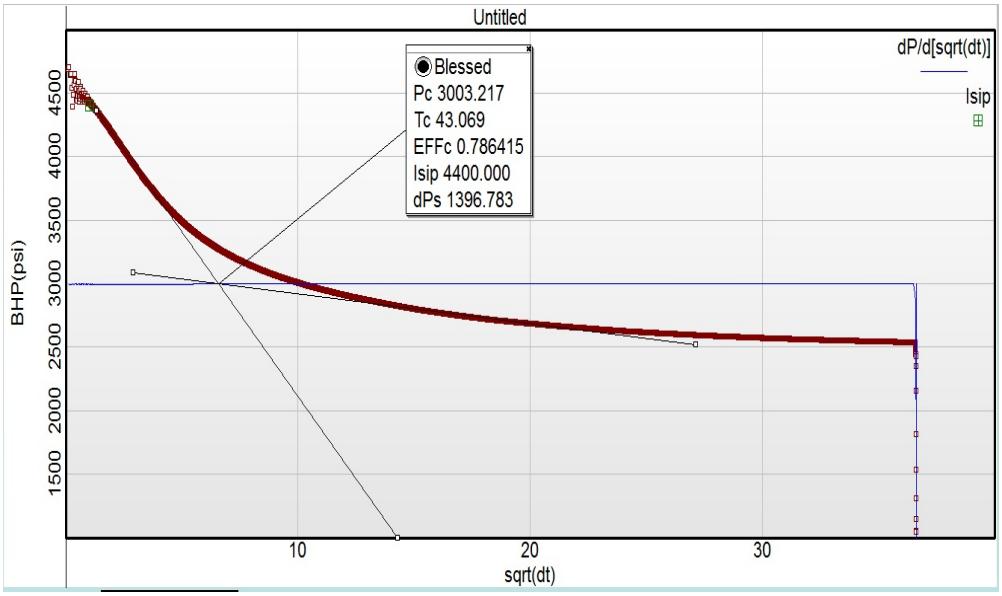

Figure 4.14.Square root of time plot showing Pc of 3003 psi

The main problem faced when using the tangent intersection technique is that the results may vary widely as shown by the example (P_c = 2847 – 3428 psi). It really depends upon the perspective and experience of the engineer how to analyze the data and how to draw tangents to the pressure decline. Accurate determination of closure stress is very important since it is directly related to fracturing parameters such net pressure and minimum in-situ stress. Any ambiguity in the determination of closure stress results in

erroneous calculations of net pressure and thus in wrong fracture geometry predictions and fluid leak off coefficients. Closure stress is the single most important parameter for the success of hydraulic fracturing treatment. Therefore above mentioned ambiguities in the determination of closure stresses should be minimized by the introduction of more definite method.

5. SQAURE ROOT OF TIME PLOT ANALYSIS FOR WATER WELL AND GAS WELL

Two wells were used in this study, including a water well in southwestern Missouri and gas well from Canadian gas formations. This section discusses the tests and square root of time plot analysis for these tests.

5.1 CU PROJECT EXPLORATORY WELL # 1 (WATER WELL)

The data for this study is gathered from a city utilities project well # 1 which is a CO_2 sequestration project. When injecting CO_2 into a formation, it is mandatory to make sure that the injected CO_2 does not break the formation. For this purpose it is important to know critical reservoir parameters such as minimum in situ stress, formation break down pressure. These parameters are estimated using hydraulic fracturing techniques.

Ten intervals from the bottom of the Reagan Sandstone through the Lamotte formation were selected for pressure testing. These zones were tested according to ASTM standards. The procedure uses two straddle packers set in an open hole to seal off the test interval. With the packers anchored to the borehole wall, the formation test interval is pressurized hydraulically by pumping at a constant flow rate. The general principle is to affect hydrofracturing with a minute or so from the beginning of interval pressure rise. Packer pressure must be maintained during testing to minimize leakoffs. As the rock hydrofractures, a critical (or breakdown) pressure is reached. When pumping is stopped, the pressure will drop to the instantaneous shut in pressure (ISIP). Repeated cycling of

the pressurization procedure using the same flow rate will yield the secondary breakdown pressure (the pressure required to reopen a pre-existing fracture) and additional values of the shut in pressure.

An example of hydrofrac test and hydrojack test is shown in Figure 5.1 and Figure 5.2.The testing sequence included three hydrofrac tests, followed by at least two hydrojacking tests. Each interval was approximately four feet long. Surface injection rates and pressures were recorded, along with the pressure being held on the packers. Appendix A shows the hydrofrac and hydrojack test for the rest of the test intervals.

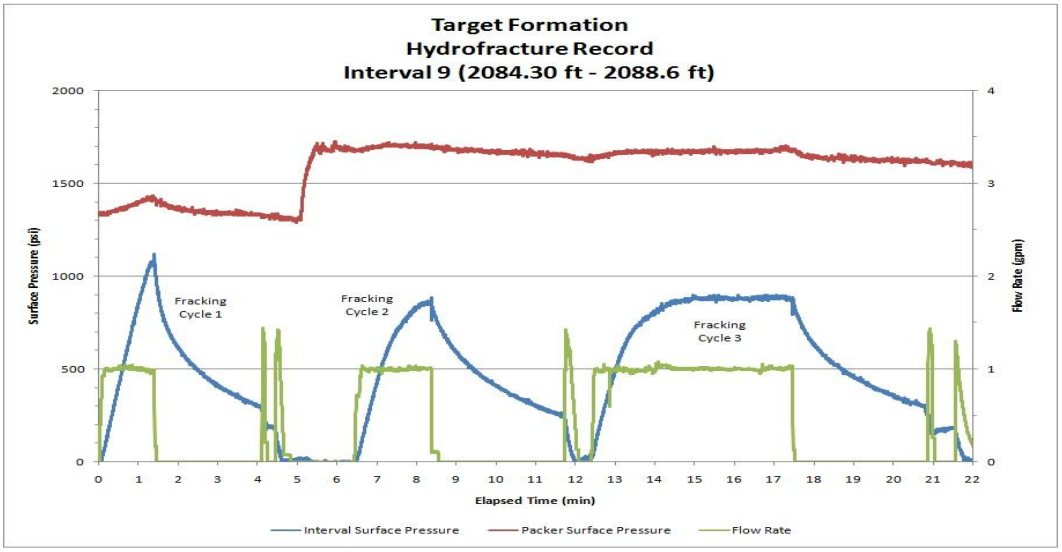

Figure 5.1.Hydrofrac test performed on test interval 9 (2084.3ft – 2088.6ft)

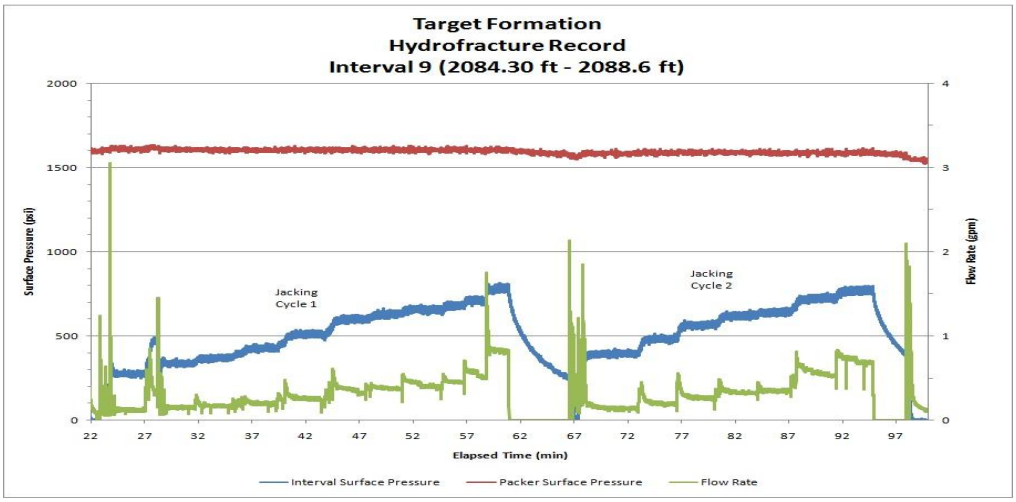

Figure 5.2.Hydrojack test performed on test interval 9 (2084.3ft – 2088.6ft)

In this analysis, all surface test data were adjusted to bottomhole pressures using the hydrostatic head of fresh water. In addition, the tests have been reordered on depth, and are presented from the bottom of the well upward. Hence, the test interval numbers are not in numerical order.

Formation breakdown pressure was determined by reading this highest pressure of the first breakdown cycle, unless a later hydrofrac cycle had a significantly higher pressure. In those cases, the later cycle was used. Typically, after a fracture initiates, its reopening pressure should be less, as the initial fracture has already overcome the tensile strength in the rock. Interval 9 did exhibit a reduction in the hydrofrac breakdown pressure. Intervals 4 and 10 did not exhibit the highest breakdown in their first pump-in cycle, and Interval 8 could not be broken down at all.

Closure stress (minimum in-situ stress) was determined from the falloff period of the final pump in test for each interval, as the last pump-in period generally had the longest injection and falloff time. StimPlan software was used to analyze the fall off period using the standard pressure square root of time plot. Figure 5.3 shows the square root of time plot analysis for the test interval 9. Analysis for rest of the intervals is shown in appendix A.

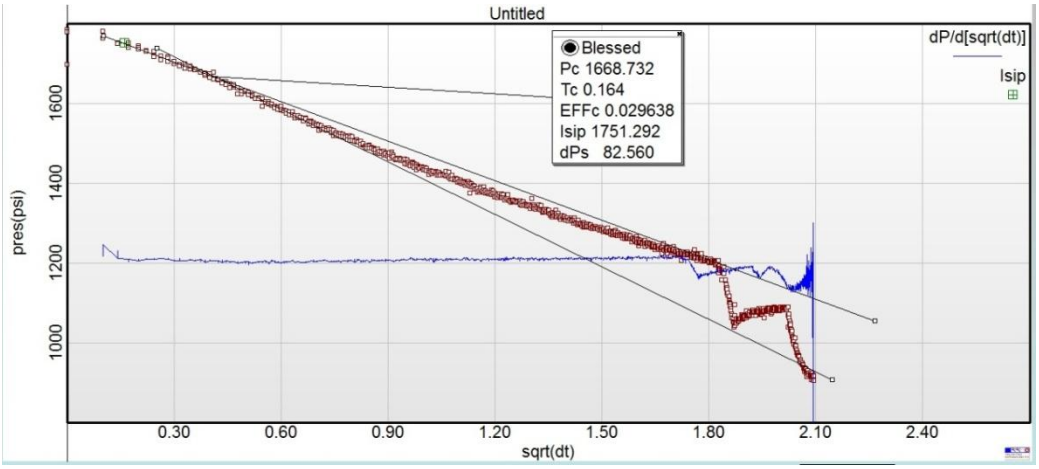

Figure 5.3.Square root time plot analysis using for test interval 9 (2084.3ft – 2088.6ft)

5.2 CANADIAN GAS WELL # 2

Canadian gas well # 2 is a new producing well in an existing major gas field. The well has been drilled and logged and preparations are being made to fracture stimulate the well. This well is a planned Canadian formation completion with perforation at a depth of 1983 m – 1989 m. The objective is to design and place the optimum fracture stimulation on this well to maximize both the initial potential and profitability of this new well. Fracturing fluid planned for this job is water based cross linked gel and 20/40 Ottawa sand. Prior to fracture stimulation job a series of pre fracture tests were conducted on the well. Out of those, a stress test and a minifrac are taken for analysis purpose in this study.

Prior to mobilizing the fracture fleet, the well is perforated at 2020 meters and an in situ stress and a step rate test were conducted to determine fracture closure pressure. For better results, a stress test should be conducted with at least two step rate flow/flowback/decline tests with very inefficient fluid. (Thompson and Church, 1993) Figure 5.4 shows a data plot for stress test conducted on Canadian gas well # 2 at 2020 meters. It does not contain step rate part as analysis is more focused on closure stress determination. As can be seen from the plot, three successive pressurization cycles are carried out on the well, each followed by a pressure decline part. The reason for conducting three pressurization cycles is to obtain repeated value for closure stress and to minimize effect of elasticity of the rock. The second injection/decline curve was taken for analysis to calculate the closure stress.

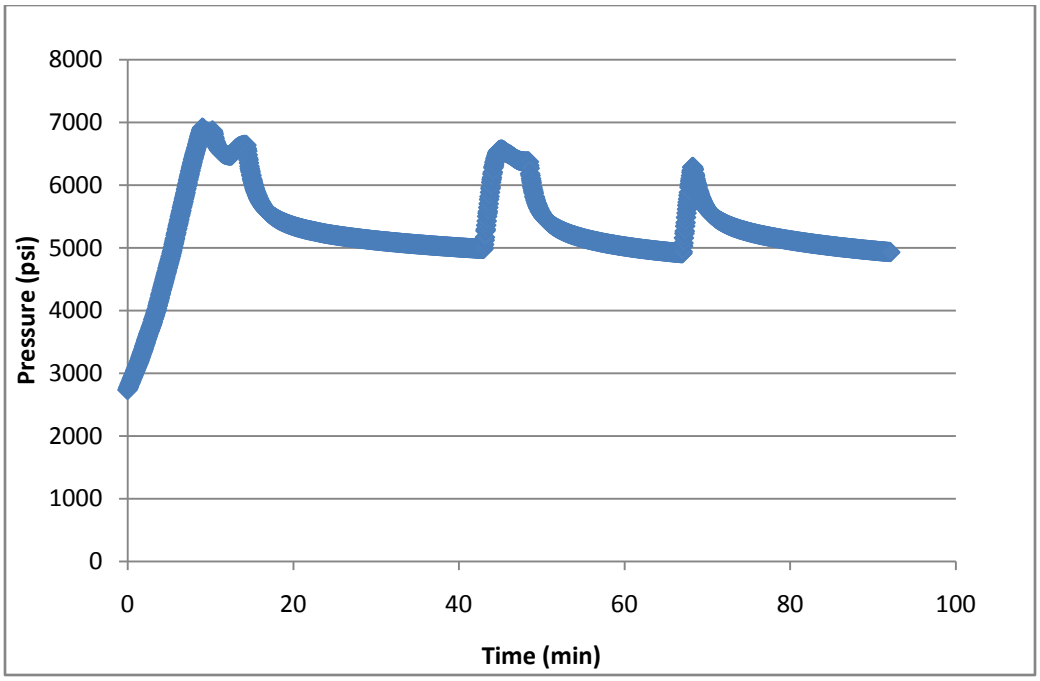

Figure 5.4.Data plot for stress test in Canadian gas well # 2

The decline part or pressure fall off period of the second pressurization cycle was analyzed for closure stress calculation. The analysis was performed by constructing a square root of time plot using StimPlan (Figure 5.5) Tangents were drawn to curves having different slopes and intersection of tangents was taken as the value for closure stress.

The gas well testing included a step rate test for fracture extension pressure, a minifrac for fluid leak off coefficient, history matching, fracture closure pressures and for redesigning the entire treatment. For the purpose of this study, only the minifrac was considered and step rate for extension pressure was neglected. Figure 5.6 shows the data plot for a minifrac conducted on well # 2.

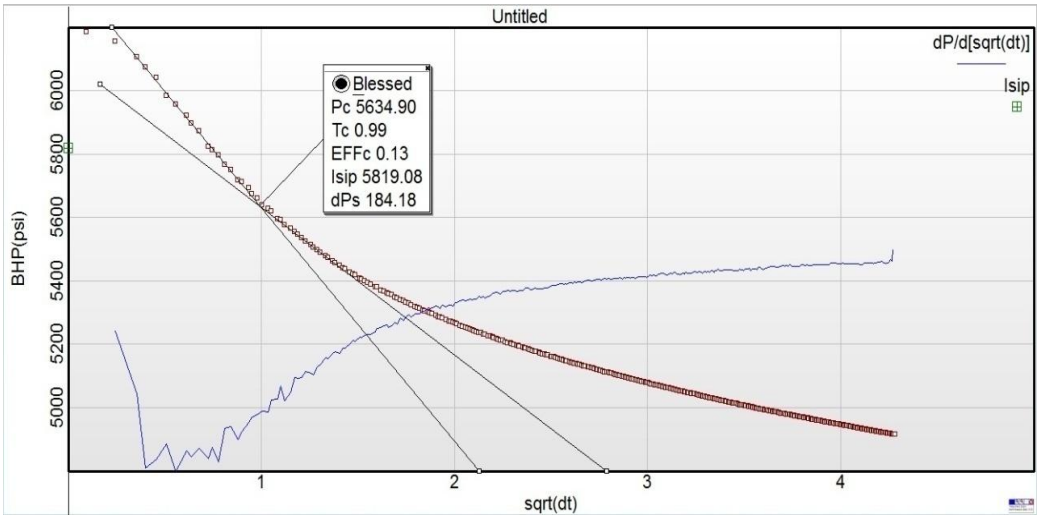

Figure 5.5.Square root time analysis for stress test in Canadian gas well # 2

Two pressurization cycles were carried out each following a decline. Here, the second pressurization cycle showed a long and prominent decline, therefore it was taken for analysis. The decline part was analyzed using square root of time plot for closure stress. Figure 5.7 shows the square root time plot analysis for minifrac test.

Results of these analyses are compared to results from statistical analysis as discussed in Section 8.

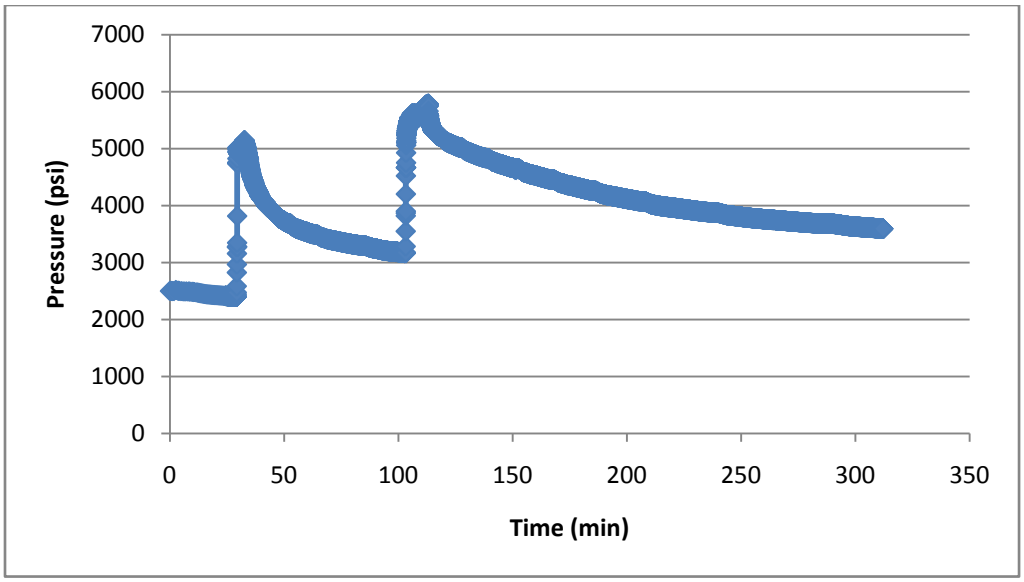

Figure 5.6.Data plot for minifrac test in Canadian gas well # 2

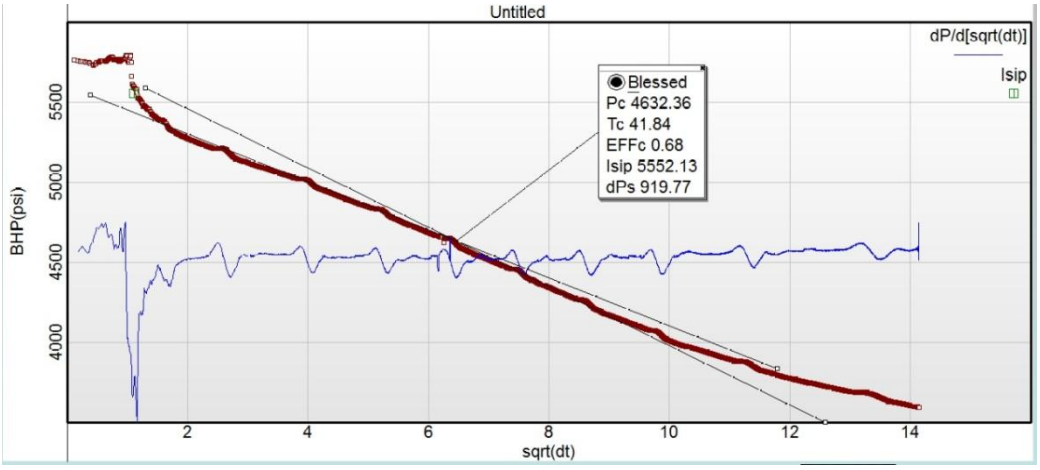

Figure 5.7.Square root time analysis for minifrac test in Canadian gas well # 2

6. STATISTICAL APPROACH FOR CLOSURE STRESS CALCULATION

This section discusses a statistical method for determining closure stress presented by Lee and Haimson (1989) and its application to this work.

6.1 NON LINEAR REGRESSION ANALYSIS (NLRA)

Statistical analysis refers to a collection of methods used to process large amounts of data and report overall trends. Statistical analysis of hydraulic fracturing data enhances the objectivity of determining closure pressures. The determination of closure pressure is straight forward when a sharp break is observed in pressure time curve after the initial fast pressure decline following pump shut-off. In some cases however the decline is gradual and P_c is indistinct. Many graphical methods such as tangent divergence, the tangent intersection and logarithmic methods have been suggested and successfully implemented over the time. Although the square root of time plot analysis, G-Function plot analysis and G-dP/dG plot analysis provide reasonable approximations, ambiguities remain when pressure decay is gradual with no obvious breaks or knees. By employing a statistical method, we provide means of improving the objective determination of P_c, applied to digitally recorded field pressure and flowrate data.

There are numerous methods to statistically evaluate the given set of data. One of these is non linear regression analysis (NLRA). Non linear regression analysis is a statistical method of fitting an arbitrary function to a given set of data points. Using

NLRA, the closed fracture segment of the pressure – time curve can be isolated by fitting it to an exponential decay model. Exponential pressure decay model can be presented as,

$$P_{pi} = \exp(d_1 t + d_2) + P_{al} \text{ for } t \geq t_L \quad \text{..... (6.1)}$$

Here t is the time since the pumps have been shut down and t_L is the time since fractures have been completely closed. The boundary condition $t \geq t_L$ implies that this equation is valid only for closed fracture segment of the pressure time curve. Muskat M. (1937) had suggested that pressure decline following the fracture closure follows the exponential pressure decay model. The interval pressure upon fracture closure P_c^{lt} would be determined first, by applying NLRA to the decaying portion of the pressure-time curve. It determines pressure decay parameters ($d_1 and\ d_2$) and the asymptote (P_{al}) by minimizing the sum of the squares of errors (SSE) between recorded data and predicted pressures based on the model. The fit can be evaluated in terms of residual mean square (RMS) of an error which represents the average deviation of the curve from the model.

$$RMS = \sqrt{\sum_{i=1}^{n} (\mathrm{P_i} - P_{pi})^2 / (\mathrm{n} - 3)} \quad \text{..... (6.2)}$$

In this equation, P_i is the actual pressure which is recorded on-field, P_{pi} is the modeled pressure which is obtained using exponential pressure decay model and n is simply number of the observation. This equation is known as RMS because it is square root of mean of square of an error. Here error is simply the difference between observed (actual) value for P_i and modeled value P_{pi}.

When these pressure decay parameters along with intial conditions and equations for RMS and exponential pressure decay are fed to simulator, an iteration procedure is invoked aimed at excluding the segment of the decaying pressure-time record before fracture closure. Starting at the time of pump shut off (t = 0), data points will be removed sequentially with each iteration. This fitting procedure would end when the decreasing RMS value stabilizes. At this point it would be assumed all the pressure data belonging to the open fracture time segment ($t < t_l$) have been removed from the curve fitting process. Figure 6.1 shows the process of curve fitting and determination closure stress using fitted model over the actual data.

The largest pressure value of the fitted pressure-time curve (P_c^{lt}) is interpreted as the level at which the induced fracture has completely closed, hence it is the lower limit of the expected shut in pressure value. The extrapolated pressure level obtained by fitted exponential curve at time t = 0 (P_c^{et}) represents the pressure at which pure radial flow would have commenced were the fracture to close instantaneously upon pump shut off. It is thus the upper limit of the range of values within which P_c is to be found. (Lee and Haimson, 1989)

$$P_c^{lt} < P_c < P_c^{et} \quad \text{..... (6.3)}$$

Generally the value of P_c^{et} yields more accurate approximation for the value of closure stress (Lee and Haimson, 1989). Expected value of the closure stress should lie within ±100 psi of P_c^{et}. Aamodt and Kuriyagawa have also recommended using P_c^{et} as the closure pressure value.

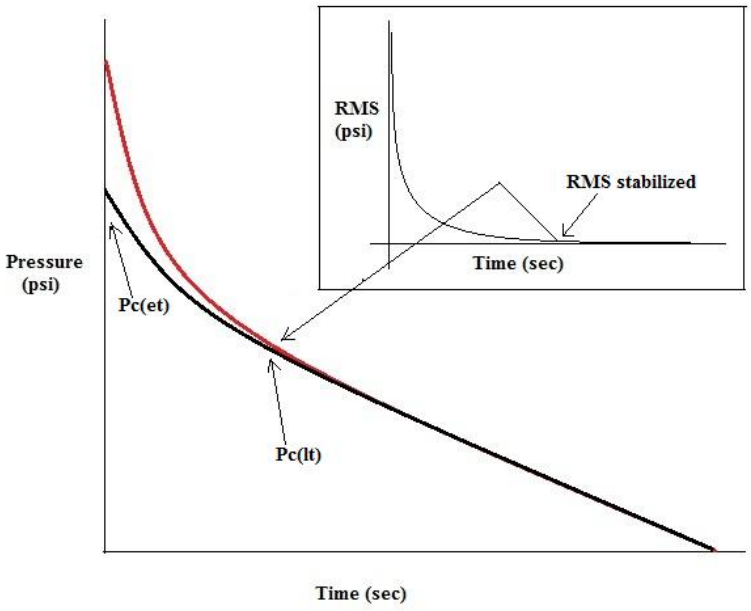

Figure 6.1.Curve fitting process and RMS graph using NLRA (Lee and Haimson, 1989)

6.2 SAS

All the statistical analysis of data for this study is done programmed a software SAS. Before describing the actual work, this section provides basic information on SAS and SAS programming.

SAS was developed in early 1970's at North Carolina State University. It was originally intended for management and agricultural field experiments. It is now most widely used statistical software. The name 'SAS' used to be an abbreviation for 'Statistical Analysis System' however it is no longer an acronym for anything.

SAS system provides a powerful framework for statistical analysis. It has extensive data manipulation capabilities to prepare for analytic and modeling work. It has reporting tools for presenting results. Enterprise Guide (EG) enables to get answers without having to write programs, through a point-and-click interface making selections from a series of menus. As a benefit even for experienced SAS programmers, EG provides a framework within which to organize the data, tasks, and results involved in performing a statistical analysis, through the creation and maintenance of "projects". (Hallahan and Atkinson, USDA)

In SAS, we can create new projects, open existing projects, save projects, we can access data from outside. Enterprise Guide reads the data and brings it up in a data viewer. Figure 6.2 shows a window that pops up after we create a new project. The empty space in the middle is being provided for writing the program.

6.3 SAS PROGRAMMING

SAS as a programming language can be learned quickly and a user can begin writing programs within hours of being introduced to SAS if there is the correct information being taught.

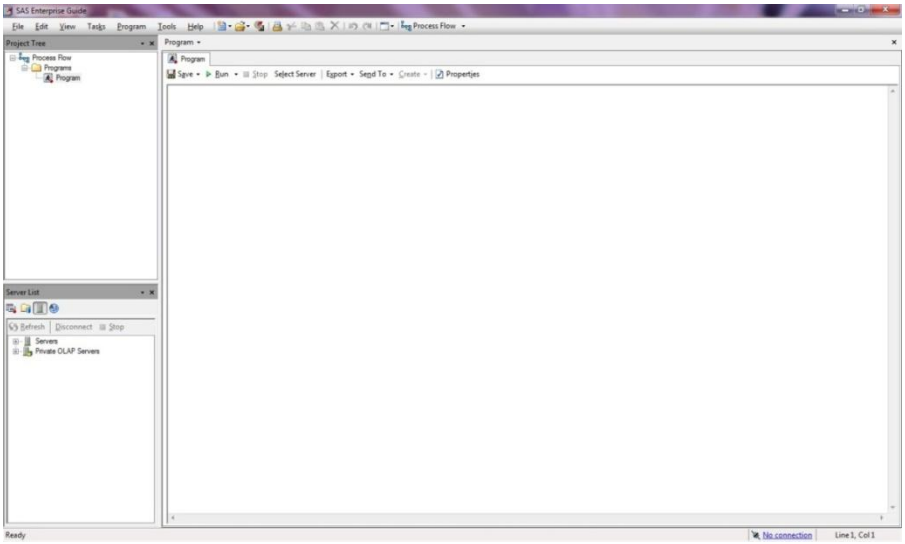

Figure 6.2.SAS enterprise guide showing program window

SAS programming is easy to understand if the concept of ‘Step Boundaries’ is understood thoroughly. Step boundaries are denoted by ‘DATA’ and ‘PROC’ or Procedure statements. SAS runs whatever code it finds within the step, processes the data, then goes to the next step in the next DATA or PROC step, repeats the cycle within the step, and so on until the end of the SAS job. When writing a SAS job, it should begin with either DATA or PROC statement. (Clarence Jackson, CSQA)

A very important concept to understand is the computing cycle, which is simply ‘input process - output’.

- Input is the start of any compute cycle. There must be something coming in to be processed before any output can occur. Input for SAS programs can be from raw data files, in stream cards or data lines, or SAS dataset/files. Input is what you want to process.

- Process is the part of the cycle that turns the input into something that can be used, a very important part of the cycle.
- Output is the part of the cycle that gives you what you need from the computer.

Every program requires input, processes the input, then returns the results as output. SAS does that in so many different ways. It uses DATA step as an input and PROC step as an output. (Clarence Jackson, CSQA)

6.3.1 SAS Programming Statements SAS programs are done by using SAS statements that describe the action to be taken by SAS. SAS statements are delimited by ';' or a semi-colon. This denotes then end of a statement segment. SAS is a free form programming language, which means there are no rules regarding where on the line of code statements need to be. Each statement contains a SAS keyword, at least one blank between words, and a semi-colon. One can write SAS where one statement can span multiple lines of code, which makes it possible to write code that is easy to read and maintain.

SAS DATA steps usually create SAS datasets or datafiles from raw input data. SAS uses the following keyword statements to perform the input process within the DATA step:

- INFILE statements defines the raw source file of data to be read into SAS
- INPUT statements defines the location of fields on the record that will become variables
- CARDS/DATALINES tells SAS that data follows in the job stream. The ';' is used to tell SAS to stop reading the data as data and start back to reading SAS statements.

Figure 6.3 shows a simple program using all above defined statements. The first step marked ‘A’ consists of two statements; DATA and Input. The second step marked ‘B’ consists of one statement; Cards. Cards defines the input to the program. Step ‘C’ is Proc Print statement which is used to present output data in the tabular form or as a list. Last step ‘C’ is a Proc Corr statement. This statement is used when an output data needs to be represented in some form of correlation.

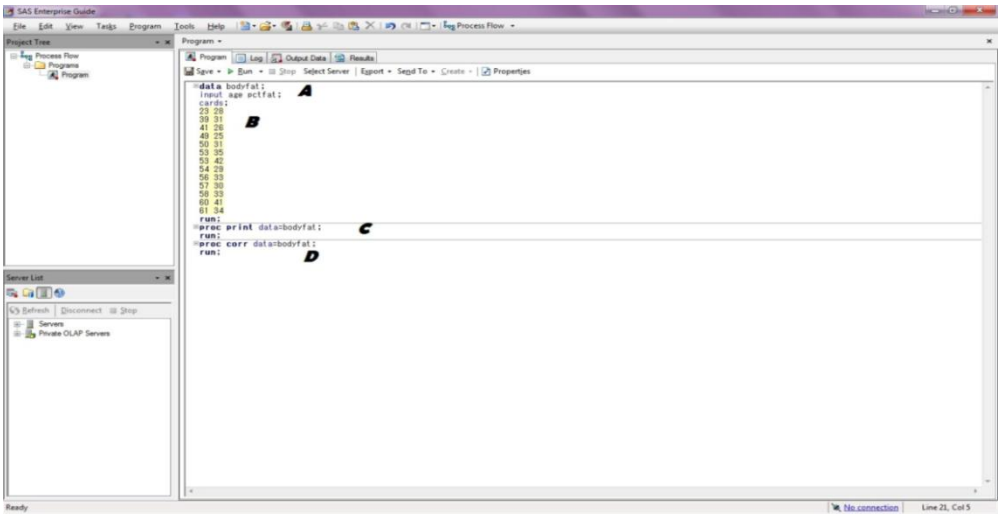

Figure 6.3.A simple SAS program showing use of different statements

6.3.2 SAS Log File and Results File If SAS program stops running, SAS log should be reviewed. The SAS Log report tells everything that SAS is doing, and will be a source of feedback regarding the execution of the SAS program. It tells if an error is being encountered, missed a record read, how many records were read and processed, and other useful information. Figure 6.4 shows the log for the last program. If there were

errors, it would be ‘ERROR:’ followed by the type of error encountered. One thing that the log will not show you are logic errors. If the results are not what are intended, a log file should be read to see what went on with your program, and should be compared with what should be done with the program.

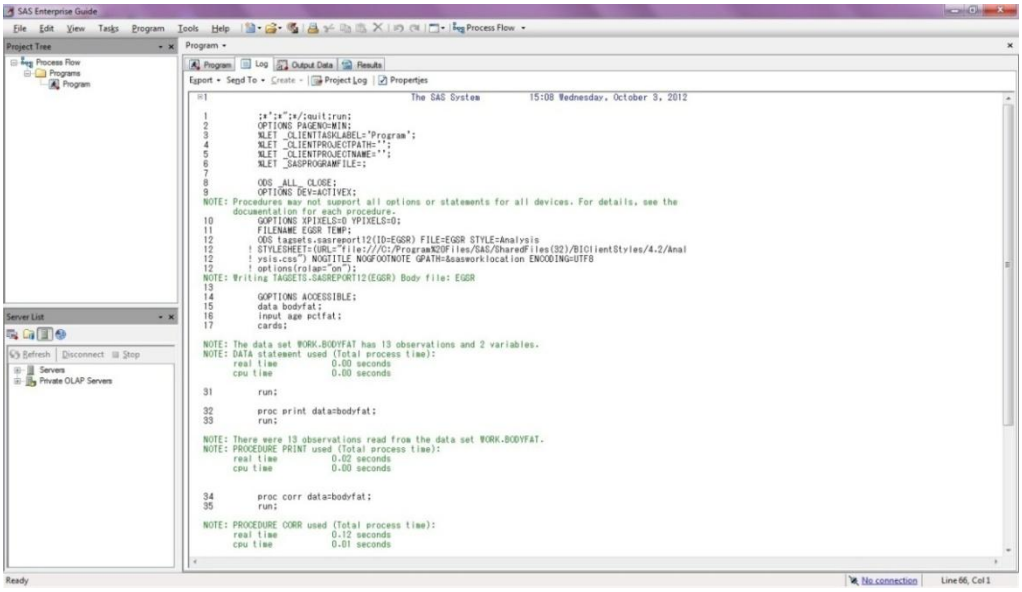

Figure 6.4.SAS log file for the sample program

Whenever a SAS program executes a PROC step that produces printed output, SAS sends the output to the procedure output file. SAS results file shows the output in the desired format. Figure 6.5 shows the output file for the above program. Figure 6.6 shows results file for the same program. It reflects the results of Proc Corr statement. It summarizes the input data into different quantities such as mean, standard deviation, minimum, maximum etc. SAS results file can be used to divert results to different outputs

such as a printer, an external file, to its usual location and external file and to a remote destination. (SAS Enterprise Guide)

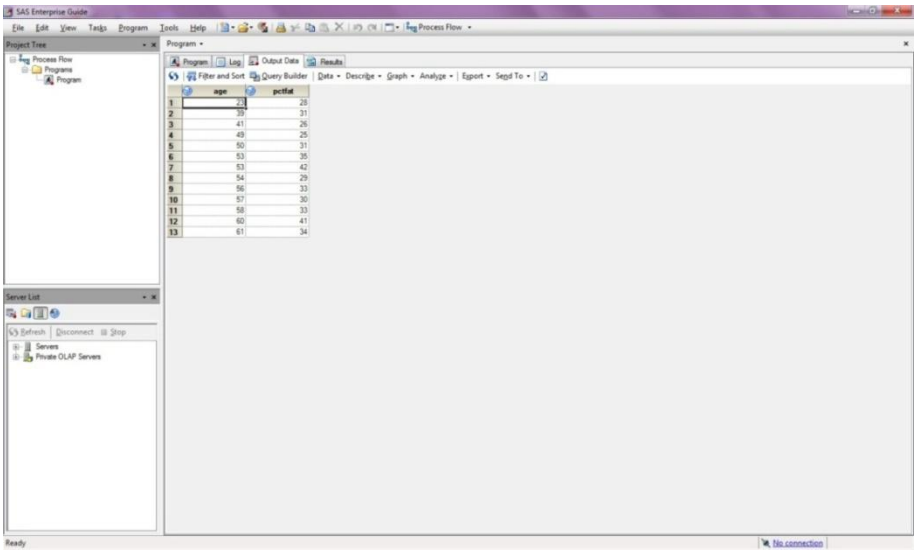

Figure 6.5.SAS output file showing results from a PROC statement

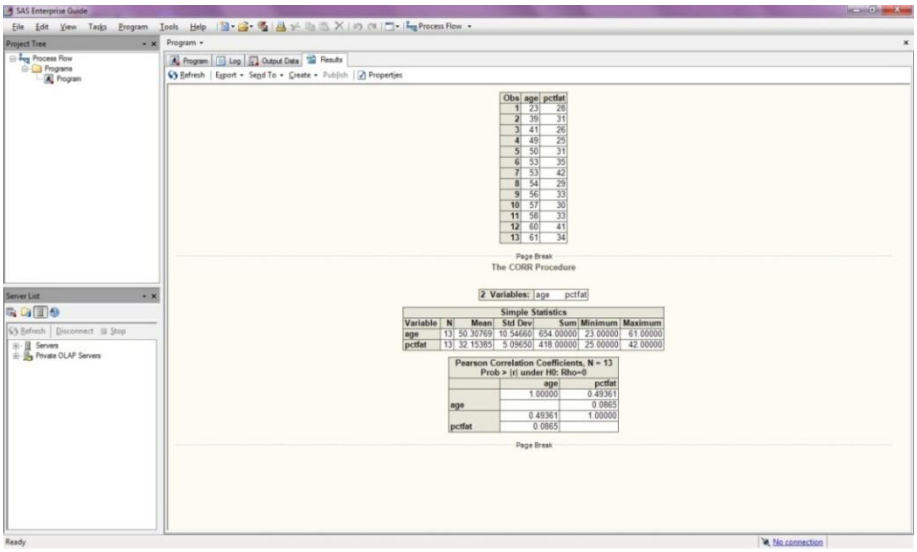

Figure 6.6.SAS results file

7. STATISTICAL ANALYSIS OF THE DATA

7.1 THE 'NLIN' PROCEDURE

For statistical analysis of the non linear data used for this study, the 'PROC NLIN' procedure in SAS was extensively used. The NLIN procedure produces least squares or weighted least squares estimates of the parameters of a nonlinear model. Nonlinear models are more difficult to specify and estimate than linear models. Instead of simply listing regressor (independent) variables, the regression expression must be written, parameter names should be declared, and initial parameter values must be supplied. Some models are difficult to fit, and there is no guarantee that the procedure can fit the model successfully. For each nonlinear model to be analyzed, a model must be specified (using a single dependent variable) and also, the names and starting values of the parameters to be estimated must be specified.

Estimation of a nonlinear model is an iterative process. To begin this process the NLIN procedure first examines the starting value specifications of the parameters. If a grid of values is specified, PROC NLIN evaluates the residual sum of squares at each combination of parameter values to determine the set of parameter values producing the lowest residual sum of squares. These parameter values are used for the initial step of the iteration. (SAS Online doc version)

Then PROC NLIN uses one of these five iterative methods:

1. steepest-descent or gradient method
2. Newton method

3. modified Gauss-Newton method

4. Marquardt method

5. multivariate secant or false position (DUD) method

These methods use derivatives or approximations to derivatives of the SSE (sum of squares of the errors) with respect to the parameters to guide the search for the parameters producing the smallest SSE.

Statistical analysis of the data used for this study used Gauss – Newton method for non linear regression analysis. Figure 7.1 shows the program used for NLRA using nlin procedure and Gauss – Newton method.

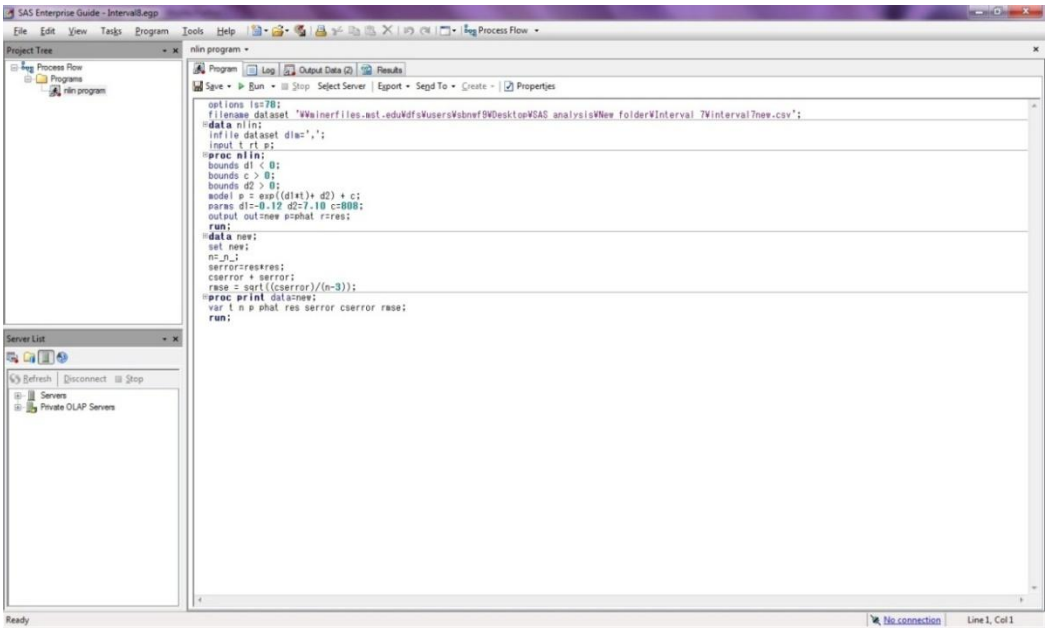

Figure 7.1.SAS program used for the study showing ‘nlin’ procedure.

7.2. CU PROJECT EXPLORATORY WELL # 1 (WATER WELL)

A large amount of pressure data was collected when Lamotte and Reagan sandstones were subjected to hydrofrac and hydrojack test cycles. As previously stated, this zone of interest was divided into 10 intervals each approximately 4 feet tall and each interval was pressure tested for breakdown pressures and extension pressures. For the purpose of this study, each interval was analyzed statistically using NLRA for the closure stress. Data corresponding to only the shut in part of the pressure – time curve was selected. This is because closure stress can be calculated by analyzing only the decline part of the pump in – fall off data. This data was then imported into SAS and proc nlin procedure using Gauss – Newton method was implemented. Equation 6.1 was used to fit exponential pressure decay model to the decline part of the data. As stated in section 7.1, the proc nlin procedure requires initial parameters to start the iterative procedure. Considering Equation 6.1, the initial parameters required to start iterations are d_1, d_2 and C. Here d_1, d_2 are pressure decay constants. These parameters were calculated independently for each test interval using sum of square of errors (SSE) between recorded data and predicted pressures based on the model. The formation pressure was selected as an asymptotic pressure for the calculation of initial parameters. The fit was evaluated in terms of RMS using equation 6.2. An iteration procedure was invoked and data points corresponding to open fracture segment were removed sequentially. The fitting procedure ended when decreasing RMS values were stabilized. However, because the program written to analyze the data was not so advanced that it would remove points sequentially on its own, data points were remove manually and each time program was run to do the iteration. Output from the simulator was analyzed each time to check if the

RMS had stabilized or not. If it was observed that RMS had not stabilized then again next few data points were removed and again the program was run to get output from next iteration. This process was continued until decreasing value of RMS was stabilized. This process was repeated for each interval. After RMS was stabilized, all the data points corresponding to open fracture segment were assumed to be removed. Table 7.1 shows an example for the output from SAS. Column 1 is an observation column which shows number of observations read or number of data points read by SAS. Column 2 is a time column which is the time in minutes from which pressure decline has started. Column 3 is again number of observation which serves as a denominator for equation 6.2. Column 4 is digitally recorded downhole pressure data. Column 5 is modeled pressure calculated using equation 6.1. Column 6 is an error which represents the amount by which modeled pressure value has deviated from the observed one. Column 7, 8 and 9 represent square of error, cumulative square of error and root mean square of error (RMSE) respectively. Column 10 is a manipulated time which is calculated by considering first observation in column 2 to be equal to zero. Figure 7.2 shows RMS graph, which is a graph of column 10 v/s column 9 in table 7.1, for the data analyzed for interval 9 (2084.3ft – 2088.6ft).

Table 7.1.Example table showing output from SAS for interval 9 (2084.3ft – 2088.6ft)

	1	2	3	4	5	6	7	8	9	10
Obs	**Obs**	**t**	**n**	**P**	**P Mod**	**Error**	**SQ Error**	**CUM SQ Error**	**RMSE**	**MAN Time**
1	**1**	.	1	.	.	.	.	0	0	0
2	**2**	17.95	2	1549.97	1544.03	5.9393	35.275	35.28	.	0
3	**3**	17.95	3	1547.53	1544.03	3.4979	12.235	47.51	.	0
4	**4**	17.95	4	1542.65	1544.03	-1.385	1.918	49.43	7.0306	0
5	**5**	17.96	5	1545.09	1541.61	3.4819	12.123	61.55	5.5476	0.01
6	**6**	17.96	6	1547.53	1541.61	5.9234	35.086	96.64	5.6756	0.01

Table 7.1.Example table showing output from SAS for interval 9 (2084.3ft – 2088.6ft) (cont.)

8	**8**	17.97	8	1537.77	1539.2	-1.4326	2.052	99.77	4.4671	0.02
9	**9**	17.97	9	1530.44	1539.2	-8.7568	76.682	176.46	5.423	0.02
10	**10**	17.97	10	1545.09	1539.2	5.8916	34.711	211.17	5.4924	0.02
11	**11**	17.98	11	1537.77	1536.8	0.9614	0.924	212.09	5.1489	0.03
12	**12**	17.98	12	1535.32	1536.8	-1.48	2.19	214.28	4.8795	0.03
13	**13**	17.98	13	1542.65	1536.8	5.8442	34.155	248.44	4.9843	0.03
14	**14**	17.99	14	1532.88	1534.43	-1.5429	2.38	250.82	4.7751	0.04
15	**15**	17.99	15	1537.77	1534.43	3.3399	11.155	261.97	4.6724	0.04
16	**16**	17.99	16	1532.88	1534.43	-1.5429	2.38	264.35	4.5094	0.04
17	**17**	18	17	1537.77	1532.06	5.703	32.524	296.88	4.6049	0.05
18	**18**	18	18	1535.32	1532.06	3.2616	10.638	307.51	4.5278	0.05
19	**19**	18	19	1530.44	1532.06	-1.6212	2.628	310.14	4.4027	0.05
20	**20**	18.01	20	1537.77	1529.71	8.0507	64.813	374.96	4.6964	0.06
21	**21**	18.01	21	1530.44	1529.71	0.7265	0.528	375.48	4.5673	0.06
22	**22**	18.01	22	1532.88	1529.71	3.1679	10.035	385.52	4.5045	0.06
23	**23**	18.02	23	1528	1527.38	0.6175	0.381	385.9	4.3926	0.07
24	**24**	18.02	24	1532.88	1527.38	5.5003	30.253	416.15	4.4516	0.07
25	**25**	18.02	25	1525.56	1527.38	-1.8239	3.327	419.48	4.3666	0.07
26	**26**	18.03	26	1528	1525.07	2.9348	8.613	428.09	4.3142	0.08
27	**27**	18.03	27	1518.23	1525.07	-6.8308	46.66	474.75	4.4476	0.08
28	**28**	18.03	28	1530.44	1525.07	5.3762	28.903	503.66	4.4885	0.08
29	**29**	18.04	29	1518.23	1522.76	-4.5286	20.508	524.16	4.49	0.09
30	**30**	18.04	30	1525.56	1522.76	2.7956	7.815	531.98	4.4388	0.09
31	**31**	18.04	31	1520.68	1522.76	-2.0872	4.356	536.34	4.3766	0.09
32	**32**	18.05	32	1520.68	1520.48	0.2	0.04	536.38	4.3007	0.1
33	**33**	18.05	33	1520.68	1520.48	0.2	0.04	536.42	4.2285	0.1
34	**34**	18.05	34	1518.23	1520.48	-2.2414	5.024	541.44	4.1792	0.1
35	**35**	18.06	35	1520.68	1518.2	2.4724	6.113	547.55	4.1366	0.11
36	**36**	18.06	36	1523.12	1518.2	4.9138	24.146	571.7	4.1622	0.11
37	**37**	18.06	37	1515.79	1518.2	-2.4104	5.81	577.51	4.1214	0.11
38	**38**	18.07	38	1520.68	1515.95	4.7301	22.374	599.88	4.14	0.12
39	**39**	18.07	39	1513.35	1515.95	-2.5941	6.729	606.61	4.1049	0.12
40	**40**	18.07	40	1515.79	1515.95	-0.1527	0.023	606.63	4.0491	0.12
41	**41**	18.08	41	1515.79	1513.7	2.0902	4.369	611	4.0099	0.13
42	**42**	18.08	42	1518.23	1513.7	4.5316	20.536	631.54	4.0241	0.13
43	**43**	18.08	43	1513.35	1513.7	-0.3512	0.123	631.66	3.9739	0.13
44	**44**	18.09	44	1513.35	1511.47	1.8772	3.524	635.19	3.936	0.14
45	**45**	18.09	45	1515.79	1511.47	4.3186	18.651	653.84	3.9456	0.14

Table 7.1.Example table showing output from SAS for interval 9 (2084.3ft – 2088.6ft) (cont.)

46	**46**	18.09	46	1508.47	1511.47	-3.0056	9.033	662.87	3.9263	0.14
47	**47**	18.1	47	1518.23	1509.26	8.9739	80.532	743.4	4.1104	0.15
48	**48**	18.1	48	1513.35	1509.26	4.0911	16.737	760.14	4.11	0.15
49	**49**	18.1	49	1506.03	1509.26	-3.2332	10.453	770.59	4.0929	0.15
50	**50**	18.11	50	1506.03	1507.06	-1.0336	1.068	771.66	4.052	0.16

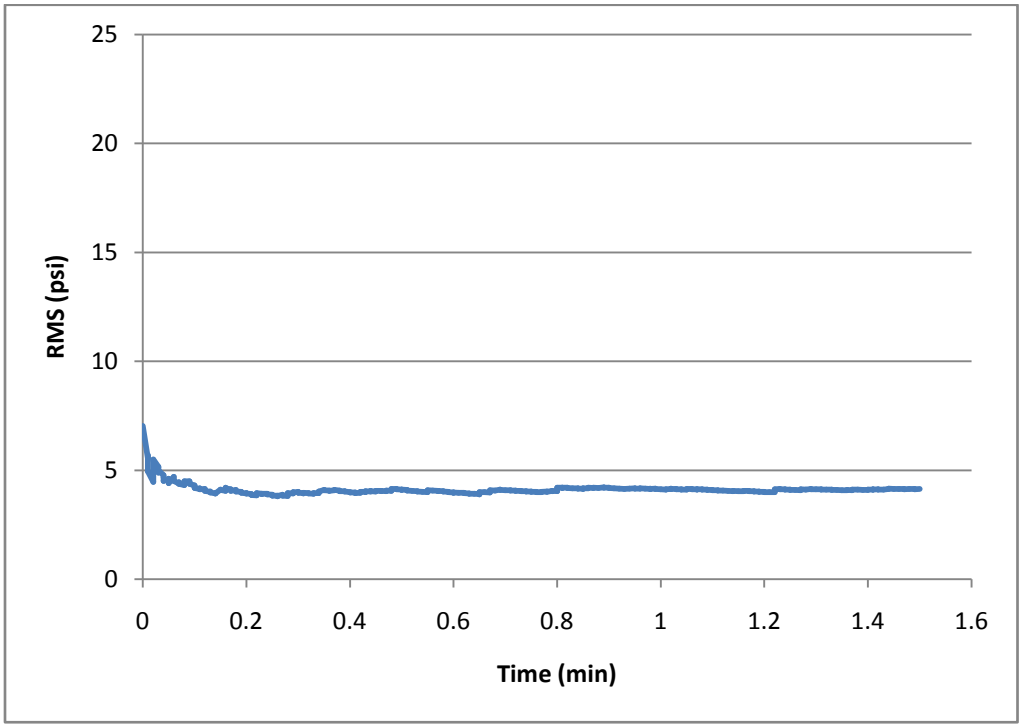

Figure 7.2.Graph showing stabilized value of RMS for interval 9 (2084.3ft – 2088.6ft)

It is clear from Figure 7.2 that RMS value stabilizes well before first minute from the time the pump has shut off. Figure 7.3 shows modeled curve using equation 6.1 fitted

over digitally recorded data. The modeled curve starts to deviate from recorded one, before first minute. The data corresponding to fitted part (where blue curve fits over the red one) is the data corresponding to closed fracture segment. The point at which modeled curve (blue) starts to deviate from the digitally recorded curve (red), is the lower bound on the value of closure stress. The extrapolation of modeled curve on Y axis is the upper bound on the expected value of the closure stress.

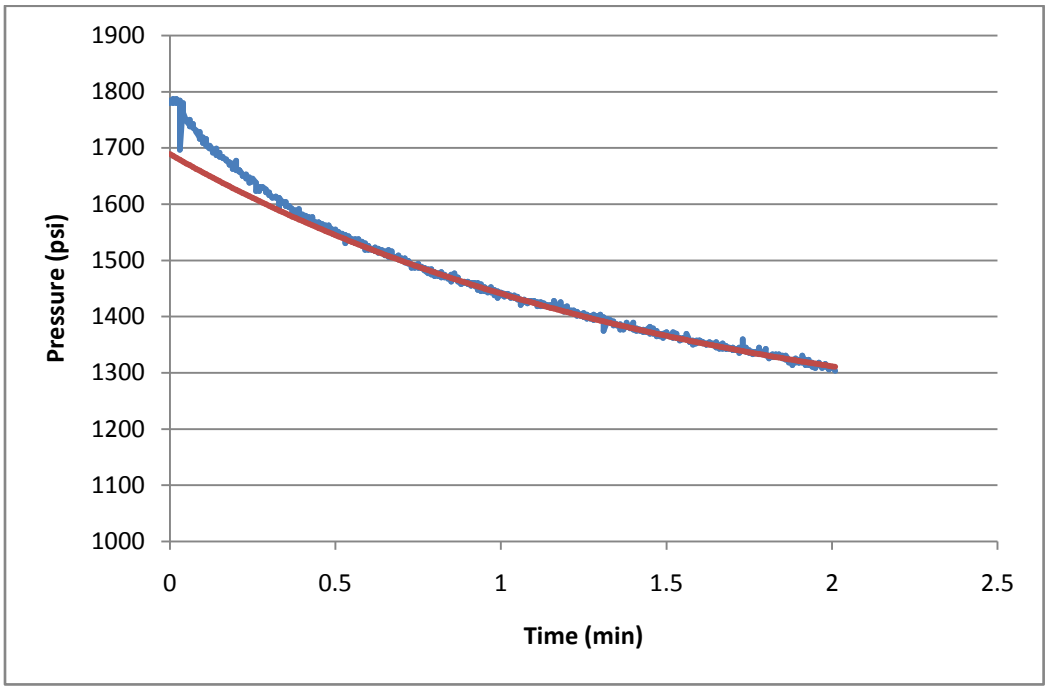

Figure 7.3.Modeled curve (blue) extrapolated to Y axis for interval 9(2084.3ft – 2088.6ft)

From Figure 7.3 we can conclude that the largest pressure value of the fitted pressure-time curve (P_c^{lt}) is 1590 psi and it is considered as the lower limit for the

expected value of closure stress and (P_c^{et}) is close to 1690 psi which is upper limit for the expected value of closure stress.

7.3 CANADIAN GAS WELL # 2

Similar to water well, data obtained from Canadian gas well # 2 was analyzed using regression analysis. Two tests, a stress test and a minifrac test, are analyzed using NLRA. As previously stated, data corresponding to second pressurization cycle, of the stress test, was considered for analysis. Data corresponding to decline part of the pressure time plot was imported in SAS and the same procedure used for water wells was followed to obtain stabilized value of RMS. Stabilized value of RMS indicates that data points corresponding to open fracture segment was removed completely and the fit corresponding to only the closed fracture segment has been obtained. Table 7.2 shows the results obtained from SAS. Figure 7.4 shows the RMS graph for the stress test that was done on Canadian gas well # 2. RMS starts to stabilize after 8th minute and stabilizes completely at 12th minute.

Table 7.2.Example table showing output from SAS for in-situ stress test

1	2	3	4	5	6	7	8	9	10
Obs	**t**	**n**	**P**	**P Mod**	**Error**	**SQ Error**	**CUM SQ Error**	**RMSE**	**MAN Time**
1	2.2	1	5496.13	5449.36	46.7656	2187	2187.02	.	0
2	2.3	2	5490.27	5445.1	45.1723	2040.5	4227.56	.	0.05
3	2.3	3	5477.79	5439.5	38.296	1466.6	5694.14	.	0.117
4	2.3	4	5473.22	5436.7	36.5186	1333.6	7027.75	83.832	0.15
5	2.4	5	5462.16	5431.17	30.9881	960.26	7988.01	63.198	0.217
6	2.4	6	5456.63	5428.42	28.2138	796.02	8784.03	54.111	0.25
7	2.5	7	5448.19	5422.97	25.2174	635.92	9419.94	48.528	0.317
8	2.6	8	5440.52	5418.91	21.6045	466.75	9886.7	44.467	0.367

Table 7.2.Example table showing output from SAS for in-situ stress test (cont.)

9	2.6	9	5436.69	5416.22	20.4622	418.7	10305.4	41.444	0.4
10	2.7	10	5427.78	5410.91	16.8687	284.55	10589.95	38.895	0.467
11	2.7	11	5422.28	5406.94	15.3404	235.33	10825.28	36.785	0.517
12	2.7	12	5417.21	5404.31	12.8981	166.36	10991.64	34.947	0.55
13	2.8	13	5408.89	5399.1	9.7887	95.82	11087.46	33.298	0.617
14	2.8	14	5405.49	5396.52	8.9705	80.47	11167.93	31.863	0.65
15	2.9	15	5398.75	5392.65	6.1017	37.23	11205.16	30.558	0.7
16	3.0	16	5394.05	5388.83	5.2174	27.22	11232.38	29.394	0.75
17	3.0	17	5389.54	5385.05	4.4938	20.19	11252.57	28.351	0.8
18	3.1	18	5380.94	5380.03	0.9029	0.82	11253.39	27.39	0.867
19	3.1	19	5379.37	5377.54	1.8345	3.37	11256.76	26.525	0.9
20	3.2	20	5370.84	5372.6	-1.7559	3.08	11259.84	25.736	0.967
21	3.2	21	5367.25	5368.92	-1.6664	2.78	11262.62	25.014	1.017

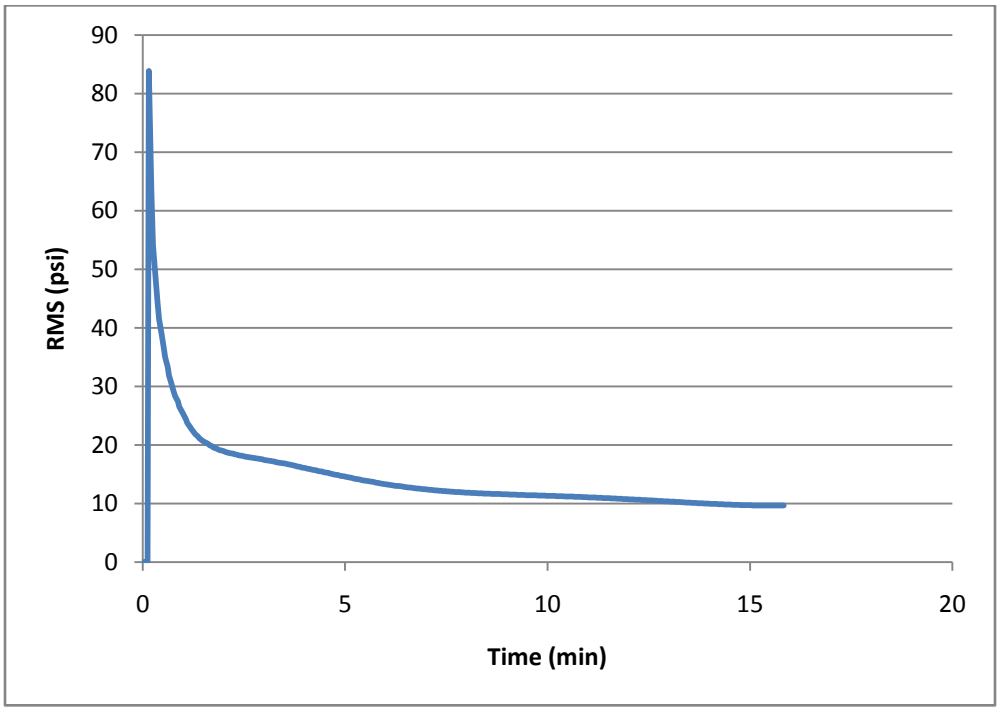

Figure 7.4.RMS graph for stress test on Canadian gas well # 2

Figure 7.5 shows the modeled curve for stress test. The modeled curve starts to deviate from the recorded one at a pressure value of around 5400 psi. Modeled curve extrapolates on Y axis to give upper bound on closure pressure value. This value is around 5675 psi.

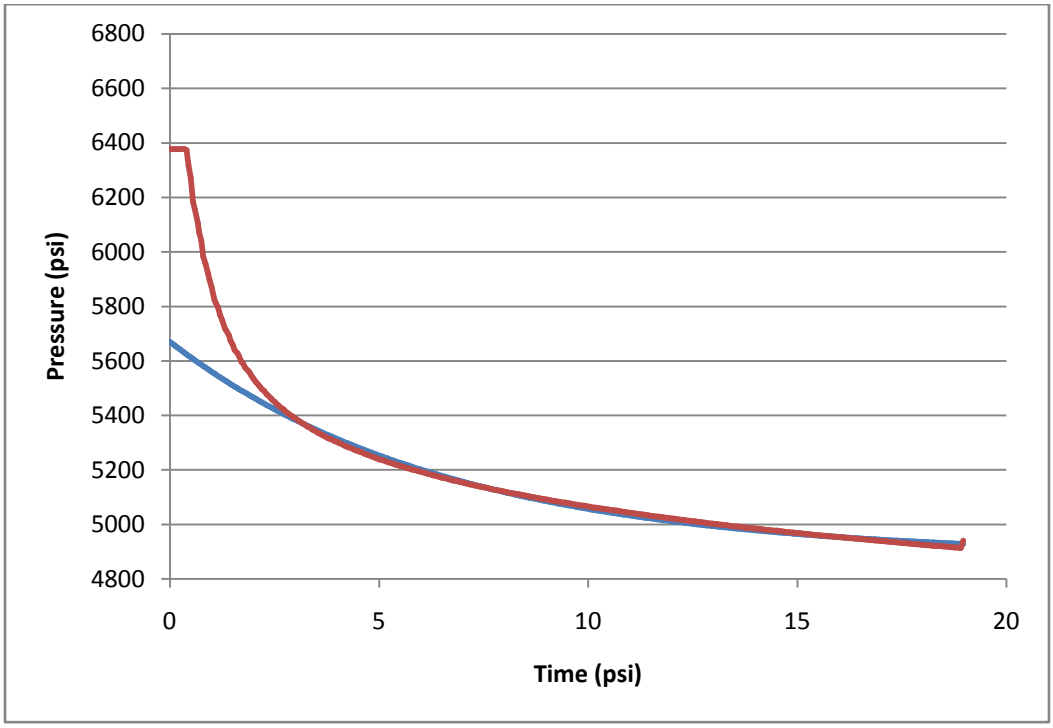

Figure 7.5.Modeled curve (blue) extrapolated to Y axis for stress test

Similar analysis was done on data obtained from the minifrac test. As stated before, data pertaining to second pressurization cycle was taken under consideration for

analysis purpose. Because large data was analyzed, output from SAS showing simulated results is not shown here. Figure 7.6 shows the matched curve for digitally recorded curve. Modeled curve (red) starts from to deviate at around 4750 psi and it extrapolates to a value of around 5300 psi. These are lower bounds and upper bounds on closure pressure values obtained from minifrac test.

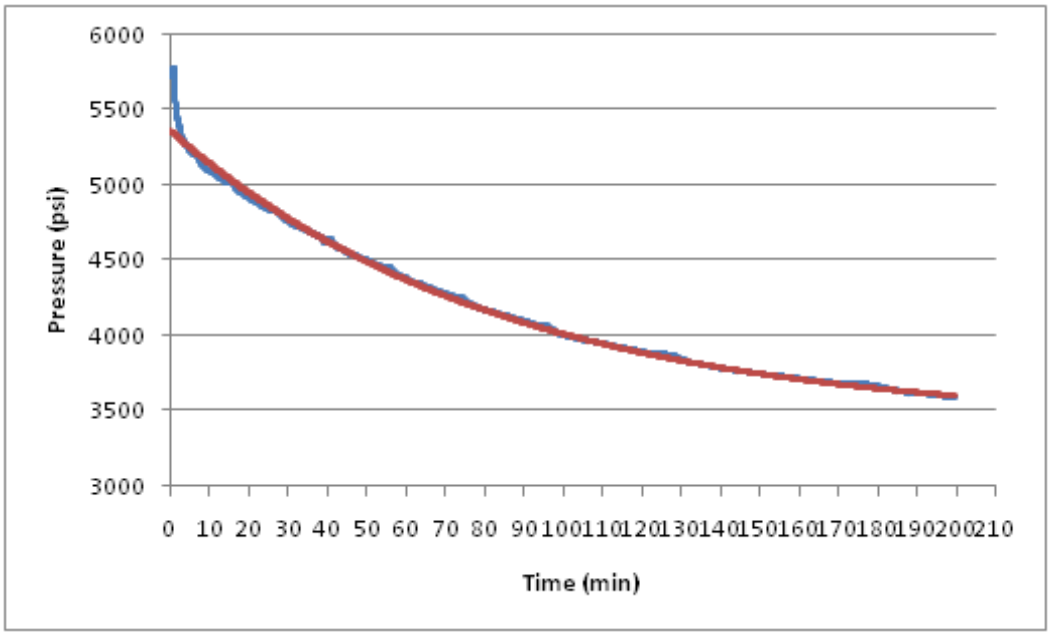

Figure 7.6.Modeled curve extrapolated to Y axis for minifrac test

8. RESULTS AND DISCUSSION

All the 10 intervals in CU Exploratory well # 1 were analyzed, for closure pressures, using statistical method as well as using square root of time plot analysis and results were obtained. Table 8.1 summarizes the results for closure pressures for 10 intervals in CU Exploratory well # 1 calculated using statistical analysis and StimPlan.

Table 8.2 summarizes the results obtained for stress test and minifrac test conducted on Canadian gas well # 2.

Table 8.1.Results showing closure pressures obtained for different intervals using statistical analysis and StimPlan analysis (Water Well)

Interval	Depth (ft)	Statistical Analysis		Square Root of Time Analysis
		Pc (et) (psi)	Pc (lt) (psi)	(psi)
Interval 8	1795	1799	1600	1627
Interval 7	1864.7	2001	1952	1718
Interval 6	1880.3	1701	1643	1647
Interval 5	1942.3	1700	1621	1571
Interval 4	1995	1094	1069	1064
Interval 10	2013	-	-	-
Interval 3	2022	1062	1040	1047
Interval 2	2065	1236	1186	1154
Interval 9	2084.3	1688	1542	1668
Interval 1	2102	1784	1409	1580

Table 8.2.Results showing closure pressures obtained for different tests using statistical analysis and StimPlan analysis (Gas Well)

Test	Statistical Analysis		Square Root Time analysis
	Pc (et) (psi)	Pc (lt) (psi)	(psi)
In-situ stress test	5670	5448	5634.9
Minifrac test	5300	4750	4632.36

As can be seen from Table 8.1, statistically determined value of closure stress Pc(et) yields a value for closure stress, which is consistently close to the value obtained from square root of time analysis. In water well domain, there is a little difference in results. However, for the gas well analysis there is a nearly 200 psi difference between the statistically determined closure stress and the value determined from the square root of time plot. The value obtained from statistical procedure for P_c appears to be greater in oil/gas well domain.

As previously stated, in order to implement the nlin procedure, the data should be non linear and it must have an exponential decline pattern. However, decline curve for interval 10 did not exhibit exponential pressure decay. Therefore it could not be analyzed using nlin procedure and results could not be obtained.

9. CONCLUSION

In this study, statistical analysis and it's applicability to determine closure stress was studied. The study included a comparison of closure stress using a standard square rot of time plot and a statistical approach in which Non Linear Regression Analysis was carried out. The data used for this study was from the to CU project Exploratory Well # 1, which is a water well drilled in Lamotte and Reagan sandstone formations. The data from Canadian gas well # 2 was also used for comparing the oil/ gas domain to the water well domain.

In CU exploratory well, all the intervals showed good results using NLRA except for interval 10, for which results could not be obtained because of non-exponential nature of the decline. Closure pressures obtained for each interval was in a range of ± 100 psi of the square root time analysis results. In Canadian gas well, NLRA results obtained for in-situ stress test were in good agreement with the square root time analysis results, indicating there is greater applicability for the statistical method in the oil/gas well domain. For a minifrac test conducted in same formation, NLRA gave closure stress value which was comparable with closure stress obtained from in-situ stress test. However square root time analysis results for a minifrac test were ambiguous and were in no close proximity of the results obtained from NLRA.

There are few limitations about the study. The program used for the analysis of data was case specific. It was only built for an exponential pressure decay model. Also, the method used here can be applied only for the determination of closure stress. Other fracturing parameters such as fracture re-opening pressure, fracture extension pressure

could not be determined using this (exponential pressure decay) method. This does not mean that statistical approach cannot be used for determining these parameters and should be considered as a future work for this study. The approach taken in this study can be taken as a reference and other methods can be applied to analyze the data statistically. Further work is also recommended for developing the program which would do successive iterations on its own for getting the best possible fit.

Statistical analysis is a handy tool for the objective determination of closure stress. Along with all the graphical methods that are used in the industry today, statistical analysis should be given an equal consideration as it can become a powerful method to determine the closure stress objectively.

APPENDIX A

STIMPLAN ANALYSIS, DIGITALLY RECORDED CURVES AND MODELED CURVES

Interval 8

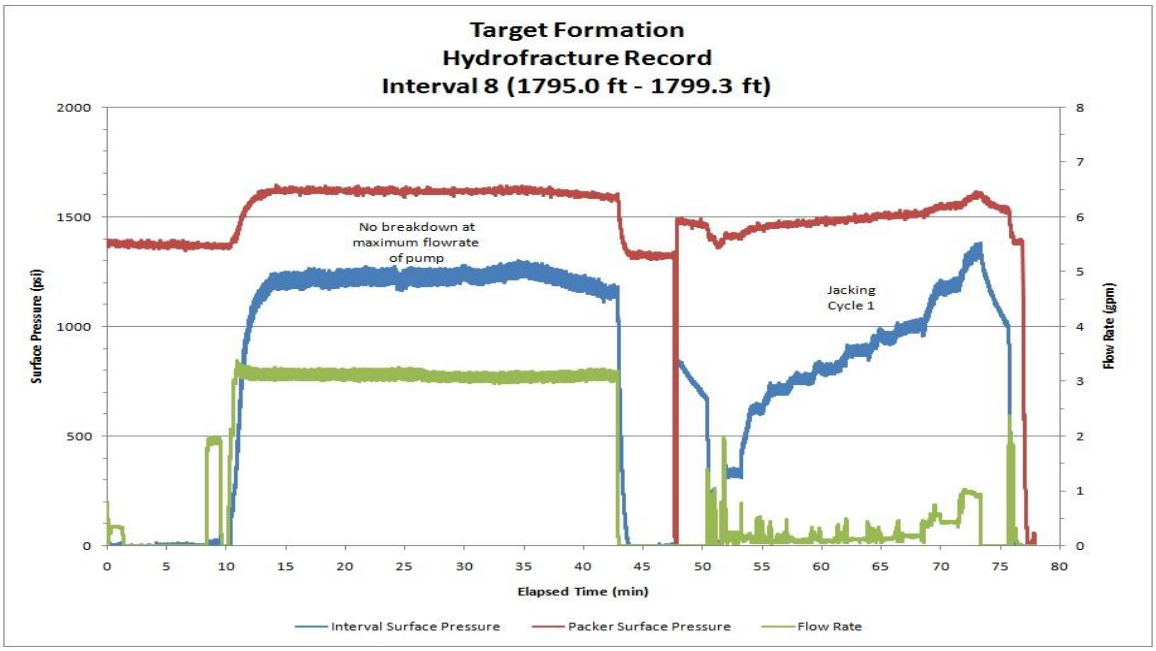

Hydrofrac and Hydrojack Pressure Test for Interval 8 (1795.0 ft – 1799.3 ft)

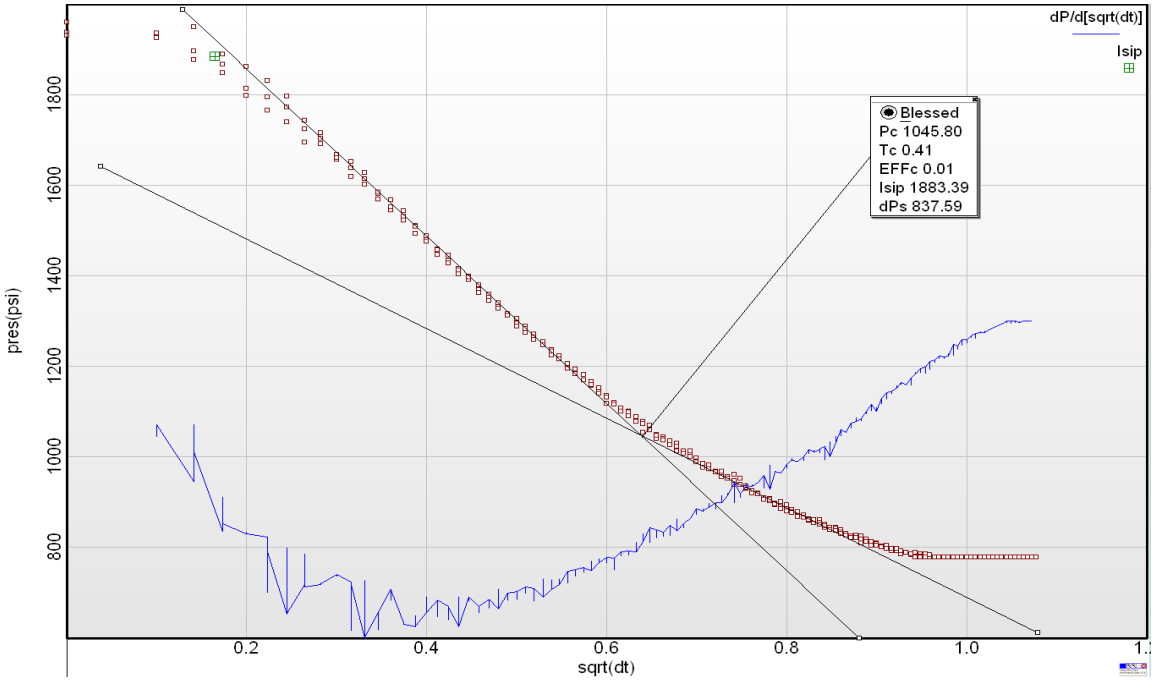

Square Root Time Plot for Interval 8 (1795.0 ft – 1799.3 ft)

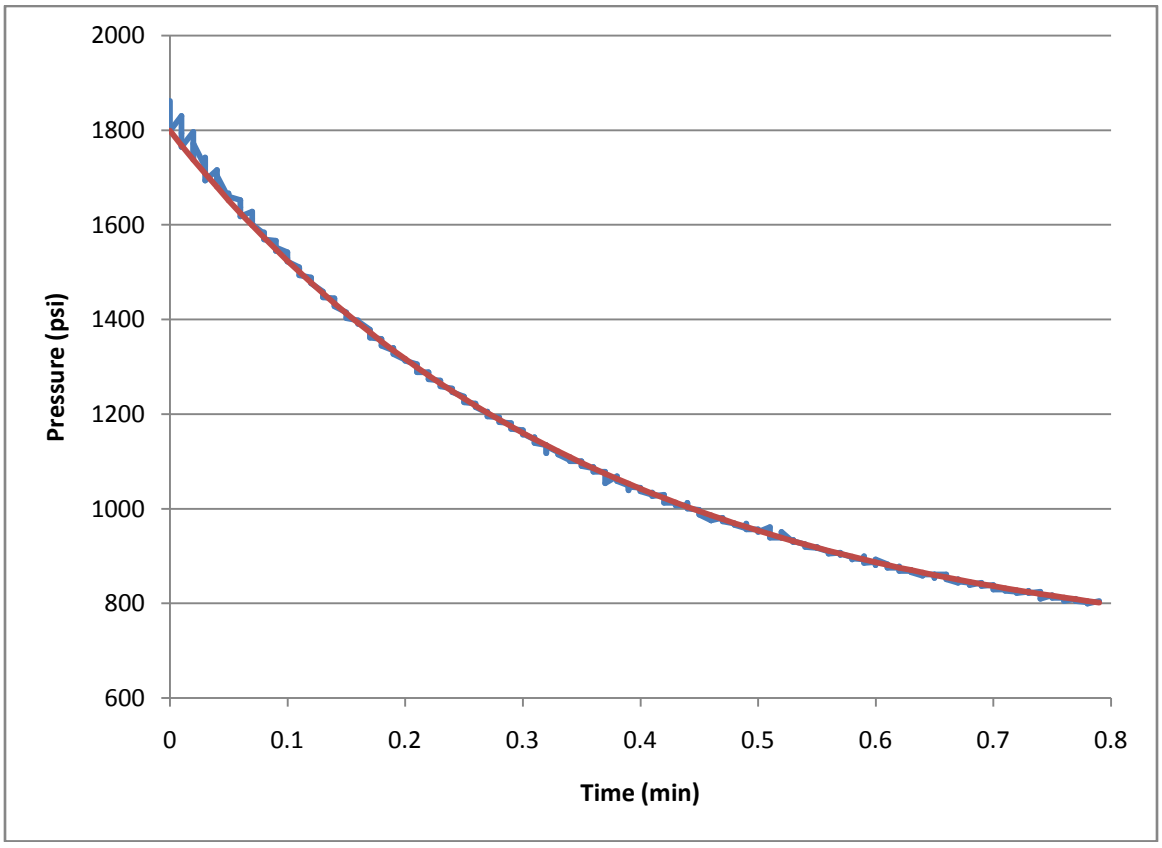

Digitally recorded and modeled curve for interval 8 (1795.0 ft – 1799.3 ft)

Interval 7

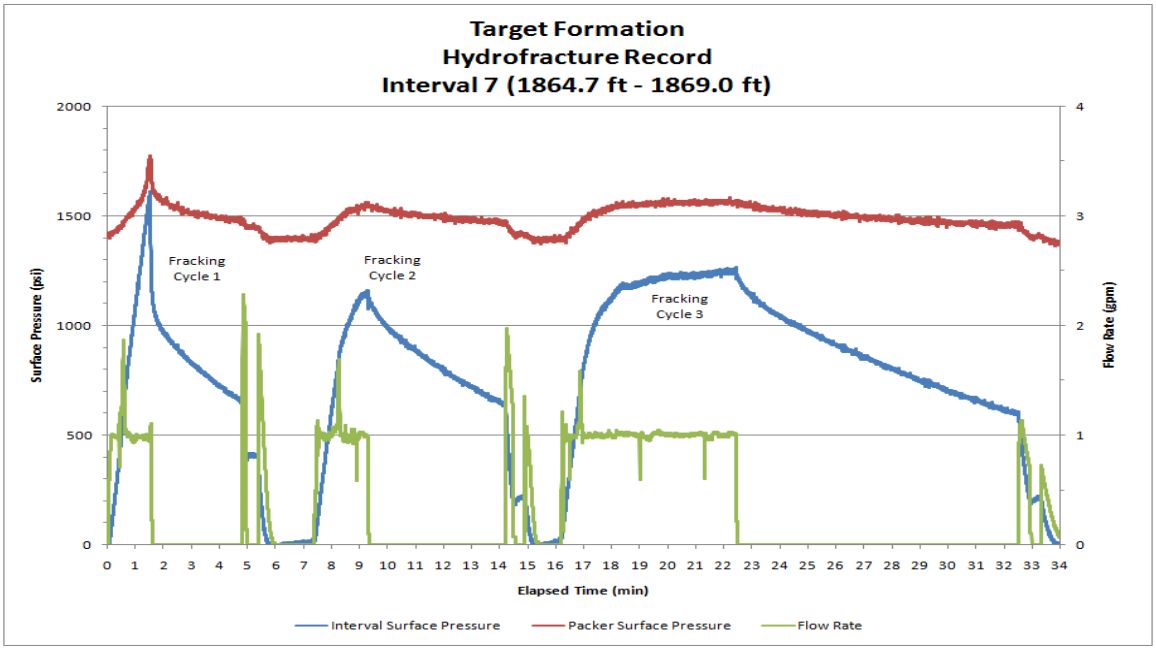

Hydrofrac Pressure Test for Interval 7 (1864.7 ft – 1869.0 ft)

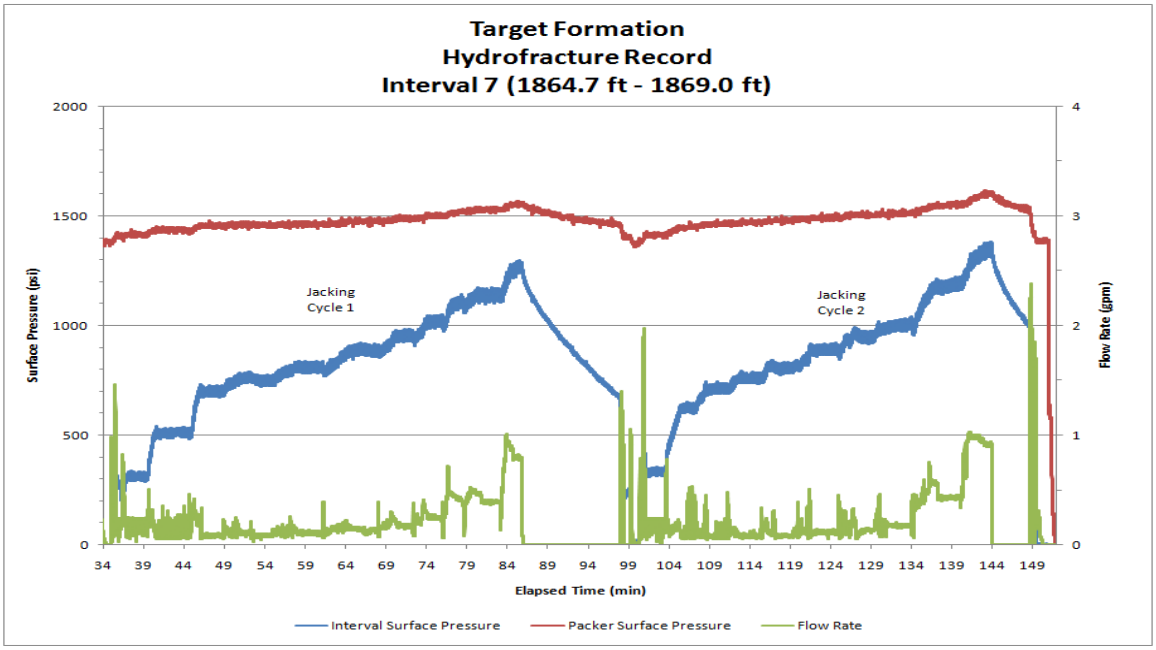

Hydrojack Pressure Test for Interval 7 (1864.7 ft – 1869.0 ft)

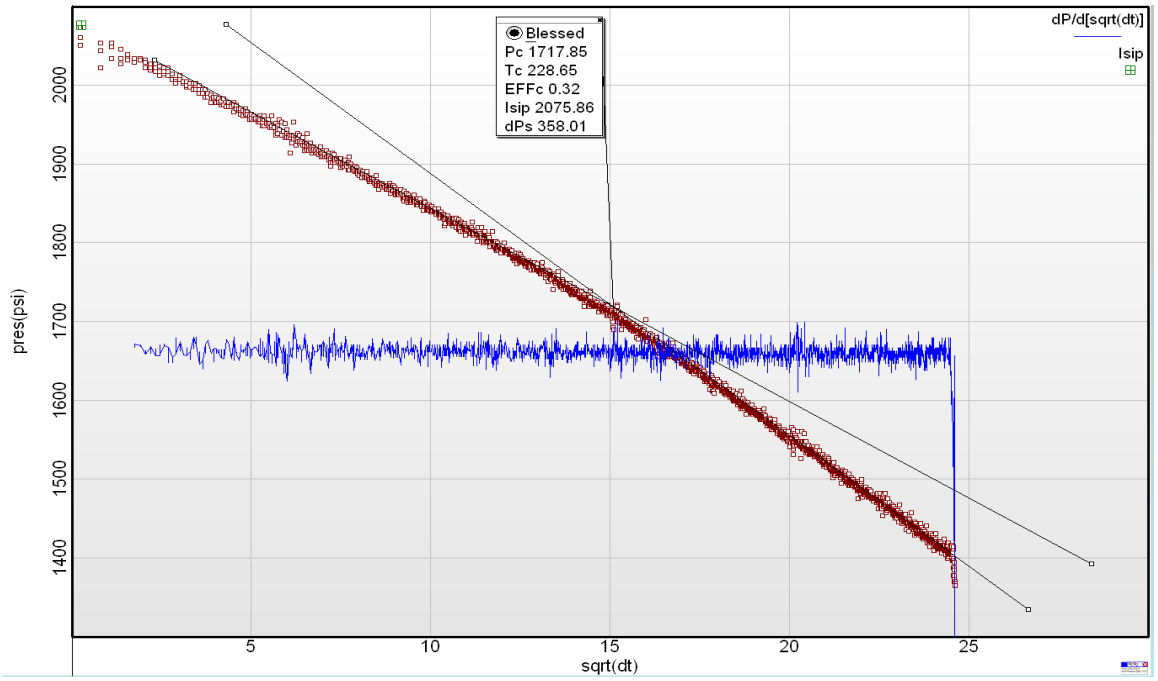

Square Root Time Plot for Interval 7 (1864.7 ft – 1869.0 ft)

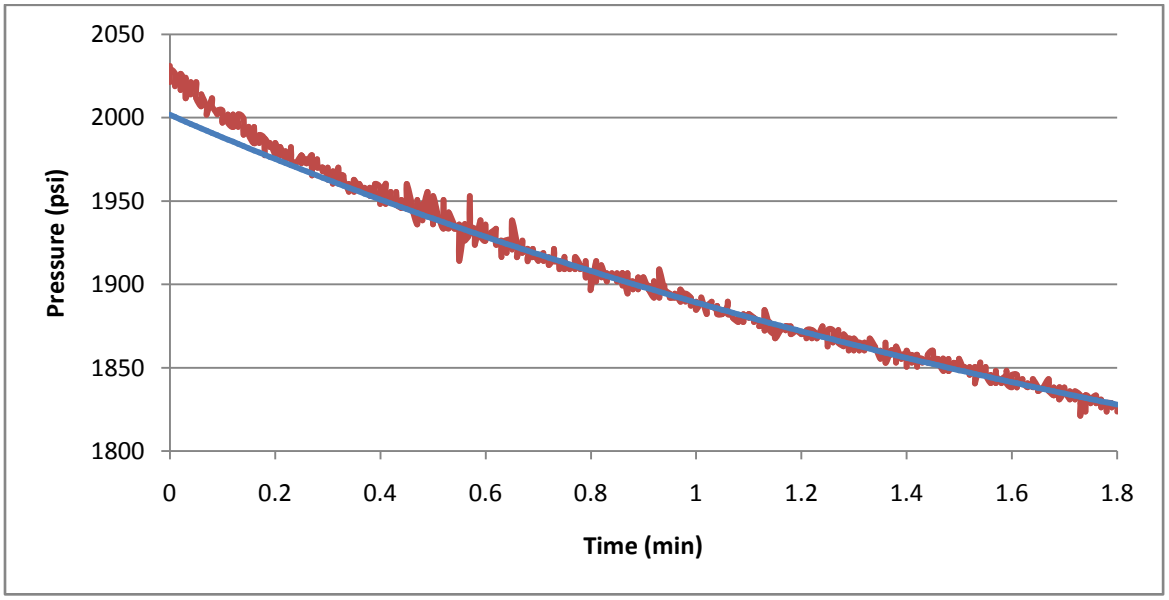

Digitally recorded and modeled curve for interval 7 (1864.7 ft – 1869.0 ft)

Interval 6

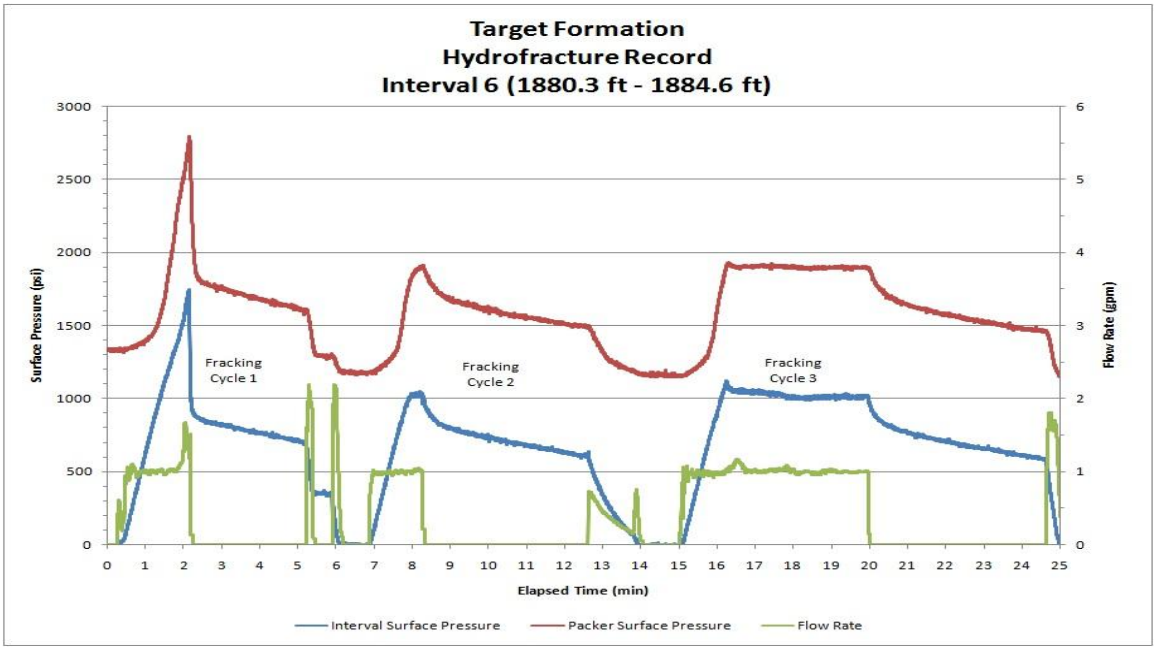

Hydrofrac Pressure Test for Interval 6 (1880.3 ft – 1884.6 ft)

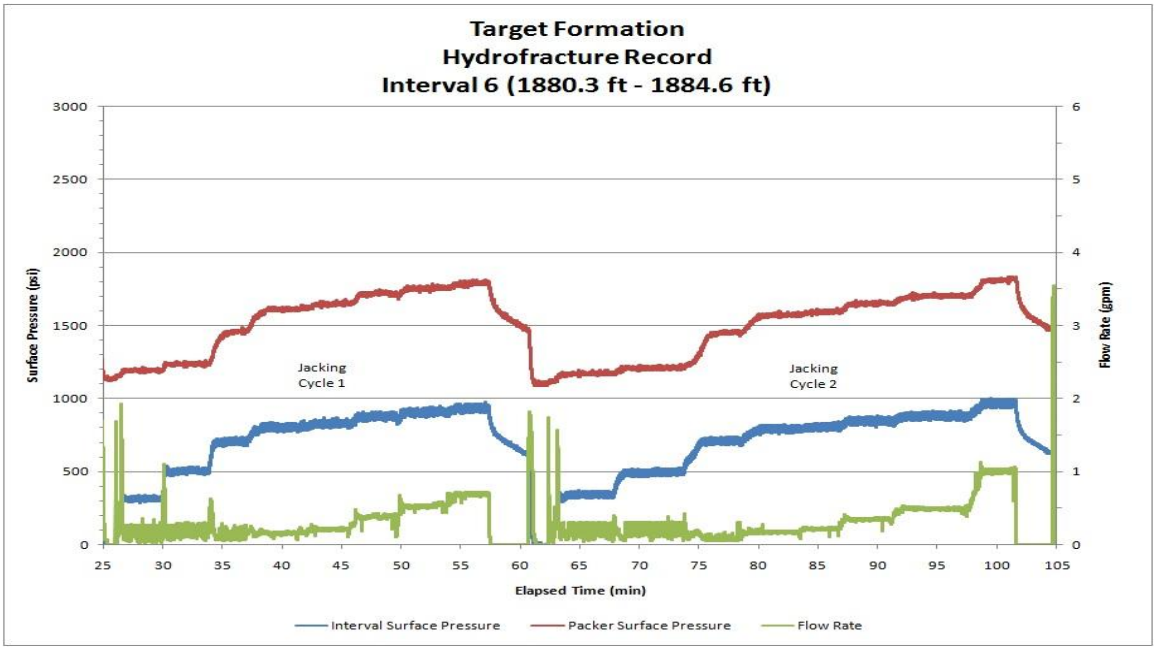

Hydrojack Pressure Test for Interval 6 (1880.3 ft – 1884.6 ft)

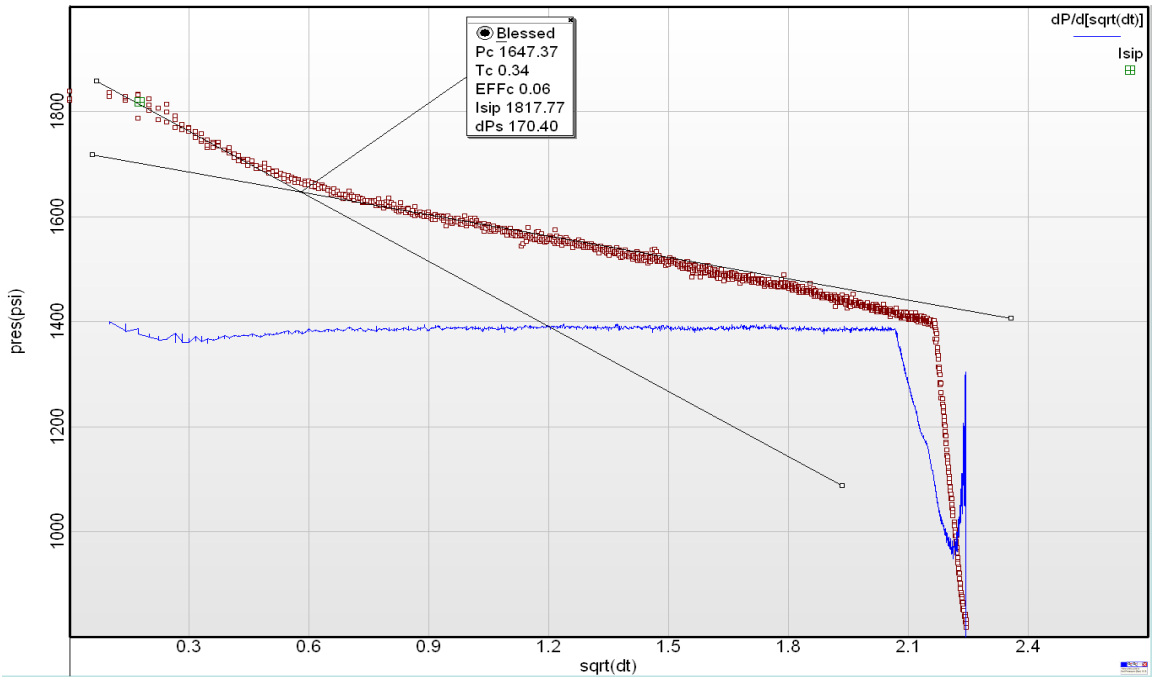

Square Root Time Plot for Interval 6 (1880.3 ft – 1884.6 ft)

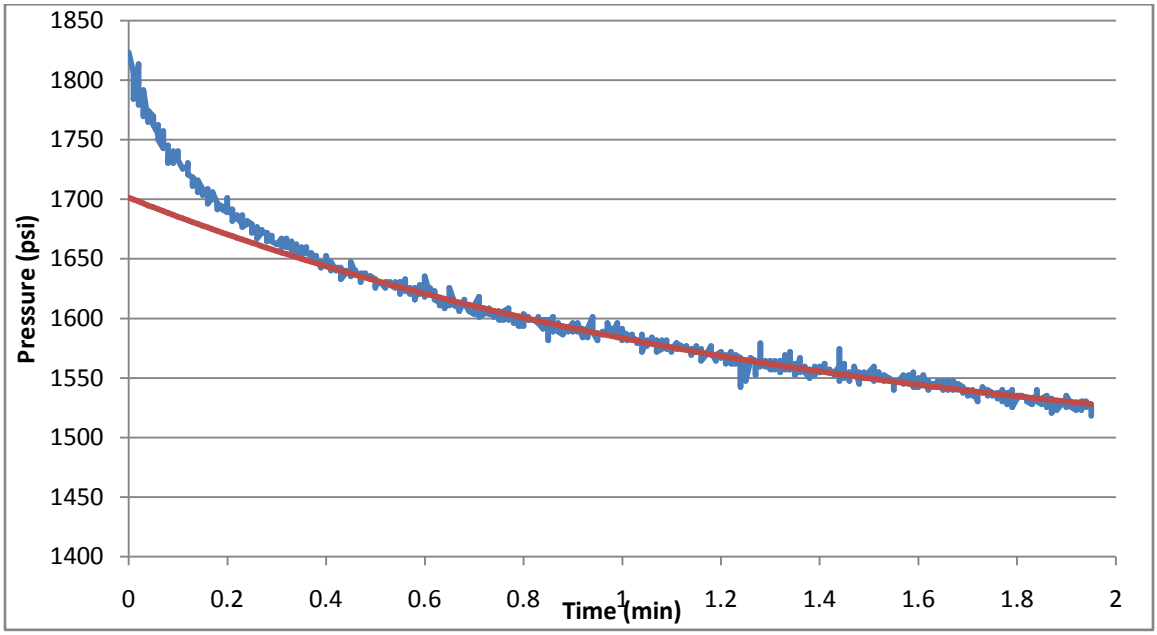

Digitally recorded and modeled curve for interval 6 (1880.3 ft – 1884.6 ft)

Interval 5

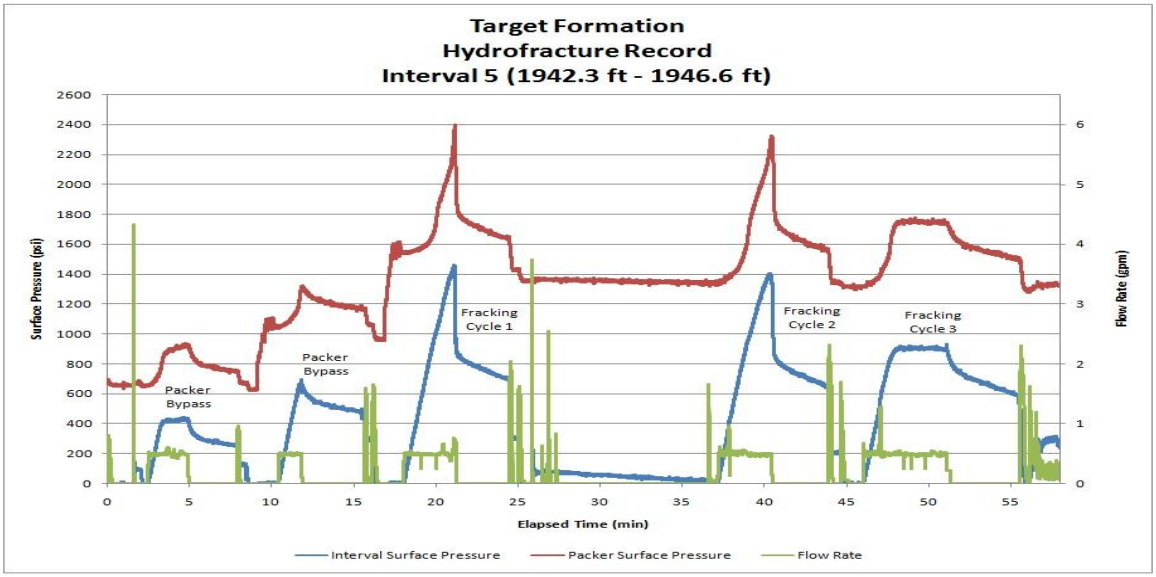

Hydrofrac Pressure Test for Interval 5 (1942.3 ft – 1946.6 ft)

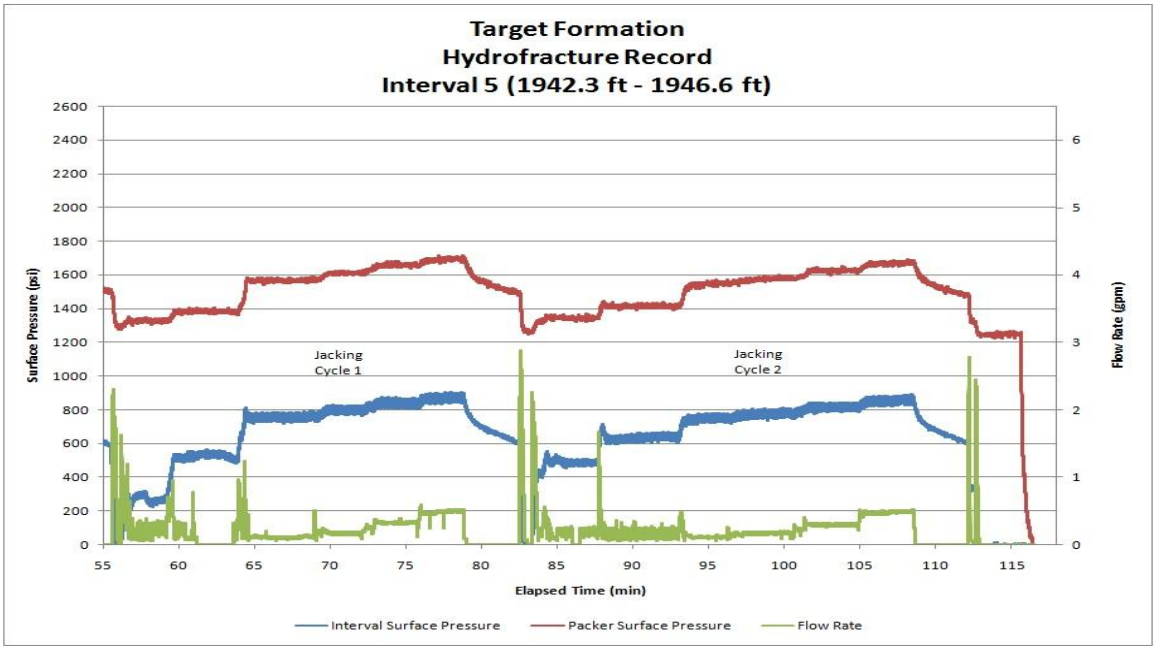

Hydrojack Pressure Test for Interval 5 (1942.3 ft – 1946.6 ft)

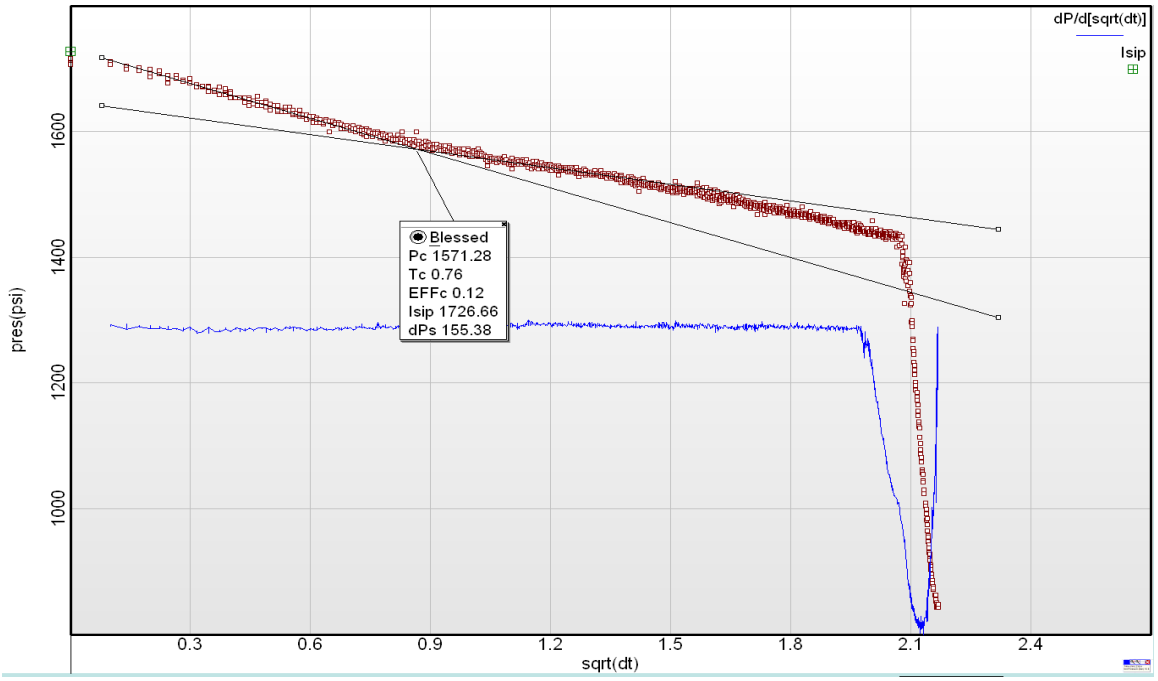

Square Root Time Plot for Interval 5 (1942.3 ft – 1946.6 ft)

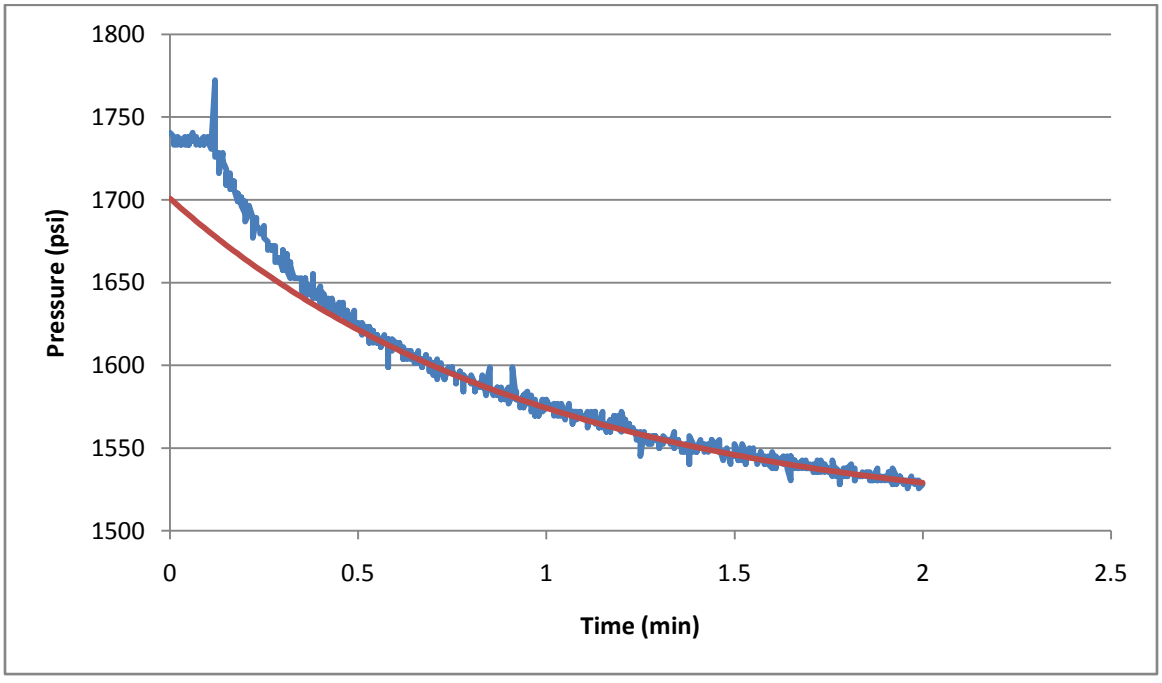

Digitally recorded and modeled curve for interval 5

(1942.3 ft – 1946.6 ft)

Interval 4

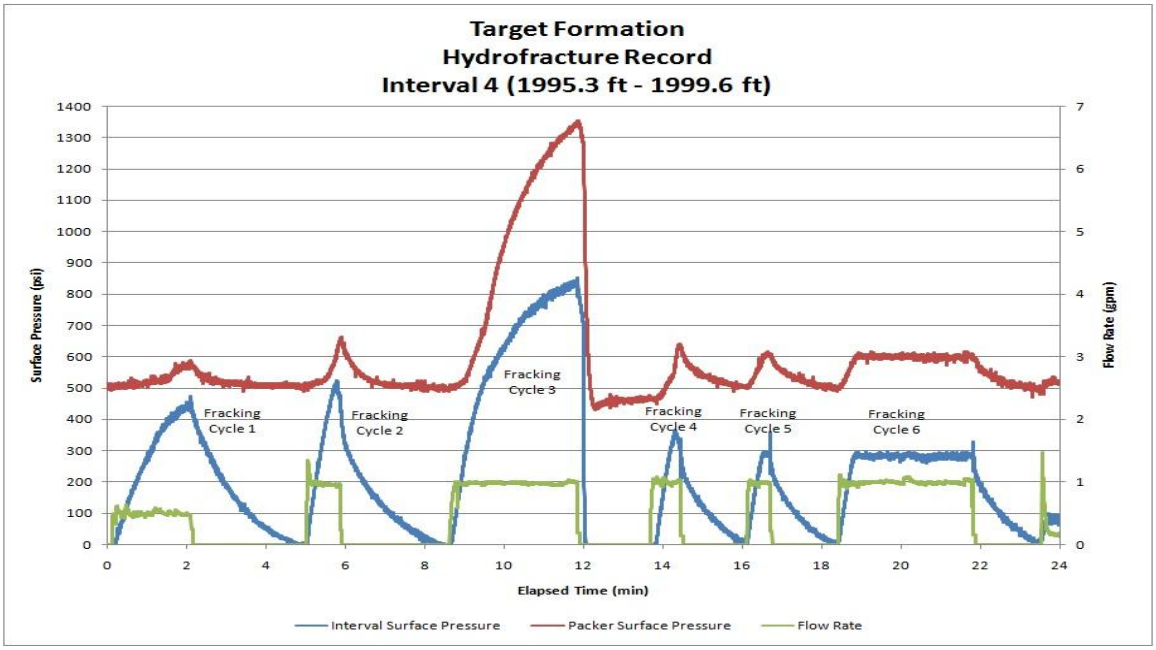

Hydrofrac Pressure Test for Interval 4 (1995.3 ft – 1996.3 ft)

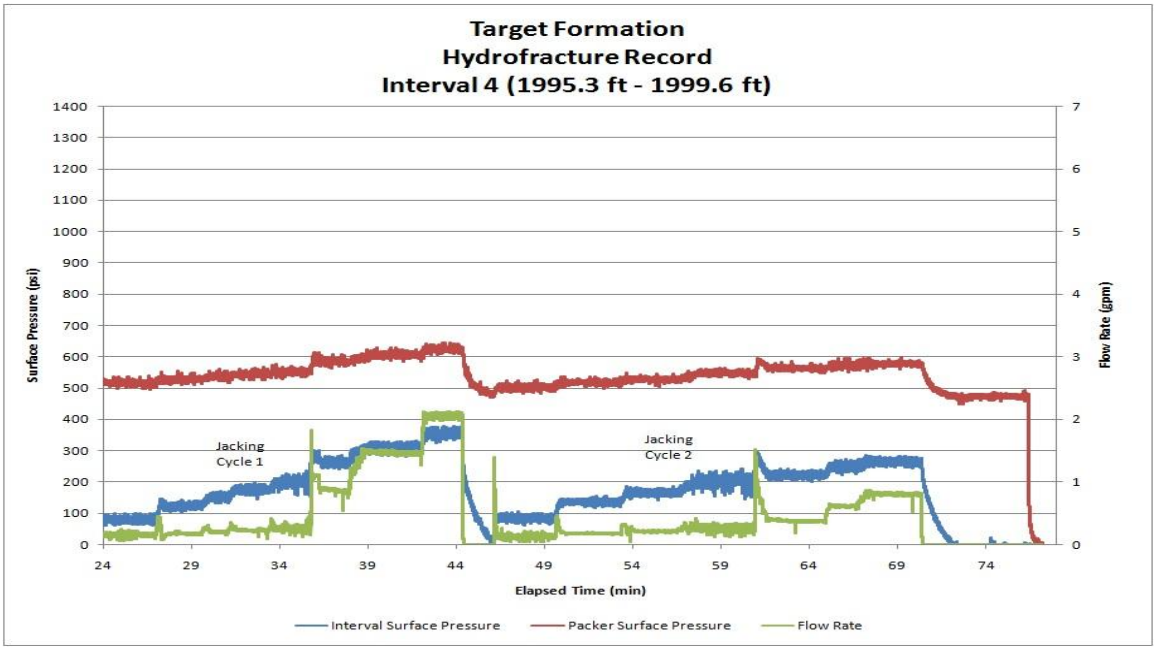

Hydrojack Pressure Test for Interval 4 (1995.3 ft – 1996.3 ft)

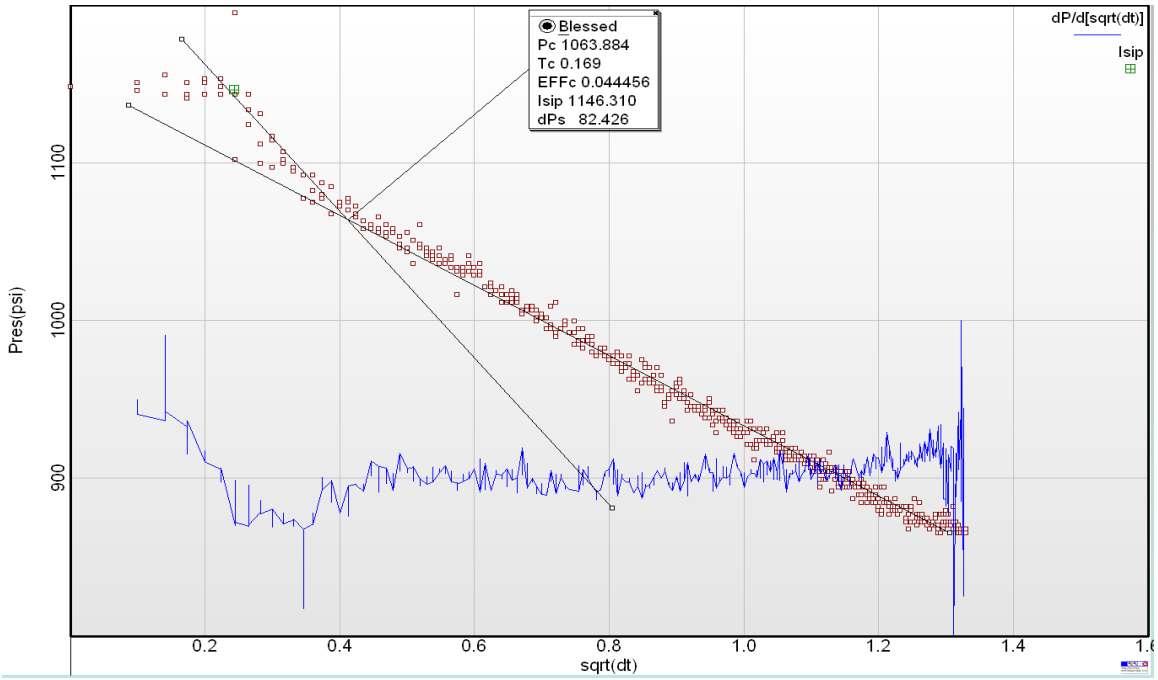

Square Root Time Plot for Interval 4 (1995.3 ft – 1999.6 ft)

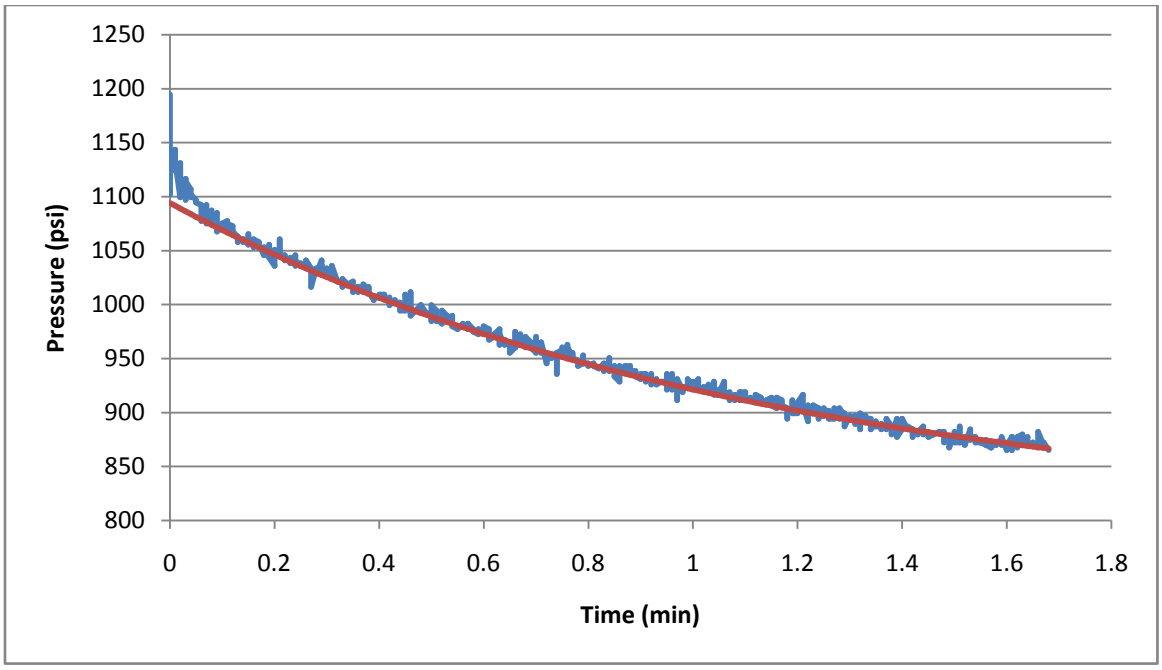

Digitally recorded and modeled curve for interval 4

(1995.3 ft – 1999.6 ft)

Interval 10

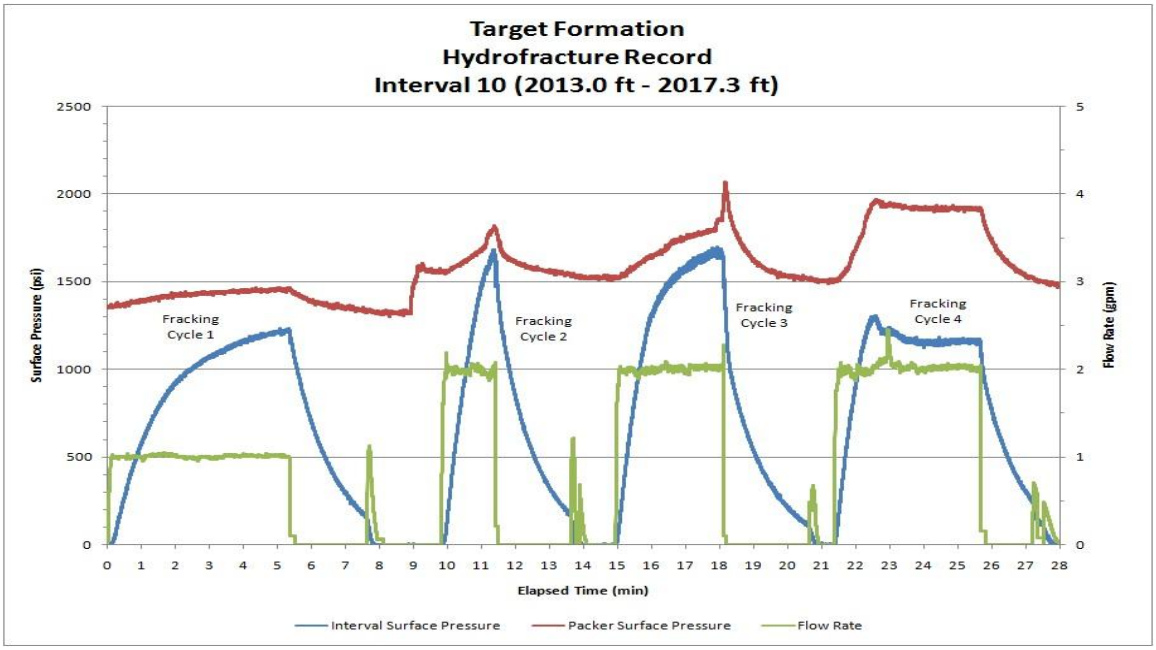

Hydrofrac Pressure Test for Interval 10 (2013.0 ft – 2017.3 ft)

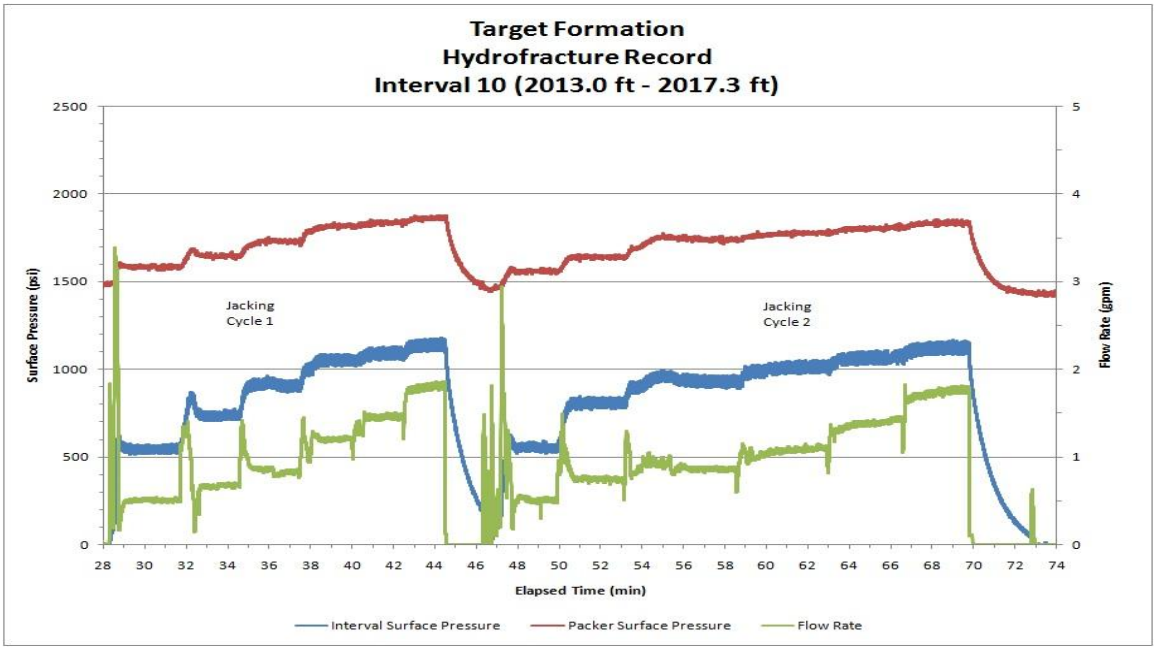

Hydrojack Pressure Test for Interval 10 (2013.0 ft – 2017.3 ft)

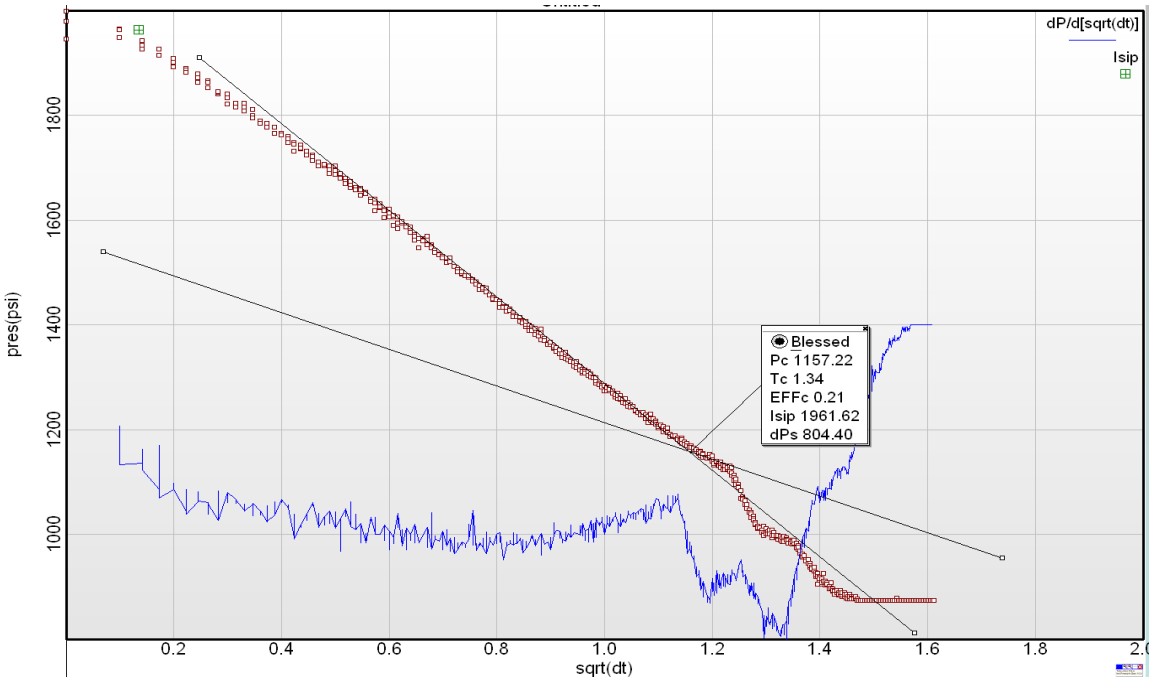

Square Root Time Plot for Interval 10 (2013.0 ft – 2017.3 ft)

Interval 3

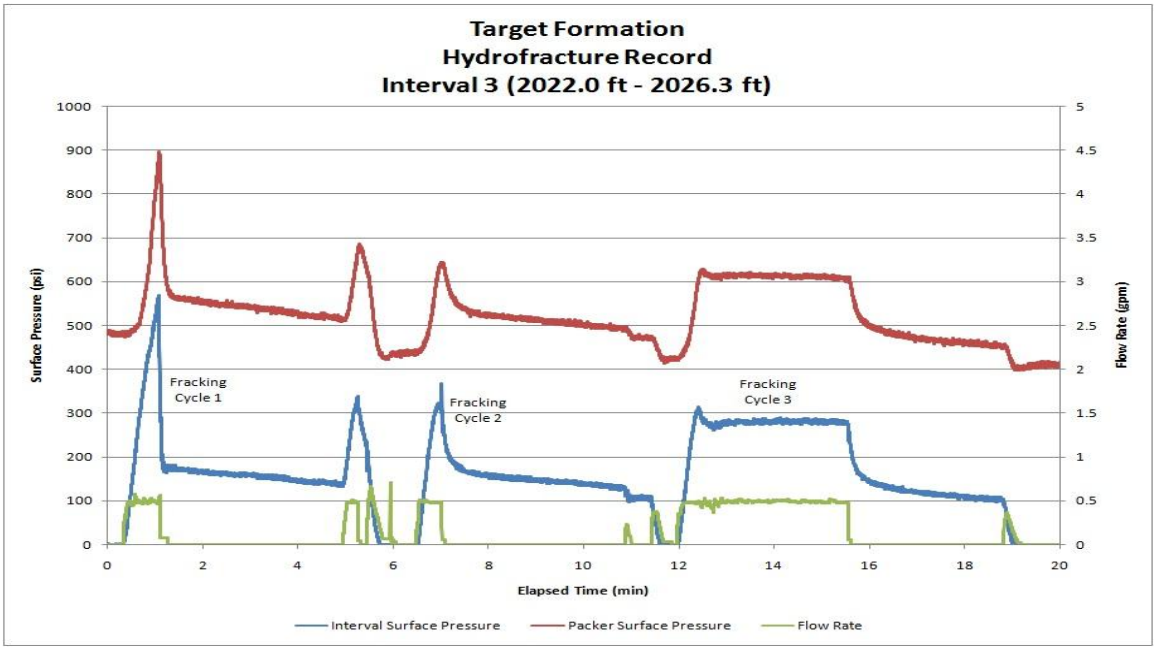

Hydrofrac Pressure Test for Interval 3 (2022.0 ft – 2026.3ft)

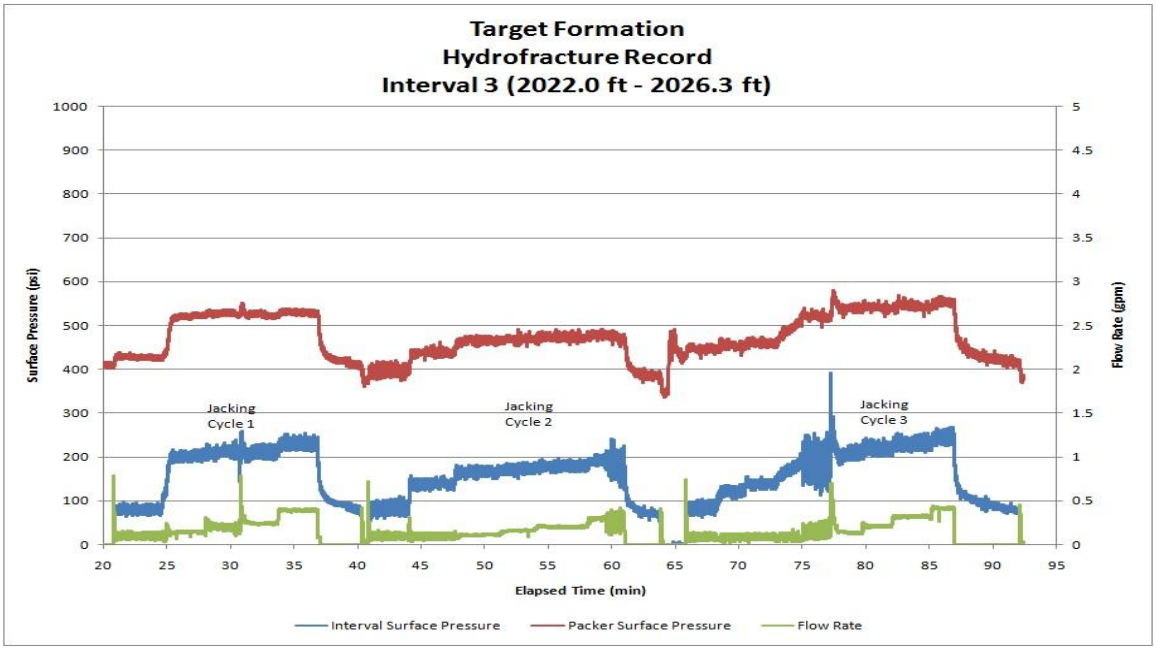

Hydrojack Pressure Test for Interval 3 (2022.0 ft – 2026.3ft)

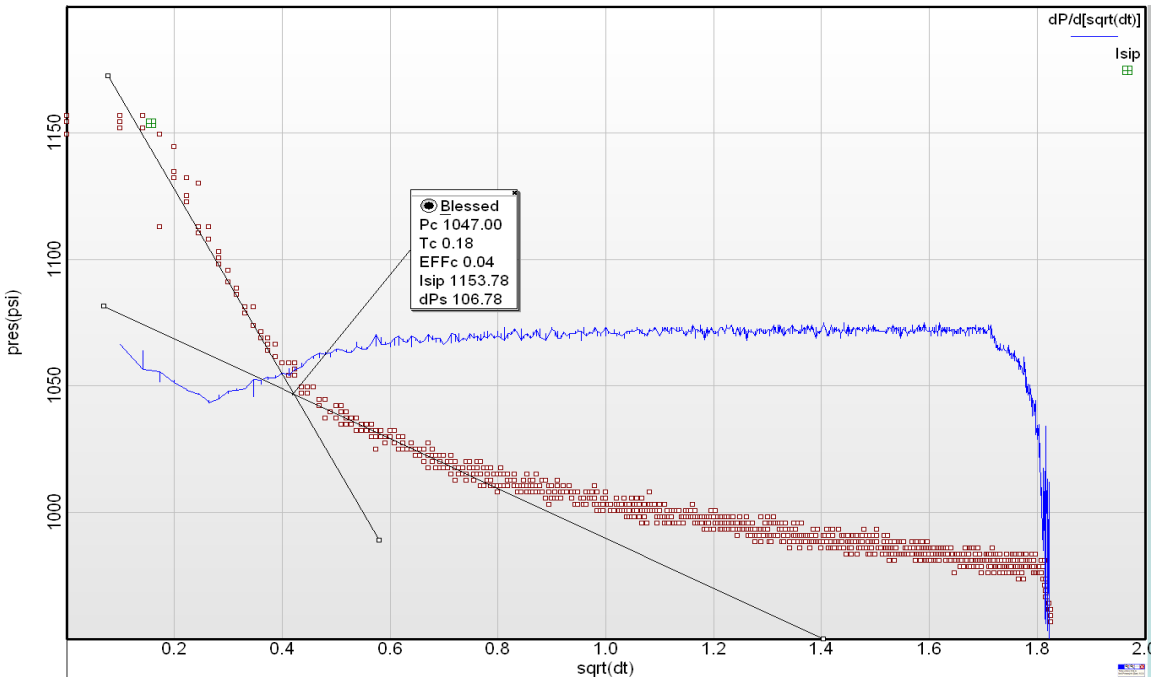

Square Root Time Plot for Interval 3 (2022.0 ft – 2026.3 ft)

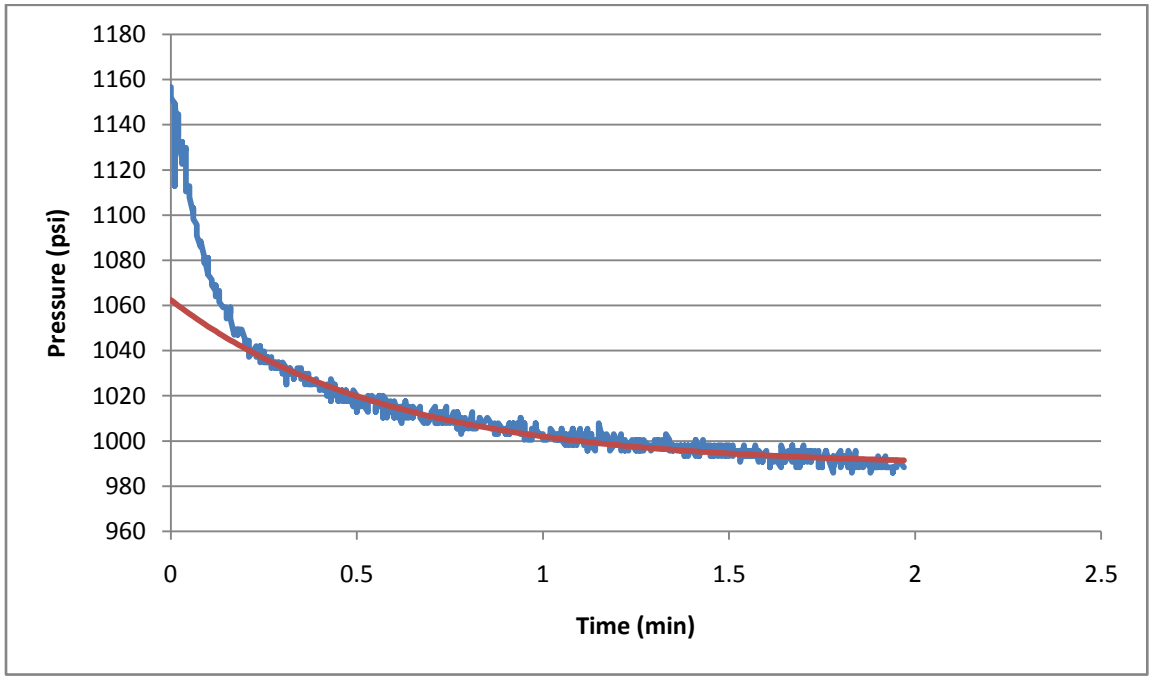

Digitally recorded and modeled curve for interval 3

(2022.0 ft – 2026.3 ft)

Interval 2

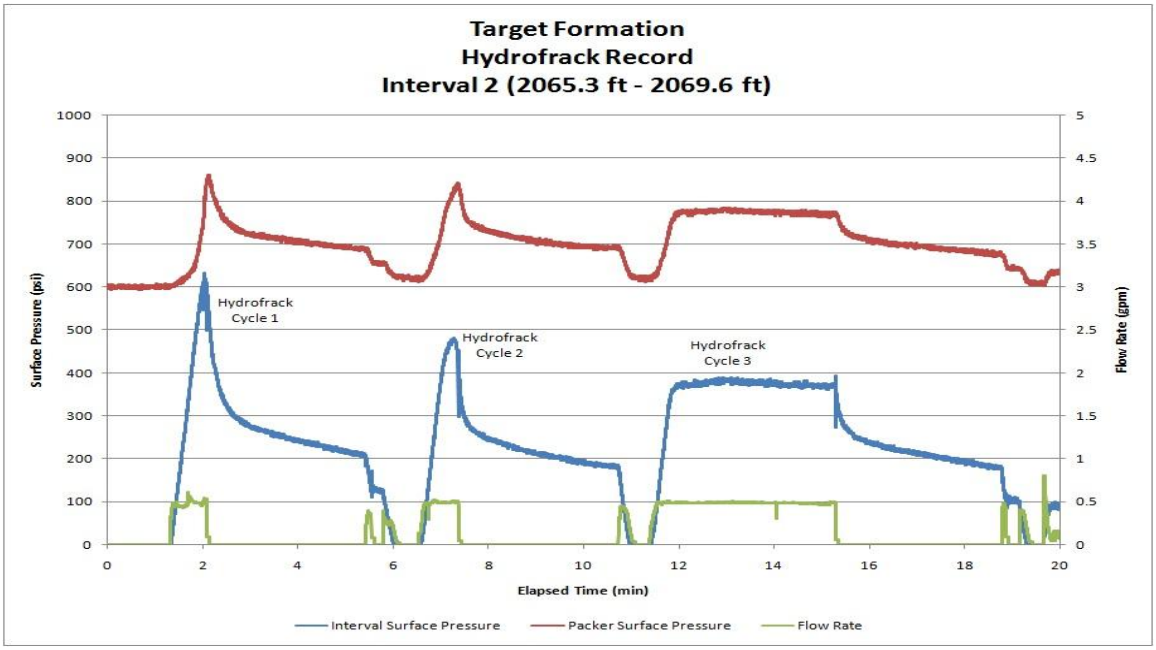

Hydrofrac Pressure Test for Interval 2 (2065.3ft – 2069.6ft)

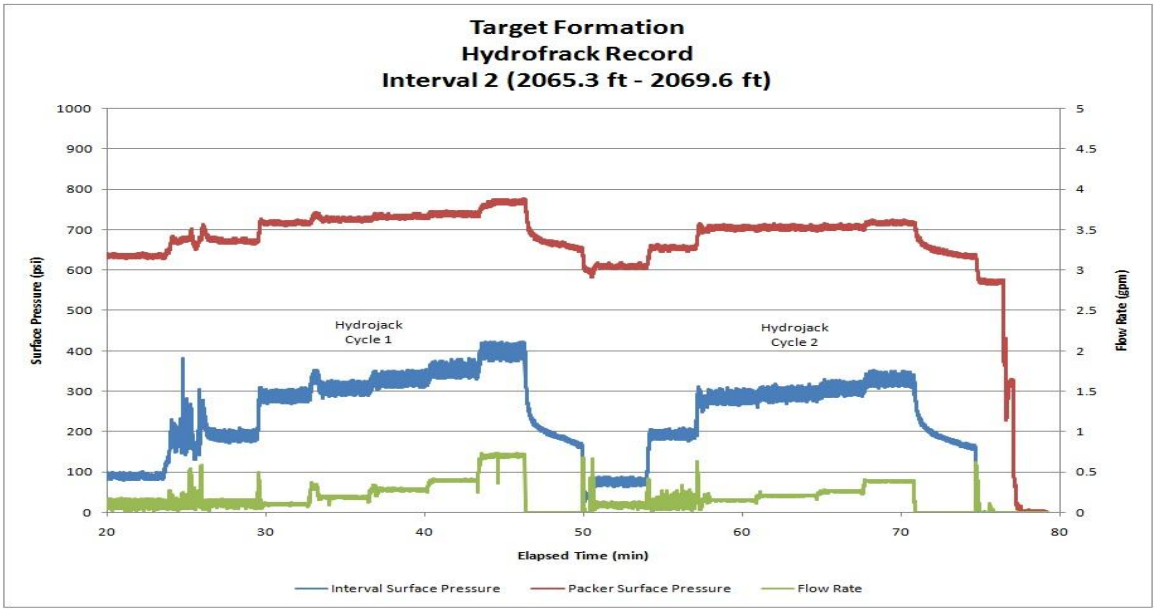

Hydrojack Pressure Test for Interval 2 (2065.3ft – 2069.6ft)

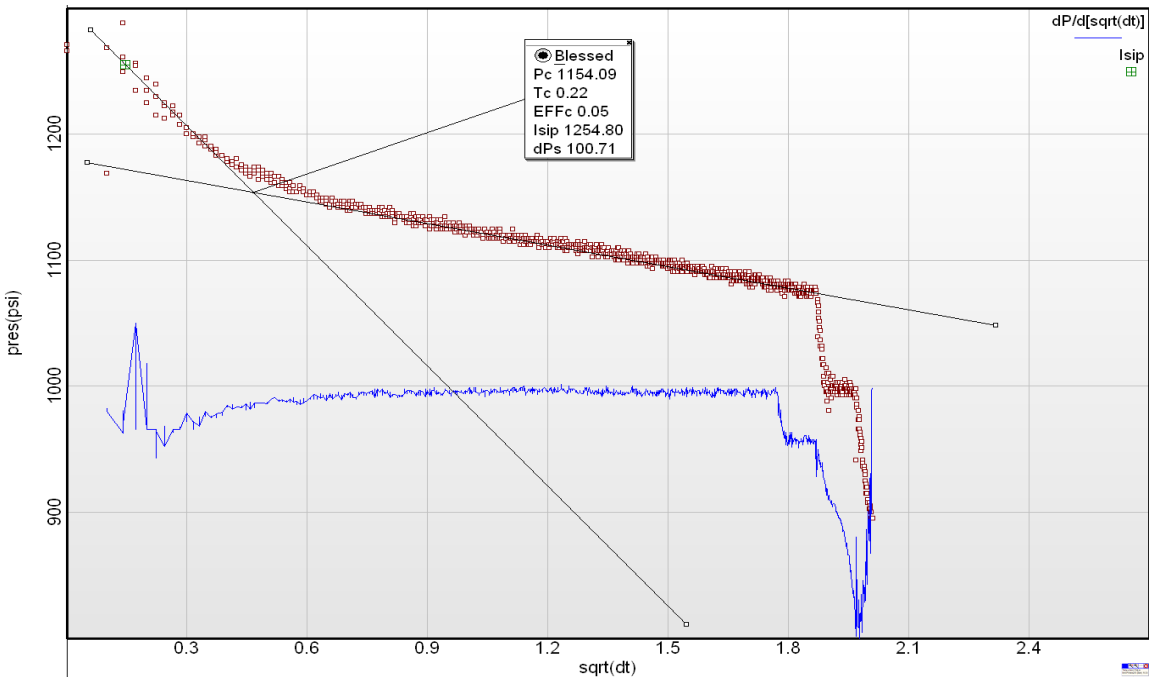

Square Root Time Plot for Interval 2 (2065.3 ft – 2069.6 ft)

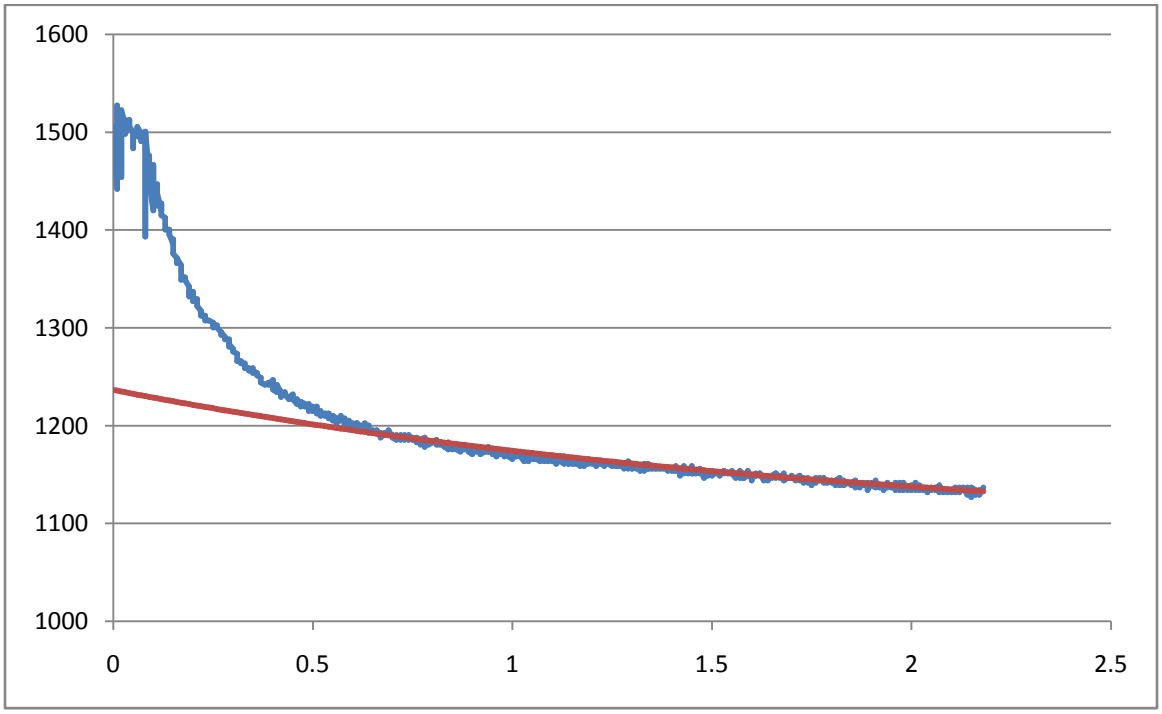

Digitally recorded and modeled curve for interval 2

(2065.3 ft – 2069.5 ft)

Interval 1

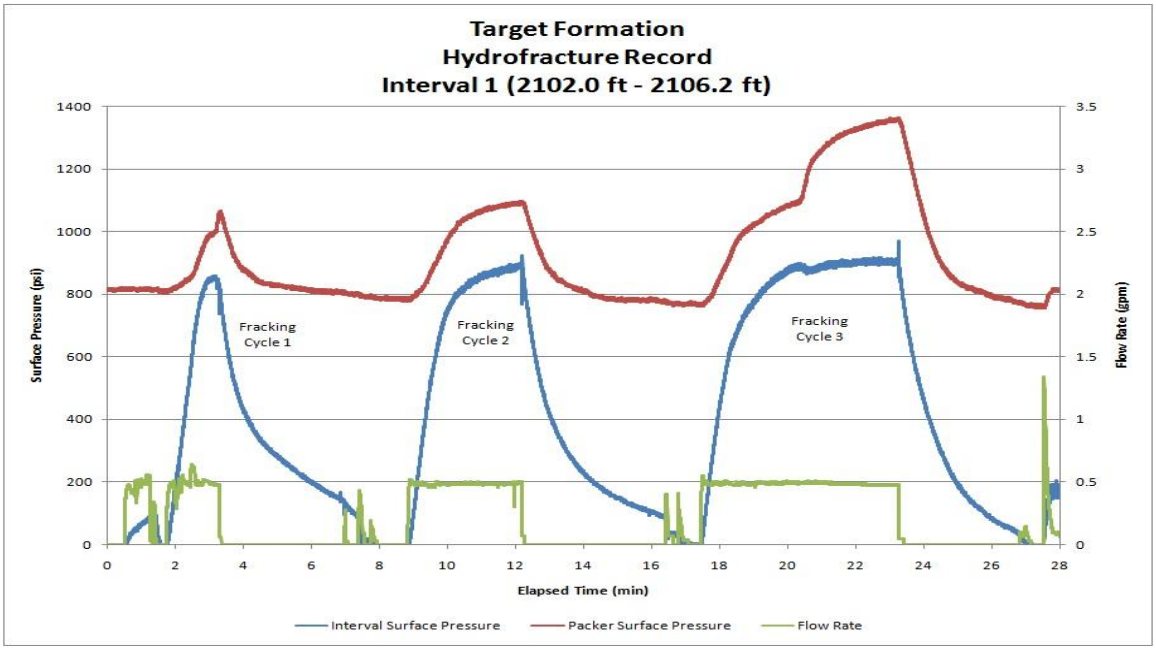

Hydrofrac Pressure Test for Interval 1 (2102.0 ft – 2106.2 ft)

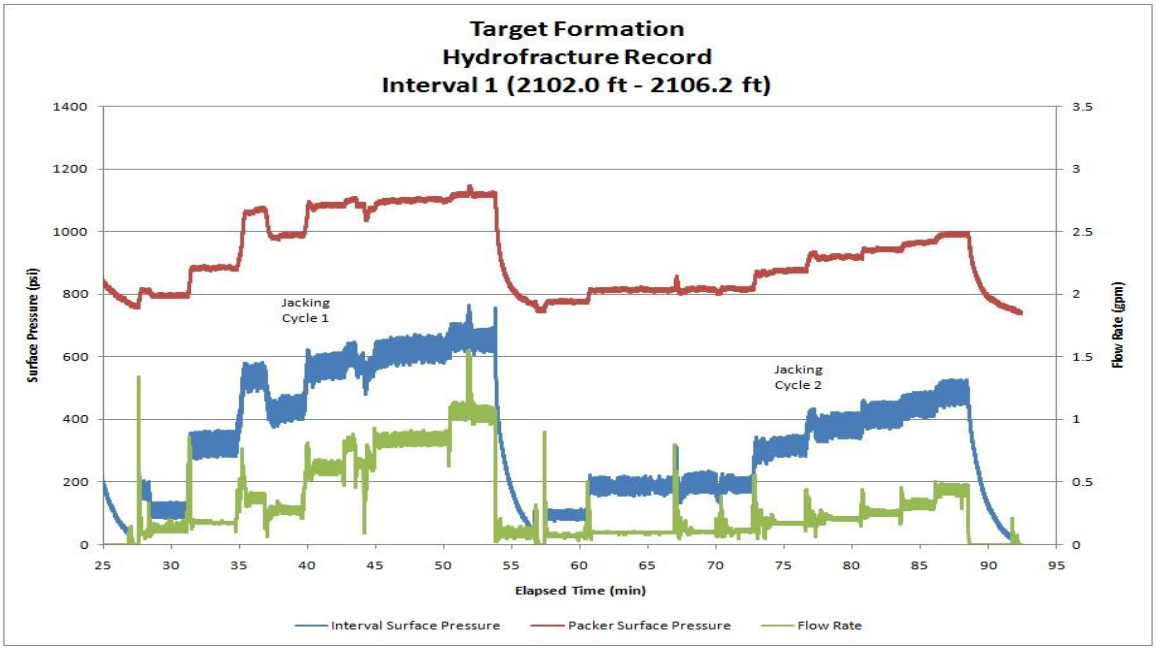

Hydrojack Pressure Test for Interval 1 (2102.0 ft – 2106.2 ft)

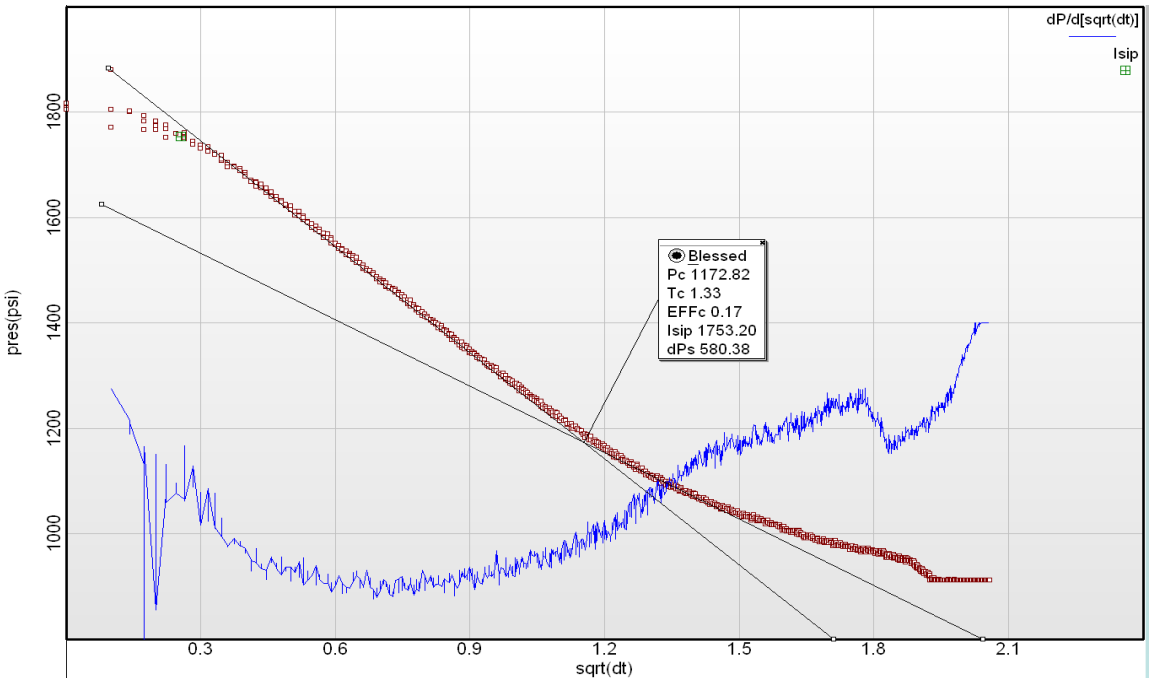

Square Root Time Plot for Interval 1 (2102.0 ft – 2106.2 ft)

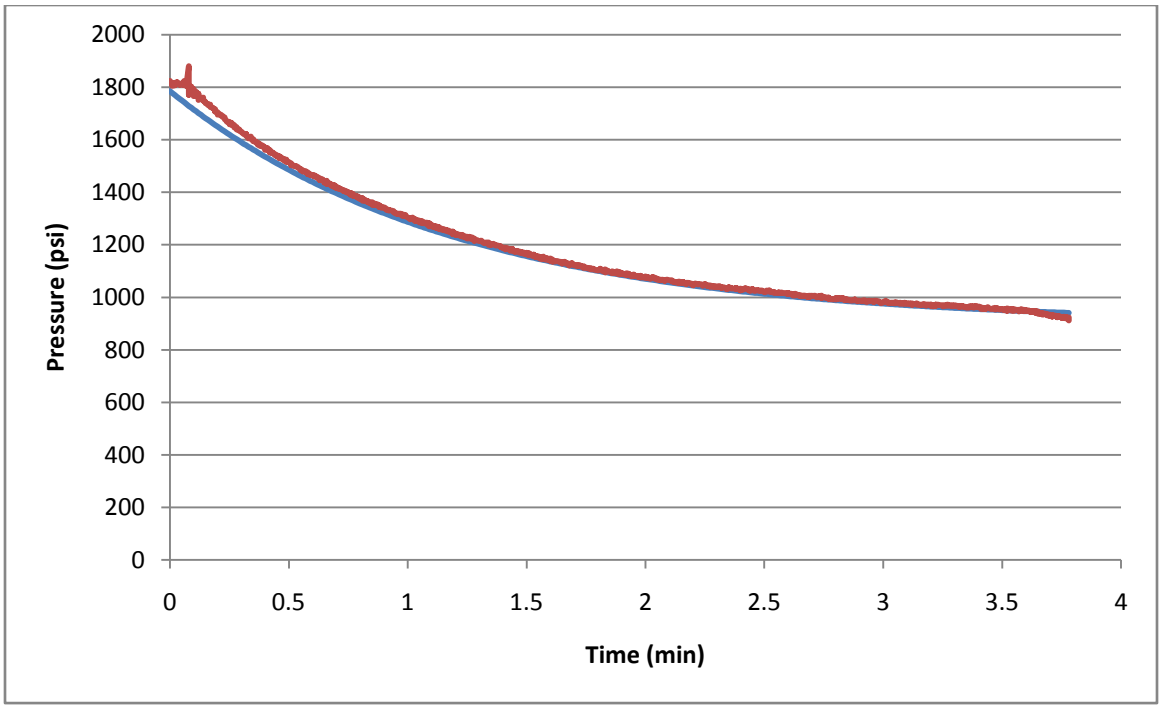

Digitally recorded and modeled curve for interval 1

(2102.0 ft – 2106.2 ft)

APPENDIX B

OUTPUT TABLES FROM SAS

Table showing output from SAS for interval 9 (2084.3ft – 2088.6ft)

1	2	3	4	5	6	7	8	9	10
Obs	**t**	**n**	**P**	**P Mod**	**Error**	**SQ Error**	**CUM SQ Error**	**RMSE**	**MAN Time**
1	.	1	.	.	.	.	0	0	0
2	17.95	2	1549.97	1544.03	5.9393	35.275	35.28	.	0
3	17.95	3	1547.53	1544.03	3.4979	12.235	47.51	.	0
4	17.95	4	1542.65	1544.03	-1.385	1.918	49.43	7.0306	0
5	17.96	5	1545.09	1541.61	3.4819	12.123	61.55	5.5476	0.01
6	17.96	6	1547.53	1541.61	5.9234	35.086	96.64	5.6756	0.01
7	17.96	7	1542.65	1541.61	1.0405	1.083	97.72	4.9427	0.01
8	17.97	8	1537.77	1539.2	-1.4326	2.052	99.77	4.4671	0.02
9	17.97	9	1530.44	1539.2	-8.7568	76.682	176.46	5.423	0.02
10	17.97	10	1545.09	1539.2	5.8916	34.711	211.17	5.4924	0.02
11	17.98	11	1537.77	1536.8	0.9614	0.924	212.09	5.1489	0.03
12	17.98	12	1535.32	1536.8	-1.48	2.19	214.28	4.8795	0.03
13	17.98	13	1542.65	1536.8	5.8442	34.155	248.44	4.9843	0.03
14	17.99	14	1532.88	1534.43	-1.5429	2.38	250.82	4.7751	0.04
15	17.99	15	1537.77	1534.43	3.3399	11.155	261.97	4.6724	0.04
16	17.99	16	1532.88	1534.43	-1.5429	2.38	264.35	4.5094	0.04
17	18	17	1537.77	1532.06	5.703	32.524	296.88	4.6049	0.05
18	18	18	1535.32	1532.06	3.2616	10.638	307.51	4.5278	0.05
19	18	19	1530.44	1532.06	-1.6212	2.628	310.14	4.4027	0.05
20	18.01	20	1537.77	1529.71	8.0507	64.813	374.96	4.6964	0.06
21	18.01	21	1530.44	1529.71	0.7265	0.528	375.48	4.5673	0.06
22	18.01	22	1532.88	1529.71	3.1679	10.035	385.52	4.5045	0.06
23	18.02	23	1528	1527.38	0.6175	0.381	385.9	4.3926	0.07
24	18.02	24	1532.88	1527.38	5.5003	30.253	416.15	4.4516	0.07
25	18.02	25	1525.56	1527.38	-1.8239	3.327	419.48	4.3666	0.07
26	18.03	26	1528	1525.07	2.9348	8.613	428.09	4.3142	0.08
27	18.03	27	1518.23	1525.07	-6.8308	46.66	474.75	4.4476	0.08
28	18.03	28	1530.44	1525.07	5.3762	28.903	503.66	4.4885	0.08
29	18.04	29	1518.23	1522.76	-4.5286	20.508	524.16	4.49	0.09
30	18.04	30	1525.56	1522.76	2.7956	7.815	531.98	4.4388	0.09
31	18.04	31	1520.68	1522.76	-2.0872	4.356	536.34	4.3766	0.09
32	18.05	32	1520.68	1520.48	0.2	0.04	536.38	4.3007	0.1
33	18.05	33	1520.68	1520.48	0.2	0.04	536.42	4.2285	0.1
34	18.05	34	1518.23	1520.48	-2.2414	5.024	541.44	4.1792	0.1
35	18.06	35	1520.68	1518.2	2.4724	6.113	547.55	4.1366	0.11
36	18.06	36	1523.12	1518.2	4.9138	24.146	571.7	4.1622	0.11
37	18.06	37	1515.79	1518.2	-2.4104	5.81	577.51	4.1214	0.11

38	18.07	38	1520.68	1515.95	4.7301	22.374	599.88	4.14	0.12
39	18.07	39	1513.35	1515.95	-2.5941	6.729	606.61	4.1049	0.12
40	18.07	40	1515.79	1515.95	-0.1527	0.023	606.63	4.0491	0.12
41	18.08	41	1515.79	1513.7	2.0902	4.369	611	4.0099	0.13
42	18.08	42	1518.23	1513.7	4.5316	20.536	631.54	4.0241	0.13
43	18.08	43	1513.35	1513.7	-0.3512	0.123	631.66	3.9739	0.13
44	18.09	44	1513.35	1511.47	1.8772	3.524	635.19	3.936	0.14
45	18.09	45	1515.79	1511.47	4.3186	18.651	653.84	3.9456	0.14
46	18.09	46	1508.47	1511.47	-3.0056	9.033	662.87	3.9263	0.14
47	18.1	47	1518.23	1509.26	8.9739	80.532	743.4	4.1104	0.15
48	18.1	48	1513.35	1509.26	4.0911	16.737	760.14	4.11	0.15
49	18.1	49	1506.03	1509.26	-3.2332	10.453	770.59	4.0929	0.15
50	18.11	50	1506.03	1507.06	-1.0336	1.068	771.66	4.052	0.16
51	18.11	51	1515.79	1507.06	8.7321	76.249	847.91	4.203	0.16
52	18.11	52	1506.03	1507.06	-1.0336	1.068	848.98	4.1625	0.16
53	18.12	53	1506.03	1504.88	1.1516	1.326	850.31	4.1239	0.17
54	18.12	54	1503.59	1504.88	-1.2898	1.664	851.97	4.0872	0.17
55	18.12	55	1503.59	1504.88	-1.2898	1.664	853.63	4.0517	0.17
56	18.13	56	1508.47	1502.7	5.7641	33.225	886.86	4.0906	0.18
57	18.13	57	1501.14	1502.7	-1.5602	2.434	889.29	4.0581	0.18
58	18.13	58	1503.59	1502.7	0.8812	0.777	890.07	4.0228	0.18
59	18.14	59	1503.59	1500.55	3.0382	9.231	899.3	4.0074	0.19
60	18.14	60	1503.59	1500.55	3.0382	9.231	908.53	3.9924	0.19
61	18.14	61	1501.14	1500.55	0.5968	0.356	908.89	3.9586	0.19
62	18.15	62	1498.7	1498.4	0.2983	0.089	908.97	3.9251	0.2
63	18.15	63	1503.59	1498.4	5.1811	26.844	935.82	3.9493	0.2
64	18.15	64	1496.26	1498.4	-2.1431	4.593	940.41	3.9264	0.2
65	18.16	65	1493.82	1496.28	-2.4555	6.03	946.44	3.9071	0.21
66	18.16	66	1496.26	1496.28	-0.0141	0	946.44	3.8759	0.21
67	18.16	67	1498.7	1496.28	2.4273	5.892	952.33	3.8575	0.21
68	18.17	68	1491.38	1494.16	-2.7818	7.738	960.07	3.8432	0.22
69	18.17	69	1488.94	1494.16	-5.2232	27.281	987.35	3.8678	0.22
70	18.17	70	1486.5	1494.16	-7.6646	58.745	1046.1	3.9514	0.22
71	18.18	71	1491.38	1492.06	-0.6803	0.463	1046.6	3.9231	0.23
72	18.18	72	1491.38	1492.06	-0.6803	0.463	1047	3.8954	0.23
73	18.18	73	1486.5	1492.06	-5.5631	30.949	1078	3.9242	0.23
74	18.19	74	1493.82	1489.97	3.8488	14.813	1092.8	3.9232	0.24
75	18.19	75	1491.38	1489.97	1.4074	1.981	1094.8	3.8994	0.24
76	18.19	76	1486.5	1489.97	-3.4754	12.078	1106.8	3.8939	0.24
77	18.2	77	1486.5	1487.9	-1.4012	1.963	1108.8	3.8709	0.25
78	18.2	78	1488.94	1487.9	1.0402	1.082	1109.9	3.8469	0.25

79	18.2	79	1486.5	1487.9	-1.4012	1.963	1111.9	3.8249	0.25
80	18.21	80	1481.61	1485.84	-4.2233	17.836	1129.7	3.8303	0.26
81	18.21	81	1486.5	1485.84	0.6595	0.435	1130.1	3.8064	0.26
82	18.21	82	1481.61	1485.84	-4.2233	17.836	1148	3.812	0.26
83	18.22	83	1476.73	1483.79	-7.0587	49.826	1197.8	3.8694	0.27
84	18.22	84	1484.05	1483.79	0.2655	0.07	1197.9	3.8456	0.27
85	18.22	85	1481.61	1483.79	-2.1759	4.735	1202.6	3.8296	0.27
86	18.23	86	1484.05	1481.76	2.2995	5.288	1207.9	3.8148	0.28
87	18.23	87	1474.29	1481.76	-7.4661	55.743	1263.6	3.8786	0.28
88	18.23	88	1474.29	1481.76	-7.4661	55.743	1319.4	3.9398	0.28
89	18.24	89	1476.73	1479.73	-3.0039	9.023	1328.4	3.9302	0.29
90	18.24	90	1471.85	1479.73	-7.8867	62.2	1390.6	3.998	0.29
91	18.24	91	1479.17	1479.73	-0.5625	0.316	1390.9	3.9756	0.29
92	18.25	92	1471.85	1477.73	-5.879	34.563	1425.5	4.0021	0.3
93	18.25	93	1476.73	1477.73	-0.9962	0.992	1426.5	3.9812	0.3
94	18.25	94	1476.73	1477.73	-0.9962	0.992	1427.5	3.9606	0.3
95	18.26	95	1476.73	1475.73	0.9984	0.997	1428.5	3.9404	0.31
96	18.26	96	1479.17	1475.73	3.4398	11.832	1440.3	3.9353	0.31
97	18.26	97	1469.41	1475.73	-6.3258	40.016	1480.3	3.9684	0.31
98	18.27	98	1474.29	1473.75	0.5387	0.29	1480.6	3.9478	0.32
99	18.27	99	1469.41	1473.75	-4.3441	18.871	1499.5	3.9521	0.32
100	18.27	100	1471.85	1473.75	-1.9027	3.62	1503.1	3.9365	0.32
101	18.28	101	1469.41	1471.78	-2.3753	5.642	1508.7	3.9237	0.33
102	18.28	102	1466.96	1471.78	-4.8168	23.202	1531.9	3.9337	0.33
103	18.28	103	1466.96	1471.78	-4.8168	23.202	1555.1	3.9435	0.33
104	18.29	104	1474.29	1469.83	4.4635	19.923	1575.1	3.949	0.34
105	18.29	105	1464.52	1469.83	-5.3022	28.113	1603.2	3.9645	0.34
106	18.29	106	1462.08	1469.83	-7.7436	59.963	1663.1	4.0183	0.34
107	18.3	107	1476.73	1467.88	8.8482	78.29	1741.4	4.092	0.35
108	18.3	108	1466.96	1467.88	-0.9175	0.842	1742.3	4.0734	0.35
109	18.3	109	1471.85	1467.88	3.9654	15.724	1758	4.0724	0.35
110	18.31	110	1469.41	1465.95	3.4547	11.935	1769.9	4.0671	0.36
111	18.31	111	1462.08	1465.95	-3.8696	14.974	1784.9	4.0653	0.36
112	18.31	112	1464.52	1465.95	-1.4282	2.04	1786.9	4.0489	0.36
113	18.32	113	1457.2	1464.03	-6.8343	46.708	1833.6	4.0828	0.37
114	18.32	114	1459.64	1464.03	-4.3929	19.298	1852.9	4.0857	0.37
115	18.32	115	1459.64	1464.03	-4.3929	19.298	1872.2	4.0886	0.37
116	18.33	116	1462.08	1462.13	-0.0459	0.002	1872.2	4.0704	0.38
117	18.33	117	1462.08	1462.13	-0.0459	0.002	1872.2	4.0526	0.38
118	18.33	118	1459.64	1462.13	-2.4873	6.186	1878.4	4.0416	0.38
119	18.34	119	1462.08	1460.23	1.8474	3.413	1881.8	4.0277	0.39

120	18.34	120	1457.2	1460.23	-3.0354	9.213	1891.1	4.0203	0.39
121	18.34	121	1457.2	1460.23	-3.0354	9.213	1900.3	4.013	0.39
122	18.35	122	1459.64	1458.35	1.287	1.656	1901.9	3.9978	0.4
123	18.35	123	1454.76	1458.35	-3.5958	12.93	1914.9	3.9946	0.4
124	18.35	124	1459.64	1458.35	1.287	1.656	1916.5	3.9798	0.4
125	18.36	125	1459.64	1456.48	3.1558	9.959	1926.5	3.9738	0.41
126	18.36	126	1454.76	1456.48	-1.727	2.983	1929.5	3.9606	0.41
127	18.36	127	1454.76	1456.48	-1.727	2.983	1932.4	3.9477	0.41
128	18.37	128	1449.88	1454.63	-4.7532	22.593	1955	3.9548	0.42
129	18.37	129	1459.64	1454.63	5.0124	25.124	1980.2	3.9643	0.42
130	18.37	130	1447.43	1454.63	-7.1946	51.763	2031.9	3.9999	0.42
131	18.38	131	1457.2	1452.78	4.4155	19.497	2051.4	4.0033	0.43
132	18.38	132	1449.88	1452.78	-2.9087	8.46	2059.9	3.996	0.43
133	18.38	133	1444.99	1452.78	-7.7915	60.707	2120.6	4.0388	0.43
134	18.39	134	1449.88	1450.95	-1.0761	1.158	2121.7	4.0245	0.44
135	18.39	135	1444.99	1450.95	-5.9589	35.509	2157.2	4.0426	0.44
136	18.39	136	1452.32	1450.95	1.3653	1.864	2159.1	4.0291	0.44
137	18.4	137	1447.43	1449.13	-1.6969	2.879	2162	4.0167	0.45
138	18.4	138	1444.99	1449.13	-4.1383	17.125	2179.1	4.0177	0.45
139	18.4	139	1442.55	1449.13	-6.5797	43.292	2222.4	4.0424	0.45
140	18.41	140	1452.32	1447.32	4.9948	24.948	2247.4	4.0502	0.46
141	18.41	141	1449.88	1447.32	2.5534	6.52	2253.9	4.0413	0.46
142	18.41	142	1442.55	1447.32	-4.7708	22.761	2276.6	4.0471	0.46
143	18.42	143	1447.43	1445.52	1.9091	3.644	2280.3	4.0358	0.47
144	18.42	144	1442.55	1445.52	-2.9737	8.843	2289.1	4.0293	0.47
145	18.42	145	1437.67	1445.52	-7.8565	61.725	2350.8	4.0688	0.47
146	18.43	146	1444.99	1443.74	1.2531	1.57	2352.4	4.0559	0.48
147	18.43	147	1432.79	1443.74	-10.9539	119.99	2472.4	4.1436	0.48
148	18.43	148	1442.55	1443.74	-1.1883	1.412	2473.8	4.1305	0.48
149	18.44	149	1437.67	1441.97	-4.2974	18.467	2492.3	4.1316	0.49
150	18.44	150	1437.67	1441.97	-4.2974	18.467	2510.8	4.1328	0.49
151	18.44	151	1442.55	1441.97	0.5854	0.343	2511.1	4.1191	0.49
152	18.45	152	1440.11	1440.2	-0.0937	0.009	2511.1	4.1052	0.5
153	18.45	153	1437.67	1440.2	-2.5351	6.427	2517.5	4.0968	0.5
154	18.45	154	1435.23	1440.2	-4.9765	24.765	2542.3	4.1032	0.5
155	18.46	155	1440.11	1438.45	1.6571	2.746	2545	4.0919	0.51
156	18.46	156	1437.67	1438.45	-0.7843	0.615	2545.7	4.079	0.51
157	18.46	157	1440.11	1438.45	1.6571	2.746	2548.4	4.0679	0.51
158	18.47	158	1435.23	1436.71	-1.4862	2.209	2550.6	4.0565	0.52
159	18.47	159	1437.67	1436.71	0.9552	0.912	2551.5	4.0442	0.52
160	18.47	160	1432.79	1436.71	-3.9276	15.426	2566.9	4.0435	0.52

161	18.48	161	1437.67	1434.98	2.6833	7.2	2574.2	4.0363	0.53
162	18.48	162	1437.67	1434.98	2.6833	7.2	2581.4	4.0293	0.53
163	18.48	163	1432.79	1434.98	-2.1995	4.838	2586.2	4.0204	0.53
164	18.49	164	1435.23	1433.27	1.9588	3.837	2590	4.0109	0.54
165	18.49	165	1430.34	1433.27	-2.924	8.549	2598.6	4.0051	0.54
166	18.49	166	1430.34	1433.27	-2.924	8.549	2607.1	3.9993	0.54
167	18.5	167	1430.34	1431.56	-1.2182	1.484	2608.6	3.9883	0.55
168	18.5	168	1425.46	1431.56	-6.1011	37.223	2645.8	4.0044	0.55
169	18.5	169	1420.58	1431.56	-10.9839	120.65	2766.5	4.0823	0.55
170	18.51	170	1430.34	1429.87	0.4765	0.227	2766.7	4.0703	0.56
171	18.51	171	1430.34	1429.87	0.4765	0.227	2766.9	4.0583	0.56
172	18.51	172	1425.46	1429.87	-4.4064	19.417	2786.3	4.0605	0.56
173	18.52	173	1427.9	1428.18	-0.2814	0.079	2786.4	4.0486	0.57
174	18.52	174	1427.9	1428.18	-0.2814	0.079	2786.5	4.0368	0.57
175	18.52	175	1423.02	1428.18	-5.1642	26.668	2813.2	4.0442	0.57
176	18.53	176	1427.9	1426.51	1.3914	1.936	2815.1	4.0339	0.58
177	18.53	177	1425.46	1426.51	-1.05	1.103	2816.2	4.0231	0.58
178	18.53	178	1427.9	1426.51	1.3914	1.936	2818.1	4.0129	0.58
179	18.54	179	1425.46	1424.85	0.6118	0.374	2818.5	4.0018	0.59
180	18.54	180	1427.9	1424.85	3.0532	9.322	2827.8	3.9971	0.59
181	18.54	181	1425.46	1424.85	0.6118	0.374	2828.2	3.9861	0.59
182	18.55	182	1425.46	1423.2	2.2629	5.121	2833.3	3.9785	0.6
183	18.55	183	1423.02	1423.2	-0.1785	0.032	2833.4	3.9675	0.6
184	18.55	184	1418.14	1423.2	-5.0613	25.617	2859	3.9744	0.6
185	18.56	185	1423.02	1421.56	1.4618	2.137	2861.1	3.9649	0.61
186	18.56	186	1418.14	1421.56	-3.421	11.703	2872.8	3.9621	0.61
187	18.56	187	1425.46	1421.56	3.9032	15.235	2888.1	3.9618	0.61
188	18.57	188	1423.02	1419.93	3.0915	9.557	2897.6	3.9576	0.62
189	18.57	189	1418.14	1419.93	-1.7913	3.209	2900.8	3.9492	0.62
190	18.57	190	1418.14	1419.93	-1.7913	3.209	2904	3.9408	0.62
191	18.58	191	1420.58	1418.31	2.2692	5.149	2909.2	3.9338	0.63
192	18.58	192	1418.14	1418.31	-0.1722	0.03	2909.2	3.9234	0.63
193	18.58	193	1418.14	1418.31	-0.1722	0.03	2909.2	3.913	0.63
194	18.59	194	1420.58	1416.7	3.8777	15.037	2924.3	3.9129	0.64
195	18.59	195	1420.58	1416.7	3.8777	15.037	2939.3	3.9127	0.64
196	18.59	196	1420.58	1416.7	3.8777	15.037	2954.4	3.9125	0.64
197	18.6	197	1415.7	1415.1	0.593	0.352	2954.7	3.9026	0.65
198	18.6	198	1415.7	1415.1	0.593	0.352	2955.1	3.8928	0.65
199	18.6	199	1427.9	1415.1	12.8	163.84	3118.9	3.9891	0.65
200	18.61	200	1418.14	1413.51	4.6222	21.364	3140.3	3.9926	0.66
201	18.61	201	1415.7	1413.51	2.1808	4.756	3145	3.9855	0.66

202	18.61	202	1418.14	1413.51	4.6222	21.364	3166.4	3.9889	0.66
203	18.62	203	1413.25	1411.94	1.3168	1.734	3168.1	3.98	0.67
204	18.62	204	1425.46	1411.94	13.5238	182.89	3351	4.0831	0.67
205	18.62	205	1413.25	1411.94	1.3168	1.734	3352.7	4.074	0.67
206	18.63	206	1413.25	1410.37	2.8839	8.317	3361.1	4.069	0.68
207	18.63	207	1408.37	1410.37	-1.9989	3.995	3365.1	4.0615	0.68
208	18.63	208	1415.7	1410.37	5.3253	28.359	3393.4	4.0686	0.68
209	18.64	209	1418.14	1408.81	9.3237	86.932	3480.4	4.1103	0.69
210	18.64	210	1408.37	1408.81	-0.4419	0.195	3480.5	4.1005	0.69
211	18.64	211	1408.37	1408.81	-0.4419	0.195	3480.7	4.0908	0.69
212	18.65	212	1405.93	1407.27	-1.3364	1.786	3482.5	4.082	0.7
213	18.65	213	1410.81	1407.27	3.5464	12.577	3495.1	4.0796	0.7
214	18.65	214	1410.81	1407.27	3.5464	12.577	3507.7	4.0773	0.7
215	18.66	215	1410.81	1405.73	5.0832	25.839	3533.5	4.0826	0.71
216	18.66	216	1408.37	1405.73	2.6418	6.979	3540.5	4.077	0.71
217	18.66	217	1405.93	1405.73	0.2004	0.04	3540.5	4.0675	0.71
218	18.67	218	1405.93	1404.2	1.7272	2.983	3543.5	4.0597	0.72
219	18.67	219	1401.05	1404.2	-3.1556	9.958	3553.5	4.056	0.72
220	18.67	220	1408.37	1404.2	4.1686	17.377	3570.9	4.0565	0.72
221	18.68	221	1401.05	1402.69	-1.6387	2.685	3573.5	4.0488	0.73
222	18.68	222	1403.49	1402.69	0.8027	0.644	3574.2	4.0399	0.73
223	18.68	223	1403.49	1402.69	0.8027	0.644	3574.8	4.031	0.73
224	18.69	224	1405.93	1401.18	4.7512	22.574	3597.4	4.0346	0.74
225	18.69	225	1398.61	1401.18	-2.573	6.62	3604	4.0292	0.74
226	18.69	226	1403.49	1401.18	2.3098	5.335	3609.4	4.0231	0.74
227	18.7	227	1401.05	1399.68	1.3656	1.865	3611.2	4.0152	0.75
228	18.7	228	1396.16	1399.68	-3.5172	12.37	3623.6	4.0131	0.75
229	18.7	229	1403.49	1399.68	3.807	14.494	3638.1	4.0122	0.75
230	18.71	230	1396.16	1398.19	-2.0296	4.119	3642.2	4.0056	0.76
231	18.71	231	1401.05	1398.19	2.8532	8.141	3650.4	4.0013	0.76
232	18.71	232	1401.05	1398.19	2.8532	8.141	3658.5	3.997	0.76
233	18.72	233	1393.72	1396.72	-2.9932	8.959	3667.5	3.9932	0.77
234	18.72	234	1403.49	1396.72	6.7724	45.866	3713.3	4.0094	0.77
235	18.72	235	1401.05	1396.72	4.331	18.758	3732.1	4.0108	0.77
236	18.73	236	1401.05	1395.25	5.7993	33.632	3765.7	4.0202	0.78
237	18.73	237	1398.61	1395.25	3.3579	11.275	3777	4.0176	0.78
238	18.73	238	1396.16	1395.25	0.9165	0.84	3777.8	4.0095	0.78
239	18.74	239	1403.49	1393.79	9.6994	94.078	3871.9	4.0505	0.79
240	18.74	240	1396.16	1393.79	2.3752	5.642	3877.5	4.0449	0.79
241	18.74	241	1393.72	1393.79	-0.0662	0.004	3877.5	4.0364	0.79
242	18.75	242	1398.61	1392.34	6.2658	39.261	3916.8	4.0483	0.8

243	18.75	243	1391.28	1392.34	-1.0584	1.12	3917.9	4.0404	0.8
244	18.75	244	1374.19	1392.34	-18.1483	329.36	4247.3	4.198	0.8
245	18.76	245	1388.84	1390.9	-2.06	4.244	4251.5	4.1915	0.81
246	18.76	246	1388.84	1390.9	-2.06	4.244	4255.8	4.1849	0.81
247	18.76	247	1396.16	1390.9	5.2643	27.713	4283.5	4.1899	0.81
248	18.77	248	1393.72	1389.47	4.2533	18.091	4301.6	4.1902	0.82
249	18.77	249	1391.28	1389.47	1.8119	3.283	4304.9	4.1832	0.82
250	18.77	250	1388.84	1389.47	-0.6296	0.396	4305.3	4.1749	0.82
251	18.78	251	1391.28	1388.05	3.2331	10.453	4315.7	4.1716	0.83
252	18.78	252	1383.96	1388.05	-4.0912	16.738	4332.4	4.1713	0.83
253	18.78	253	1383.96	1388.05	-4.0912	16.738	4349.2	4.1709	0.83
254	18.79	254	1386.4	1386.64	-0.2378	0.057	4349.2	4.1627	0.84
255	18.79	255	1383.96	1386.64	-2.6792	7.178	4356.4	4.1578	0.84
256	18.79	256	1383.96	1386.64	-2.6792	7.178	4363.6	4.153	0.84
257	18.8	257	1381.52	1385.23	-3.7179	13.823	4377.4	4.1514	0.85
258	18.8	258	1386.4	1385.23	1.1649	1.357	4378.8	4.1439	0.85
259	18.8	259	1376.63	1385.23	-8.6007	73.972	4452.7	4.1706	0.85
260	18.81	260	1379.07	1383.84	-4.7656	22.711	4475.5	4.173	0.86
261	18.81	261	1376.63	1383.84	-7.207	51.941	4527.4	4.189	0.86
262	18.81	262	1379.07	1383.84	-4.7656	22.711	4550.1	4.1914	0.86
263	18.82	263	1381.52	1382.46	-0.9396	0.883	4551	4.1838	0.87
264	18.82	264	1388.84	1382.46	6.3846	40.763	4591.8	4.1944	0.87
265	18.82	265	1386.4	1382.46	3.9432	15.549	4607.3	4.1935	0.87
266	18.83	266	1379.07	1381.08	-2.0054	4.022	4611.3	4.1873	0.88
267	18.83	267	1379.07	1381.08	-2.0054	4.022	4615.3	4.1812	0.88
268	18.83	268	1379.07	1381.08	-2.0054	4.022	4619.4	4.1751	0.88
269	18.84	269	1388.84	1379.71	9.1268	83.299	4702.7	4.2047	0.89
270	18.84	270	1381.52	1379.71	1.8026	3.25	4705.9	4.1982	0.89
271	18.84	271	1376.63	1379.71	-3.0802	9.487	4715.4	4.1946	0.89
272	18.85	272	1374.19	1378.36	-4.1638	17.337	4732.7	4.1945	0.9
273	18.85	273	1379.07	1378.36	0.719	0.517	4733.3	4.187	0.9
274	18.85	274	1379.07	1378.36	0.719	0.517	4733.8	4.1795	0.9
275	18.86	275	1376.63	1377.01	-0.3734	0.139	4733.9	4.1718	0.91
276	18.86	276	1374.19	1377.01	-2.8148	7.923	4741.8	4.1677	0.91
277	18.86	277	1376.63	1377.01	-0.3734	0.139	4742	4.1601	0.91
278	18.87	278	1374.19	1375.67	-1.4746	2.175	4744.2	4.1535	0.92
279	18.87	279	1371.75	1375.67	-3.916	15.335	4759.5	4.1527	0.92
280	18.87	280	1376.63	1375.67	0.9668	0.935	4760.4	4.1456	0.92
281	18.88	281	1371.75	1374.33	-2.5845	6.68	4767.1	4.141	0.93
282	18.88	282	1376.63	1374.33	2.2983	5.282	4772.4	4.1359	0.93
283	18.88	283	1376.63	1374.33	2.2983	5.282	4777.7	4.1308	0.93

284	18.89	284	1381.52	1373.01	8.5039	72.316	4850	4.1545	0.94
285	18.89	285	1376.63	1373.01	3.6211	13.112	4863.1	4.1527	0.94
286	18.89	286	1369.31	1373.01	-3.7031	13.713	4876.8	4.1512	0.94
287	18.9	287	1379.07	1371.7	7.3767	54.416	4931.2	4.167	0.95
288	18.9	288	1369.31	1371.7	-2.3889	5.707	4936.9	4.162	0.95
289	18.9	289	1374.19	1371.7	2.4939	6.22	4943.2	4.1574	0.95
290	18.91	290	1366.87	1370.39	-3.5246	12.422	4955.6	4.1553	0.96
291	18.91	291	1374.19	1370.39	3.7996	14.437	4970	4.1542	0.96
292	18.91	292	1364.43	1370.39	-5.966	35.593	5005.6	4.1618	0.96
293	18.92	293	1369.31	1369.09	0.2141	0.046	5005.7	4.1546	0.97
294	18.92	294	1369.31	1369.09	0.2141	0.046	5005.7	4.1475	0.97
295	18.92	295	1364.43	1369.09	-4.6687	21.797	5027.5	4.1494	0.97
296	18.93	296	1369.31	1367.81	1.5029	2.259	5029.8	4.1432	0.98
297	18.93	297	1361.98	1367.81	-5.8213	33.888	5063.6	4.1501	0.98
298	18.93	298	1369.31	1367.81	1.5029	2.259	5065.9	4.144	0.98
299	18.94	299	1371.75	1366.53	5.2247	27.297	5093.2	4.1481	0.99
300	18.94	300	1366.87	1366.53	0.3419	0.117	5093.3	4.1412	0.99
301	18.94	301	1366.87	1366.53	0.3419	0.117	5093.4	4.1343	0.99
302	18.95	302	1364.43	1365.25	-0.8274	0.685	5094.1	4.1276	1
303	18.95	303	1366.87	1365.25	1.614	2.605	5096.7	4.1218	1
304	18.95	304	1366.87	1365.25	1.614	2.605	5099.3	4.116	1
305	18.96	305	1366.87	1363.99	2.8778	8.282	5107.6	4.1125	1.01
306	18.96	306	1361.98	1363.99	-2.005	4.02	5111.6	4.1073	1.01
307	18.96	307	1371.75	1363.99	7.7606	60.227	5171.9	4.1246	1.01
308	18.97	308	1369.31	1362.73	6.5748	43.228	5215.1	4.1351	1.02
309	18.97	309	1369.31	1362.73	6.5748	43.228	5258.3	4.1454	1.02
310	18.97	310	1361.98	1362.73	-0.7494	0.562	5258.9	4.1388	1.02
311	18.98	311	1359.54	1361.49	-1.9433	3.777	5262.6	4.1336	1.03
312	18.98	312	1361.98	1361.49	0.4981	0.248	5262.9	4.127	1.03
313	18.98	313	1357.1	1361.49	-4.3847	19.226	5282.1	4.1278	1.03
314	18.99	314	1359.54	1360.25	-0.704	0.496	5282.6	4.1214	1.04
315	18.99	315	1361.98	1360.25	1.7374	3.019	5285.6	4.116	1.04
316	18.99	316	1359.54	1360.25	-0.704	0.496	5286.1	4.1096	1.04
317	19	317	1364.43	1359.02	5.4101	29.269	5315.4	4.1144	1.05
318	19	318	1359.54	1359.02	0.5273	0.278	5315.7	4.1079	1.05
319	19	319	1369.31	1359.02	10.2929	105.94	5421.6	4.1421	1.05
320	19.01	320	1357.1	1357.79	-0.6908	0.477	5422.1	4.1358	1.06
321	19.01	321	1357.1	1357.79	-0.6908	0.477	5422.6	4.1294	1.06
322	19.01	322	1354.66	1357.79	-3.1322	9.811	5432.4	4.1267	1.06
323	19.02	323	1357.1	1356.58	0.5246	0.275	5432.7	4.1203	1.07
324	19.02	324	1354.66	1356.58	-1.9168	3.674	5436.3	4.1153	1.07

325	19.02	325	1349.78	1356.58	-6.7997	46.236	5482.6	4.1263	1.07
326	19.03	326	1352.22	1355.37	-3.1508	9.927	5492.5	4.1237	1.08
327	19.03	327	1357.1	1355.37	1.732	3	5495.5	4.1184	1.08
328	19.03	328	1357.1	1355.37	1.732	3	5498.5	4.1132	1.08
329	19.04	329	1357.1	1354.17	2.9316	8.594	5507.1	4.1101	1.09
330	19.04	330	1354.66	1354.17	0.4902	0.24	5507.3	4.1039	1.09
331	19.04	331	1357.1	1354.17	2.9316	8.594	5515.9	4.1008	1.09
332	19.05	332	1354.66	1352.98	1.6821	2.829	5518.8	4.0957	1.1
333	19.05	333	1352.22	1352.98	-0.7593	0.577	5519.3	4.0897	1.1
334	19.05	334	1354.66	1352.98	1.6821	2.829	5522.2	4.0845	1.1
335	19.06	335	1349.78	1351.79	-2.0168	4.067	5526.2	4.0799	1.11
336	19.06	336	1352.22	1351.79	0.4247	0.18	5526.4	4.0738	1.11
337	19.06	337	1349.78	1351.79	-2.0168	4.067	5530.5	4.0692	1.11
338	19.07	338	1354.66	1350.62	4.0425	16.342	5546.8	4.0691	1.12
339	19.07	339	1352.22	1350.62	1.6011	2.564	5549.4	4.064	1.12
340	19.07	340	1352.22	1350.62	1.6011	2.564	5551.9	4.0589	1.12
341	19.08	341	1349.78	1349.45	0.3283	0.108	5552.1	4.0529	1.13
342	19.08	342	1349.78	1349.45	0.3283	0.108	5552.2	4.047	1.13
343	19.08	343	1352.22	1349.45	2.7698	7.672	5559.8	4.0438	1.13
344	19.09	344	1344.89	1348.29	-3.3933	11.515	5571.4	4.0421	1.14
345	19.09	345	1354.66	1348.29	6.3724	40.607	5612	4.0508	1.14
346	19.09	346	1347.34	1348.29	-0.9519	0.906	5612.9	4.0453	1.14
347	19.1	347	1349.78	1347.13	2.6431	6.986	5619.9	4.0419	1.15
348	19.1	348	1349.78	1347.13	2.6431	6.986	5626.8	4.0385	1.15
349	19.1	349	1342.45	1347.13	-4.6811	21.913	5648.8	4.0405	1.15
350	19.11	350	1349.78	1345.99	3.7892	14.358	5663.1	4.0398	1.16
351	19.11	351	1342.45	1345.99	-3.535	12.496	5675.6	4.0385	1.16
352	19.11	352	1352.22	1345.99	6.2307	38.821	5714.4	4.0464	1.16
353	19.12	353	1342.45	1344.85	-2.3964	5.743	5720.2	4.0427	1.17
354	19.12	354	1347.34	1344.85	2.4864	6.182	5726.4	4.0391	1.17
355	19.12	355	1342.45	1344.85	-2.3964	5.743	5732.1	4.0354	1.17
356	19.13	356	1342.45	1343.72	-1.2651	1.601	5733.7	4.0302	1.18
357	19.13	357	1342.45	1343.72	-1.2651	1.601	5735.3	4.0251	1.18
358	19.13	358	1344.89	1343.72	1.1763	1.384	5736.7	4.0199	1.18
359	19.14	359	1340.01	1342.59	-2.5826	6.67	5743.3	4.0166	1.19
360	19.14	360	1344.89	1342.59	2.3002	5.291	5748.6	4.0128	1.19
361	19.14	361	1340.01	1342.59	-2.5826	6.67	5755.3	4.0095	1.19
362	19.15	362	1342.45	1341.48	0.9754	0.951	5756.3	4.0043	1.2
363	19.15	363	1340.01	1341.48	-1.466	2.149	5758.4	3.9995	1.2
364	19.15	364	1342.45	1341.48	0.9754	0.951	5759.4	3.9942	1.2
365	19.16	365	1342.45	1340.37	2.0847	4.346	5763.7	3.9902	1.21

366	19.16	366	1344.89	1340.37	4.5261	20.486	5784.2	3.9918	1.21
367	19.16	367	1335.13	1340.37	-5.2395	27.452	5811.6	3.9958	1.21
368	19.17	368	1342.45	1339.27	3.1869	10.156	5821.8	3.9938	1.22
369	19.17	369	1359.54	1339.27	20.2768	411.15	6232.9	4.1267	1.22
370	19.17	370	1340.01	1339.27	0.7455	0.556	6233.5	4.1213	1.22
371	19.18	371	1344.89	1338.17	6.7232	45.202	6278.7	4.1306	1.23
372	19.18	372	1340.01	1338.17	1.8404	3.387	6282.1	4.1261	1.23
373	19.18	373	1337.57	1338.17	-0.601	0.361	6282.5	4.1206	1.23
374	19.19	374	1340.01	1337.08	2.9283	8.575	6291	4.1179	1.24
375	19.19	375	1335.13	1337.08	-1.9545	3.82	6294.8	4.1136	1.24
376	19.19	376	1335.13	1337.08	-1.9545	3.82	6298.7	4.1093	1.24
377	19.2	377	1337.57	1336	1.5677	2.458	6301.1	4.1046	1.25
378	19.2	378	1337.57	1336	1.5677	2.458	6303.6	4.0999	1.25
379	19.2	379	1332.69	1336	-3.3151	10.99	6314.6	4.0981	1.25
380	19.21	380	1337.57	1334.93	2.6415	6.977	6321.6	4.0949	1.26
381	19.21	381	1337.57	1334.93	2.6415	6.977	6328.5	4.0917	1.26
382	19.21	382	1337.57	1334.93	2.6415	6.977	6335.5	4.0886	1.26
383	19.22	383	1332.69	1333.86	-1.1745	1.38	6336.9	4.0836	1.27
384	19.22	384	1344.89	1333.86	11.0325	121.72	6458.6	4.1172	1.27
385	19.22	385	1337.57	1333.86	3.7083	13.751	6472.4	4.1162	1.27
386	19.23	386	1335.13	1332.8	2.3267	5.414	6477.8	4.1126	1.28
387	19.23	387	1337.57	1332.8	4.7681	22.735	6500.5	4.1144	1.28
388	19.23	388	1332.69	1332.8	-0.1147	0.013	6500.5	4.1091	1.28
389	19.24	389	1342.45	1331.75	10.7039	114.57	6615.1	4.1398	1.29
390	19.24	390	1332.69	1331.75	0.9383	0.88	6616	4.1347	1.29
391	19.24	391	1330.25	1331.75	-1.5031	2.259	6618.2	4.1301	1.29
392	19.25	392	1330.25	1330.7	-0.457	0.209	6618.4	4.1248	1.3
393	19.25	393	1327.8	1330.7	-2.8984	8.4	6626.8	4.1221	1.3
394	19.25	394	1325.36	1330.7	-5.3398	28.513	6655.3	4.1257	1.3
395	19.26	395	1332.69	1329.66	3.0238	9.143	6664.5	4.1233	1.31
396	19.26	396	1330.25	1329.66	0.5824	0.339	6664.8	4.1181	1.31
397	19.26	397	1327.8	1329.66	-1.859	3.456	6668.3	4.114	1.31
398	19.27	398	1327.8	1328.63	-0.8264	0.683	6669	4.109	1.32
399	19.27	399	1330.25	1328.63	1.615	2.608	6671.6	4.1046	1.32
400	19.27	400	1332.69	1328.63	4.0564	16.454	6688	4.1044	1.32
401	19.28	401	1330.25	1327.61	2.6408	6.974	6695	4.1014	1.33
402	19.28	402	1332.69	1327.61	5.0822	25.829	6720.8	4.1042	1.33
403	19.28	403	1327.8	1327.61	0.1994	0.04	6720.9	4.0991	1.33
404	19.29	404	1330.25	1326.59	3.66	13.396	6734.3	4.098	1.34
405	19.29	405	1325.36	1326.59	-1.2228	1.495	6735.8	4.0934	1.34
406	19.29	406	1327.8	1326.59	1.2186	1.485	6737.3	4.0887	1.34

407	19.3	407	1322.92	1325.57	-2.6516	7.031	6744.3	4.0858	1.35
408	19.3	408	1327.8	1325.57	2.2312	4.978	6749.3	4.0823	1.35
409	19.3	409	1330.25	1325.57	4.6726	21.833	6771.1	4.0838	1.35
410	19.31	410	1322.92	1324.57	-1.6456	2.708	6773.8	4.0796	1.36
411	19.31	411	1318.04	1324.57	-6.5284	42.62	6816.4	4.0874	1.36
412	19.31	412	1320.48	1324.57	-4.087	16.703	6833.1	4.0874	1.36
413	19.32	413	1320.48	1323.57	-3.0875	9.533	6842.7	4.0853	1.37
414	19.32	414	1313.16	1323.57	-10.4117	108.4	6951.1	4.1125	1.37
415	19.32	415	1322.92	1323.57	-0.6461	0.417	6951.5	4.1076	1.37
416	19.33	416	1318.04	1322.58	-4.5359	20.575	6972.1	4.1087	1.38
417	19.33	417	1322.92	1322.58	0.3469	0.12	6972.2	4.1038	1.38
418	19.33	418	1325.36	1322.58	2.7883	7.775	6979.9	4.1011	1.38
419	19.34	419	1318.04	1321.59	-3.5494	12.598	6992.5	4.0999	1.39
420	19.34	420	1322.92	1321.59	1.3334	1.778	6994.3	4.0955	1.39
421	19.34	421	1318.04	1321.59	-3.5494	12.598	7006.9	4.0943	1.39
422	19.35	422	1318.04	1320.61	-2.5693	6.601	7013.5	4.0913	1.4
423	19.35	423	1322.92	1320.61	2.3135	5.352	7018.9	4.088	1.4
424	19.35	424	1330.25	1320.61	9.6377	92.886	7111.8	4.1101	1.4
425	19.36	425	1315.6	1319.63	-4.0369	16.297	7128.1	4.1099	1.41
426	19.36	426	1313.16	1319.63	-6.4783	41.969	7170	4.1171	1.41
427	19.36	427	1322.92	1319.63	3.2873	10.806	7180.8	4.1153	1.41
428	19.37	428	1313.16	1318.67	-5.5109	30.37	7211.2	4.1192	1.42
429	19.37	429	1322.92	1318.67	4.2547	18.102	7229.3	4.1195	1.42
430	19.37	430	1318.04	1318.67	-0.6281	0.395	7229.7	4.1148	1.42
431	19.38	431	1315.6	1317.71	-2.1084	4.445	7234.1	4.1112	1.43
432	19.38	432	1318.04	1317.71	0.333	0.111	7234.3	4.1065	1.43
433	19.38	433	1310.71	1317.71	-6.9913	48.878	7283.1	4.1155	1.43
434	19.39	434	1308.27	1316.75	-8.4778	71.873	7355	4.131	1.44
435	19.39	435	1308.27	1316.75	-8.4778	71.873	7426.9	4.1463	1.44
436	19.39	436	1313.16	1316.75	-3.5949	12.923	7439.8	4.1451	1.44
437	19.4	437	1313.16	1315.8	-2.6462	7.002	7446.8	4.1423	1.45
438	19.4	438	1318.04	1315.8	2.2366	5.002	7451.8	4.1389	1.45
439	19.4	439	1318.04	1315.8	2.2366	5.002	7456.8	4.1356	1.45
440	19.41	440	1308.27	1314.86	-6.5866	43.383	7500.2	4.1428	1.46
441	19.41	441	1313.16	1314.86	-1.7037	2.903	7503.1	4.1389	1.46
442	19.41	442	1313.16	1314.86	-1.7037	2.903	7506	4.135	1.46
443	19.42	443	1310.71	1313.92	-3.2088	10.296	7516.3	4.1331	1.47
444	19.42	444	1313.16	1313.92	-0.7673	0.589	7516.9	4.1286	1.47
445	19.42	445	1315.6	1313.92	1.6741	2.803	7519.7	4.1247	1.47
446	19.43	446	1305.83	1312.99	-7.1613	51.284	7571	4.134	1.48
447	19.43	447	1310.71	1312.99	-2.2785	5.191	7576.2	4.1308	1.48

448	19.43	448	1305.83	1312.99	-7.1613	51.284	7627.4	4.1401	1.48
449	19.44	449	1310.71	1312.07	-1.3542	1.834	7629.3	4.1359	1.49
450	19.44	450	1310.71	1312.07	-1.3542	1.834	7631.1	4.1318	1.49
451	19.44	451	1310.71	1312.07	-1.3542	1.834	7632.9	4.1277	1.49
452	19.45	452	1303.39	1311.15	-7.7602	60.22	7693.2	4.1393	1.5

Table showing output from SAS for in-situ stress test

1	2	3	4	5	6	7	8	9	10
Obs	**t**	**n**	**P**	**P Mod**	**Error**	**SQ Error**	**CUM SQ Error**	**RMSE**	**MAN Time**
1	2.2	1	5496.1	5449.36	46.7656	2187.02	2187.02	.	0
2	2.3	2	5490.3	5445.1	45.1723	2040.53	4227.56	.	0.0501
3	2.3	3	5477.8	5439.5	38.296	1466.59	5694.14	.	0.1166
4	2.3	4	5473.2	5436.7	36.5186	1333.61	7027.75	83.832	0.15
5	2.4	5	5462.2	5431.17	30.9881	960.26	7988.01	63.198	0.2166
6	2.4	6	5456.6	5428.42	28.2138	796.02	8784.03	54.111	0.25
7	2.5	7	5448.2	5422.97	25.2174	635.92	9419.94	48.528	0.3166
8	2.6	8	5440.5	5418.91	21.6045	466.75	9886.7	44.467	0.3667
9	2.6	9	5436.7	5416.22	20.4622	418.7	10305.4	41.444	0.4001
10	2.7	10	5427.8	5410.91	16.8687	284.55	10589.95	38.895	0.4665
11	2.7	11	5422.3	5406.94	15.3404	235.33	10825.28	36.785	0.5166
12	2.7	12	5417.2	5404.31	12.8981	166.36	10991.64	34.947	0.55
13	2.8	13	5408.9	5399.1	9.7887	95.82	11087.46	33.298	0.6167
14	2.8	14	5405.5	5396.52	8.9705	80.47	11167.93	31.863	0.65
15	2.9	15	5398.8	5392.65	6.1017	37.23	11205.16	30.558	0.7002
16	3.0	16	5394.1	5388.83	5.2174	27.22	11232.38	29.394	0.7501
17	3.0	17	5389.5	5385.05	4.4938	20.19	11252.57	28.351	0.8
18	3.1	18	5380.9	5380.03	0.9029	0.82	11253.39	27.39	0.8666
19	3.1	19	5379.4	5377.54	1.8345	3.37	11256.76	26.525	0.9
20	3.2	20	5370.8	5372.6	-1.7559	3.08	11259.84	25.736	0.9666
21	3.2	21	5367.3	5368.92	-1.6664	2.78	11262.62	25.014	1.0167
22	3.3	22	5361.6	5365.28	-3.7077	13.75	11276.36	24.362	1.0666
23	3.3	23	5358.4	5362.86	-4.4437	19.75	11296.11	23.766	1.1
24	3.4	24	5355.2	5359.25	-4.0366	16.29	11312.4	23.21	1.1502
25	3.4	25	5348.6	5355.69	-7.123	50.74	11363.14	22.727	1.2
26	3.5	26	5345.4	5352.13	-6.7558	45.64	11408.78	22.272	1.2501
27	3.5	27	5340.8	5348.62	-7.8098	60.99	11469.77	21.861	1.3
28	3.6	28	5335.9	5345.12	-9.2033	84.7	11554.47	21.498	1.3501
29	3.6	29	5332.3	5341.66	-9.346	87.35	11641.82	21.16	1.4
30	3.6	30	5327.4	5338.22	-10.812	116.89	11758.71	20.869	1.45
31	3.7	31	5323.5	5334.81	-11.309	127.89	11886.61	20.604	1.5
32	3.8	32	5318.2	5330.3	-12.081	145.95	12032.56	20.37	1.5666
33	3.8	33	5314.3	5326.95	-12.632	159.56	12192.12	20.16	1.6166
34	3.8	34	5313.4	5324.72	-11.294	127.56	12319.68	19.935	1.65
35	3.9	35	5307.3	5320.3	-13.004	169.1	12488.78	19.755	1.7168
36	3.9	36	5305.5	5318.12	-12.667	160.45	12649.23	19.578	1.75
37	4.0	37	5301.7	5313.75	-12.039	144.93	12794.16	19.398	1.817

38	4.0	38	5298.3	5311.62	-13.321	177.45	12971.62	19.251	1.85
39	4.1	39	5295.6	5308.39	-12.747	162.49	13134.11	19.101	1.9002
40	4.2	40	5290	5304.15	-14.17	200.79	13334.9	18.984	1.9668
41	4.2	41	5286.3	5301	-14.656	214.81	13549.72	18.883	2.0166
42	4.2	42	5284.5	5298.91	-14.42	207.92	13757.64	18.782	2.05
43	4.3	43	5281.4	5295.77	-14.369	206.48	13964.12	18.684	2.1002
44	4.4	44	5278	5291.66	-13.709	187.94	14152.06	18.579	2.1667
45	4.4	45	5272.7	5287.59	-14.844	220.34	14372.4	18.499	2.2333
46	4.5	46	5271	5285.56	-14.514	210.67	14583.07	18.416	2.2667
47	4.5	47	5268.7	5282.53	-13.869	192.35	14775.43	18.325	2.3169
48	4.6	48	5265	5279.55	-14.574	212.39	14987.82	18.25	2.3666
49	4.6	49	5263.5	5277.55	-14.035	196.99	15184.81	18.169	2.4002
50	4.7	50	5258.4	5273.63	-15.274	233.3	15418.11	18.112	2.4666
51	4.7	51	5256.2	5270.69	-14.516	210.72	15628.83	18.044	2.5167
52	4.8	52	5253.6	5267.8	-14.236	202.67	15831.5	17.975	2.5666
53	4.8	53	5250.1	5264.9	-14.837	220.13	16051.64	17.917	2.6168
54	4.9	54	5247.9	5262.04	-14.118	199.31	16250.94	17.851	2.6668
55	4.9	55	5244.2	5259.2	-15.03	225.91	16476.85	17.801	2.7167
56	5.0	56	5241.9	5256.38	-14.47	209.38	16686.23	17.744	2.7668
57	5.0	57	5238.9	5253.58	-14.735	217.13	16903.36	17.693	2.8167
58	5.1	58	5236.9	5250.81	-13.882	192.72	17096.09	17.631	2.8666
59	5.1	59	5235	5248.05	-13.023	169.59	17265.67	17.559	2.9167
60	5.2	60	5231.2	5245.32	-14.107	199	17464.67	17.504	2.9667
61	5.2	61	5230.3	5243.5	-13.161	173.21	17637.88	17.439	3.0001
62	5.3	62	5226.3	5239.9	-13.583	184.49	17822.37	17.38	3.0669
63	5.3	63	5224.4	5237.24	-12.816	164.25	17986.62	17.314	3.1166
64	5.4	64	5221.8	5234.58	-12.767	163	18149.62	17.249	3.1667
65	5.4	65	5219.8	5232.82	-12.991	168.77	18318.39	17.189	3.2001
66	5.5	66	5216.9	5229.33	-12.39	153.52	18471.91	17.123	3.2667
67	5.5	67	5215.4	5227.6	-12.228	149.51	18621.42	17.058	3.3001
68	5.6	68	5213	5225.02	-12.054	145.3	18766.72	16.992	3.3501
69	5.6	69	5211	5222.45	-11.464	131.42	18898.14	16.921	3.4001
70	5.7	70	5206.7	5219.07	-12.336	152.16	19050.3	16.862	3.4667
71	5.7	71	5204.8	5216.55	-11.733	137.66	19187.96	16.798	3.5168
72	5.8	72	5202.4	5213.22	-10.849	117.7	19305.66	16.727	3.5835
73	5.8	73	5201.3	5211.58	-10.315	106.4	19412.06	16.653	3.6166
74	5.9	74	5199.3	5209.12	-9.7926	95.89	19507.95	16.576	3.6667
75	5.9	75	5196.1	5205.86	-9.7195	94.47	19602.42	16.5	3.7334
76	6.0	76	5195	5204.25	-9.2244	85.09	19687.51	16.422	3.7668
77	6.0	77	5193.3	5202.64	-9.3591	87.59	19775.1	16.347	3.8002
78	6.1	78	5189.8	5198.66	-8.8565	78.44	19853.54	16.27	3.8836

79	6.1	79	5188.7	5197.09	-8.3724	70.1	19923.64	16.191	3.9167
80	6.2	80	5187	5195.51	-8.4653	71.66	19995.3	16.115	3.9503
81	6.2	81	5184.5	5192.4	-7.9126	62.61	20057.91	16.036	4.0167
82	6.3	82	5182.4	5190.09	-7.735	59.83	20117.74	15.958	4.0666
83	6.3	83	5179.9	5187.79	-7.9359	62.98	20180.72	15.883	4.1167
84	6.4	84	5177.3	5184.76	-7.4834	56	20236.72	15.806	4.1833
85	6.4	85	5175.6	5183.25	-7.6643	58.74	20295.46	15.732	4.2167
86	6.5	86	5173	5180.25	-7.2458	52.5	20347.96	15.658	4.2834
87	6.5	87	5171.2	5178.76	-7.6117	57.94	20405.9	15.586	4.3168
88	6.6	88	5169.7	5176.56	-6.8726	47.23	20453.13	15.512	4.3666
89	6.6	89	5167.8	5173.63	-5.8558	34.29	20487.42	15.435	4.4333
90	6.7	90	5166	5172.18	-6.1786	38.17	20525.6	15.36	4.4667
91	6.7	91	5164.5	5170.02	-5.4882	30.12	20555.72	15.284	4.5166
92	6.8	92	5161.2	5167.15	-5.9218	35.07	20590.79	15.21	4.5834
93	6.8	93	5160.4	5165.73	-5.3507	28.63	20619.42	15.136	4.6168
94	6.9	94	5159.1	5163.62	-4.5449	20.66	20640.07	15.06	4.6667
95	6.9	95	5156.6	5161.52	-4.8859	23.87	20663.95	14.987	4.7166
96	7.0	96	5154.7	5159.43	-4.6891	21.99	20685.93	14.914	4.7668
97	7.0	97	5152.1	5156.68	-4.6229	21.37	20707.3	14.842	4.8333
98	7.1	98	5151	5155.32	-4.3202	18.66	20725.97	14.771	4.8667
99	7.1	99	5149.6	5153.27	-3.6601	13.4	20739.37	14.698	4.9168
100	7.2	100	5146.7	5150.59	-3.8726	15	20754.36	14.628	4.9833
101	7.2	101	5146.2	5149.91	-3.7308	13.92	20768.28	14.558	5.0002
102	7.3	102	5143.7	5146.6	-2.9018	8.42	20776.7	14.487	5.0833
103	7.3	103	5142.4	5144.63	-2.1906	4.8	20781.5	14.416	5.1333
104	7.4	104	5141.4	5143.33	-1.9162	3.67	20785.17	14.346	5.1666
105	7.4	105	5139	5141.37	-2.3269	5.41	20790.59	14.277	5.2169
106	7.5	106	5137.7	5139.45	-1.7615	3.1	20793.69	14.209	5.2666
107	7.5	107	5135.7	5137.53	-1.8302	3.35	20797.04	14.141	5.3167
108	7.6	108	5134.5	5135.62	-1.1363	1.29	20798.33	14.074	5.3669
109	7.6	109	5133.3	5133.74	-0.4749	0.23	20798.56	14.008	5.4167
110	7.7	110	5130.8	5131.87	-1.0671	1.14	20799.69	13.942	5.4666
111	7.7	111	5129.5	5130	-0.4917	0.24	20799.94	13.878	5.5167
112	7.8	112	5127.2	5127.55	-0.3771	0.14	20800.08	13.814	5.5833
113	7.8	113	5126.3	5126.32	-0.033	0	20800.08	13.751	5.6167
114	7.9	114	5124.6	5123.9	0.6875	0.47	20800.55	13.689	5.6834
115	7.9	115	5123.6	5122.7	0.8909	0.79	20801.35	13.628	5.7166
116	8.0	116	5122	5120.91	1.0532	1.11	20802.45	13.568	5.7666
117	8.0	117	5119.6	5118.54	1.0247	1.05	20803.5	13.509	5.8333
118	8.1	118	5118.7	5117.37	1.3511	1.83	20805.33	13.451	5.8667
119	8.1	119	5116.7	5115.62	1.1208	1.26	20806.59	13.393	5.9166

120	8.2	120	5115.7	5114.45	1.2627	1.59	20808.18	13.336	5.9504
121	8.2	121	5114.1	5112.16	1.9627	3.85	20812.03	13.281	6.0166
122	8.3	122	5112.6	5110.44	2.136	4.56	20816.6	13.226	6.0667
123	8.3	123	5111.5	5108.74	2.7646	7.64	20824.24	13.173	6.1169
124	8.4	124	5110	5107.06	2.904	8.43	20832.67	13.121	6.1667
125	8.4	125	5108.4	5105.39	3.0144	9.09	20841.76	13.07	6.2167
126	8.5	126	5107.5	5104.27	3.2686	10.68	20852.44	13.02	6.2503
127	8.5	127	5105.4	5102.08	3.3113	10.96	20863.41	12.971	6.3166
128	8.6	128	5103.9	5099.9	3.9942	15.95	20879.36	12.924	6.3834
129	8.6	129	5102.6	5098.82	3.7465	14.04	20893.4	12.877	6.4167
130	8.7	130	5101.3	5097.21	4.124	17.01	20910.4	12.832	6.4666
131	8.7	131	5100.1	5095.61	4.5357	20.57	20930.98	12.788	6.5167
132	8.8	132	5098	5093.5	4.4525	19.83	20950.8	12.744	6.5831
133	8.8	133	5097.4	5092.45	4.9944	24.94	20975.75	12.702	6.6167
134	8.9	134	5095.5	5090.88	4.5728	20.91	20996.66	12.66	6.6666
135	8.9	135	5094.4	5089.33	5.0819	25.83	21022.48	12.62	6.7167
136	9.0	136	5093	5087.79	5.1619	26.65	21049.13	12.58	6.7666
137	9.0	137	5091.3	5086.26	5.0582	25.59	21074.71	12.541	6.8167
138	9.1	138	5090.3	5084.75	5.5591	30.9	21105.62	12.504	6.8666
139	9.1	139	5088.5	5083.24	5.25	27.56	21133.18	12.466	6.9167
140	9.2	140	5087.4	5081.75	5.6178	31.56	21164.74	12.429	6.9666
141	9.2	141	5086	5080.26	5.7241	32.77	21197.5	12.394	7.0167
142	9.3	142	5084.3	5078.8	5.5078	30.34	21227.84	12.358	7.0666
143	9.3	143	5083.1	5077.34	5.7492	33.05	21260.89	12.323	7.1166
144	9.4	144	5081.3	5075.89	5.4549	29.76	21290.65	12.288	7.1666
145	9.4	145	5080.5	5073.97	6.4805	42	21332.65	12.257	7.2333
146	9.5	146	5079.5	5072.54	6.9274	47.99	21380.64	12.228	7.2834
147	9.5	147	5078.5	5071.6	6.8588	47.04	21427.68	12.199	7.3166
148	9.6	148	5077.3	5070.19	7.1116	50.57	21478.25	12.171	7.3669
149	9.6	149	5075.4	5068.8	6.632	43.98	21522.24	12.141	7.4168
150	9.7	150	5074.4	5067.42	6.9742	48.64	21570.88	12.114	7.4667
151	9.7	151	5073	5066.04	6.918	47.86	21618.73	12.086	7.5168
152	9.8	152	5071.4	5064.68	6.7359	45.37	21664.11	12.058	7.5667
153	9.8	153	5070.5	5063.32	7.1531	51.17	21715.27	12.032	7.6167
154	9.9	154	5069.6	5061.98	7.5684	57.28	21772.55	12.008	7.6667
155	9.9	155	5068.7	5060.65	8.0567	64.91	21837.46	11.986	7.7166
156	10.0	156	5067.1	5059.32	7.7531	60.11	21897.57	11.963	7.7667
157	10.0	157	5065.2	5057.57	7.6683	58.8	21956.38	11.94	7.8333
158	10.1	158	5064.4	5056.7	7.7389	59.89	22016.27	11.918	7.8668
159	10.1	159	5062.5	5055.41	7.0619	49.87	22066.14	11.893	7.9167
160	10.2	160	5062	5054.13	7.858	61.75	22127.89	11.872	7.9666

161	10.2	161	5061.2	5052.85	8.3268	69.34	22197.22	11.853	8.0169
162	10.3	162	5059.8	5051.59	8.2285	67.71	22264.93	11.834	8.0666
163	10.3	163	5058.6	5050.33	8.2841	68.63	22333.56	11.815	8.1167
164	10.4	164	5056.9	5049.08	7.8608	61.79	22395.35	11.794	8.167
165	10.4	165	5056.1	5047.85	8.2311	67.75	22463.1	11.775	8.2167
166	10.5	166	5054.8	5046.21	8.6071	74.08	22537.18	11.759	8.2833
167	10.5	167	5054	5045.4	8.6028	74.01	22611.19	11.742	8.3167
168	10.6	168	5052.5	5043.79	8.6741	75.24	22686.43	11.726	8.3833
169	10.6	169	5052	5042.99	9.0428	81.77	22768.2	11.711	8.4167
170	10.7	170	5051.3	5041.8	9.5121	90.48	22858.68	11.7	8.4669
171	10.7	171	5049.9	5040.62	9.2986	86.46	22945.14	11.687	8.5167
172	10.8	172	5048.9	5039.83	9.0272	81.49	23026.64	11.673	8.5504
173	10.8	173	5046.9	5037.9	8.968	80.43	23107.06	11.659	8.6335
174	10.9	174	5046.1	5037.13	8.9717	80.49	23187.55	11.645	8.6666
175	10.9	175	5044.9	5035.61	9.2645	85.83	23273.38	11.632	8.7333
176	11.0	176	5043.6	5034.84	8.7826	77.13	23350.52	11.618	8.767
177	11.0	177	5042.7	5033.34	9.349	87.4	23437.92	11.606	8.8333
178	11.1	178	5042.3	5032.6	9.6706	93.52	23531.44	11.596	8.8667
179	11.1	179	5040	5031.11	8.9308	79.76	23611.2	11.583	8.9335
180	11.2	180	5039.5	5030.38	9.1461	83.65	23694.85	11.57	8.9667
181	11.2	181	5037.6	5029.28	8.2696	68.39	23763.24	11.554	9.0168
182	11.3	182	5037	5028.19	8.8048	77.52	23840.76	11.541	9.0668
183	11.3	183	5035.8	5026.76	9.0489	81.88	23922.65	11.528	9.1333
184	11.4	184	5034.7	5026.05	8.6426	74.69	23997.34	11.514	9.1667
185	11.4	185	5033.8	5024.98	8.847	78.27	24075.61	11.502	9.2169
186	11.5	186	5032.9	5023.93	8.9586	80.26	24155.87	11.489	9.2667
187	11.5	187	5031.7	5022.88	8.8262	77.9	24233.77	11.476	9.3167
188	11.6	188	5030.5	5021.84	8.6557	74.92	24308.69	11.463	9.3668
189	11.6	189	5029.7	5020.81	8.8992	79.2	24387.89	11.451	9.4167
190	11.7	190	5029.1	5019.79	9.3561	87.54	24475.42	11.441	9.4666
191	11.7	191	5027.8	5018.43	9.3918	88.21	24563.63	11.431	9.5334
192	11.8	192	5027.3	5017.77	9.4819	89.91	24653.54	11.421	9.5666
193	11.8	193	5025.7	5016.76	8.9448	80.01	24733.55	11.41	9.6167
194	11.9	194	5024.9	5015.76	9.1132	83.05	24816.6	11.399	9.6669
195	11.9	195	5024.1	5014.78	9.3022	86.53	24903.13	11.389	9.7167
196	12.0	196	5022.5	5013.81	8.6727	75.22	24978.34	11.376	9.7666
197	12.0	197	5021.8	5012.83	8.9138	79.46	25057.8	11.365	9.8167
198	12.1	198	5020.8	5011.55	9.2957	86.41	25144.21	11.355	9.8836
199	12.1	199	5019.2	5010.6	8.6449	74.74	25218.94	11.343	9.9334
200	12.2	200	5018.6	5009.96	8.6021	74	25292.94	11.331	9.9669
201	12.2	201	5017.3	5008.71	8.6046	74.04	25366.98	11.319	10.033

202	12.3	202	5016.7	5007.78	8.8774	78.81	25445.79	11.308	10.083
203	12.3	203	5016.3	5007.16	9.0918	82.66	25528.45	11.298	10.117
204	12.4	204	5014.3	5005.93	8.3397	69.55	25598	11.285	10.183
205	12.4	205	5013.6	5005.33	8.2902	68.73	25666.73	11.272	10.217
206	12.5	206	5012.7	5004.42	8.2262	67.67	25734.4	11.259	10.267
207	12.5	207	5012.2	5003.52	8.6405	74.66	25809.05	11.248	10.317
208	12.6	208	5011.4	5002.63	8.7972	77.39	25886.45	11.237	10.367
209	12.6	209	5009.1	5001.44	7.6798	58.98	25945.43	11.223	10.434
210	12.7	210	5008.9	5000.86	8.0196	64.31	26009.74	11.209	10.467
211	12.7	211	5008.1	4999.99	8.1503	66.43	26076.17	11.197	10.517
212	12.8	212	5007.1	4998.83	8.2498	68.06	26144.23	11.185	10.583
213	12.8	213	5006.1	4997.97	8.1269	66.05	26210.27	11.172	10.633
214	12.9	214	5005.1	4997.41	7.6514	58.54	26268.82	11.158	10.667
215	12.9	215	5004	4996.28	7.6687	58.81	26327.62	11.144	10.733
216	13.0	216	5003.3	4995.72	7.5321	56.73	26384.36	11.13	10.767
217	13.0	217	5002.7	4994.88	7.8098	60.99	26445.35	11.117	10.817
218	13.1	218	5001.4	4993.78	7.6255	58.15	26503.5	11.103	10.883
219	13.1	219	5000.4	4993.23	7.198	51.81	26555.31	11.088	10.917
220	13.2	220	4999.4	4992.42	7.0153	49.21	26604.52	11.073	10.967
221	13.2	221	4998.3	4991.61	6.7149	45.09	26649.61	11.057	11.017
222	13.3	222	4997.7	4990.81	6.8682	47.17	26696.79	11.041	11.067
223	13.3	223	4997.2	4990.01	7.2249	52.2	26748.99	11.027	11.117
224	13.4	224	4995.6	4988.95	6.6007	43.57	26792.56	11.011	11.183
225	13.4	225	4994.8	4988.43	6.3971	40.92	26833.48	10.994	11.217
226	13.5	226	4993.5	4987.39	6.0816	36.99	26870.46	10.977	11.283
227	13.5	227	4993	4986.62	6.3421	40.22	26910.69	10.961	11.333
228	13.6	228	4992.6	4986.11	6.45	41.6	26952.29	10.945	11.367
229	13.6	229	4991.5	4985.09	6.394	40.88	26993.17	10.929	11.433
230	13.7	230	4991.3	4984.59	6.7153	45.09	27038.27	10.914	11.467
231	13.7	231	4989	4983.59	5.3601	28.73	27067	10.896	11.533
232	13.8	232	4988.6	4983.09	5.5034	30.29	27097.29	10.878	11.567
233	13.8	233	4987.6	4982.11	5.4676	29.89	27127.18	10.86	11.633
234	13.9	234	4987	4981.62	5.374	28.88	27156.06	10.842	11.667
235	13.9	235	4986.1	4980.65	5.4799	30.03	27186.09	10.825	11.733
236	14.0	236	4985.4	4980.17	5.2355	27.41	27213.5	10.807	11.767
237	14.0	237	4985.1	4979.45	5.6064	31.43	27244.93	10.79	11.817
238	14.1	238	4984.3	4978.74	5.5401	30.69	27275.62	10.773	11.867
239	14.1	239	4983.5	4978.03	5.4534	29.74	27305.36	10.756	11.917
240	14.2	240	4982.1	4977.33	4.7385	22.45	27327.82	10.738	11.967
241	14.2	241	4980.8	4976.64	4.1155	16.94	27344.75	10.719	12.017
242	14.3	242	4980.2	4975.95	4.228	17.88	27362.63	10.7	12.067

243	14.3	243	4979.5	4975.26	4.2782	18.3	27380.93	10.681	12.117
244	14.4	244	4978.9	4974.58	4.3047	18.53	27399.46	10.663	12.167
245	14.4	245	4978.2	4973.9	4.3174	18.64	27418.1	10.644	12.217
246	14.5	246	4977.4	4973.01	4.343	18.86	27436.97	10.626	12.283
247	14.5	247	4977.2	4972.57	4.6705	21.81	27458.78	10.608	12.317
248	14.6	248	4976.4	4971.91	4.451	19.81	27478.59	10.59	12.367
249	14.6	249	4975.4	4971.25	4.1562	17.27	27495.86	10.572	12.417
250	14.7	250	4974.1	4970.6	3.4523	11.92	27507.78	10.553	12.467
251	14.7	251	4973	4969.96	3.0711	9.43	27517.21	10.534	12.517
252	14.8	252	4972.2	4969.11	3.1122	9.69	27526.9	10.514	12.583
253	14.8	253	4971.7	4968.68	3.0416	9.25	27536.15	10.495	12.617
254	14.9	254	4970.8	4967.84	2.9692	8.82	27544.97	10.476	12.683
255	14.9	255	4970.2	4967.43	2.7398	7.51	27552.47	10.456	12.717
256	15.0	256	4969.5	4966.8	2.7	7.29	27559.76	10.437	12.767
257	15.0	257	4968.7	4965.98	2.6818	7.19	27566.96	10.418	12.833
258	15.1	258	4968.1	4965.57	2.4982	6.24	27573.2	10.399	12.867
259	15.1	259	4967.4	4964.97	2.4271	5.89	27579.09	10.379	12.917
260	15.2	260	4966.3	4964.17	2.1395	4.58	27583.66	10.36	12.983
261	15.2	261	4965.9	4963.76	2.1119	4.46	27588.12	10.341	13.017
262	15.3	262	4965.3	4963.17	2.1401	4.58	27592.7	10.322	13.067
263	15.3	263	4963.1	4962.39	0.7392	0.55	27593.25	10.302	13.133
264	15.4	264	4962.8	4962	0.7914	0.63	27593.88	10.282	13.167
265	15.4	265	4961.8	4961.42	0.3511	0.12	27594	10.263	13.217
266	15.5	266	4961.3	4960.84	0.4235	0.18	27594.18	10.243	13.267
267	15.5	267	4960.4	4960.08	0.3323	0.11	27594.29	10.224	13.333
268	15.6	268	4959.8	4959.7	0.1181	0.01	27594.3	10.204	13.367
269	15.6	269	4959.3	4959.14	0.1272	0.02	27594.32	10.185	13.417
270	15.7	270	4958.4	4958.58	-0.1936	0.04	27594.36	10.166	13.467
271	15.7	271	4957.8	4958.02	-0.2521	0.06	27594.42	10.147	13.517
272	15.8	272	4957.1	4957.48	-0.3635	0.13	27594.55	10.128	13.567
273	15.8	273	4956.2	4956.93	-0.7467	0.56	27595.11	10.11	13.617
274	15.9	274	4955.7	4956.39	-0.7079	0.5	27595.61	10.091	13.667
275	15.9	275	4954.8	4955.85	-1.0253	1.05	27596.66	10.073	13.717
276	16.0	276	4954.2	4955.14	-0.9557	0.91	27597.58	10.054	13.783
277	16.0	277	4953.4	4954.61	-1.1649	1.36	27598.93	10.036	13.833
278	16.1	278	4952.9	4954.26	-1.4094	1.99	27600.92	10.018	13.867
279	16.1	279	4952.1	4953.73	-1.6165	2.61	27603.53	10.001	13.917
280	16.2	280	4951.3	4953.22	-1.889	3.57	27607.1	9.9832	13.967
281	16.2	281	4950.4	4952.53	-2.1619	4.67	27611.78	9.9661	14.034
282	16.3	282	4949.9	4952.19	-2.3031	5.3	27617.08	9.9492	14.067
283	16.3	283	4949.2	4951.69	-2.5029	6.26	27623.34	9.9325	14.117

284	16.4	284	4948.4	4951.01	-2.6347	6.94	27630.29	9.9161	14.183
285	16.4	285	4947.8	4950.68	-2.8536	8.14	27638.43	9.8999	14.217
286	16.5	286	4947.2	4950.19	-2.9579	8.75	27647.18	9.884	14.267
287	16.5	287	4946.3	4949.53	-3.2813	10.77	27657.95	9.8685	14.334
288	16.6	288	4945.8	4949.21	-3.382	11.44	27669.38	9.8532	14.367
289	16.6	289	4944.9	4948.56	-3.7021	13.71	27683.09	9.8384	14.433
290	16.7	290	4944.4	4948.24	-3.8944	15.17	27698.26	9.8239	14.467
291	16.7	291	4943.7	4947.77	-4.0409	16.33	27714.59	9.8098	14.517
292	16.8	292	4942.9	4947.29	-4.3504	18.93	27733.51	9.7961	14.567
293	16.8	293	4942.3	4946.82	-4.4925	20.18	27753.69	9.7828	14.617
294	16.9	294	4941.6	4946.36	-4.7427	22.49	27776.19	9.7699	14.667
295	16.9	295	4940.8	4945.89	-5.1125	26.14	27802.33	9.7577	14.717
296	17.0	296	4940.2	4945.43	-5.1949	26.99	27829.31	9.7458	14.767
297	17.0	297	4939.4	4944.98	-5.6165	31.55	27860.86	9.7347	14.817
298	17.1	298	4938.5	4944.38	-5.8413	34.12	27894.98	9.7242	14.883
299	17.1	299	4938.1	4944.08	-5.9385	35.27	27930.24	9.7139	14.917
300	17.2	300	4937.3	4943.63	-6.3477	40.29	27970.54	9.7045	14.967
301	17.2	301	4936.7	4943.19	-6.5167	42.47	28013.01	9.6955	15.017
302	17.3	302	4935.9	4942.75	-6.8994	47.6	28060.61	9.6875	15.067
303	17.3	303	4935.2	4942.32	-7.104	50.47	28111.07	9.6801	15.117
304	17.4	304	4934.3	4941.74	-7.4068	54.86	28165.94	9.6734	15.183
305	17.4	305	4933.8	4941.45	-7.6733	58.88	28224.81	9.6675	15.217
306	17.5	306	4933.2	4941.03	-7.8621	61.81	28286.63	9.662	15.267
307	17.5	307	4932.3	4940.61	-8.3192	69.21	28355.84	9.6579	15.317
308	17.6	308	4931.6	4940.18	-8.5571	73.22	28429.06	9.6545	15.367
309	17.6	309	4931.1	4939.77	-8.6803	75.35	28504.41	9.6515	15.417
310	17.7	310	4930.3	4939.36	-9.1013	82.83	28587.24	9.6498	15.467
311	17.7	311	4929.7	4938.95	-9.2911	86.32	28673.56	9.6486	15.517
312	17.8	312	4928.7	4938.54	-9.8195	96.42	28769.99	9.6492	15.567
313	17.8	313	4928.1	4938.14	-10.041	100.83	28870.82	9.6505	15.617
314	17.9	314	4927.5	4937.74	-10.268	105.42	28976.24	9.6525	15.667
315	17.9	315	4926.7	4937.34	-10.634	113.07	29089.31	9.6558	15.717
316	18.0	316	4926.1	4936.94	-10.867	118.1	29207.41	9.6599	15.767
317	18.0	317	4925.1	4936.42	-11.319	128.12	29335.53	9.6657	15.833
318	18.1	318	4924.8	4936.16	-11.408	130.14	29465.67	9.6717	15.867
319	18.1	319	4924.1	4935.78	-11.694	136.74	29602.41	9.6788	15.917
320	18.2	320	4923.1	4935.39	-12.267	150.49	29752.9	9.688	15.967
321	18.2	321	4922.5	4935.01	-12.505	156.38	29909.28	9.6982	16.017
322	18.3	322	4921.6	4934.64	-13.007	169.19	30078.47	9.7103	16.067
323	18.3	323	4921.5	4934.14	-12.649	159.99	30238.45	9.7209	16.133
324	18.4	324	4921.4	4933.89	-12.453	155.07	30393.52	9.7306	16.167

325	18.4	325	4920.8	4933.52	-12.712	161.6	30555.12	9.7412	16.217
326	18.5	326	4920.3	4933.16	-12.857	165.29	30720.41	9.7524	16.267
327	18.5	327	4919.5	4932.79	-13.299	176.87	30897.28	9.7653	16.317
328	18.6	328	4918.6	4932.31	-13.751	189.08	31086.36	9.7801	16.383
329	18.6	329	4917.7	4931.95	-14.231	202.53	31288.89	9.7968	16.433
330	18.7	330	4917.2	4931.72	-14.522	210.89	31499.77	9.8148	16.467
331	18.7	331	4916.5	4931.25	-14.751	217.61	31717.38	9.8336	16.533
332	18.8	332	4915.8	4931.02	-15.186	230.6	31947.98	9.8543	16.567
333	18.8	333	4915.5	4930.67	-15.212	231.39	32179.37	9.8749	16.617
334	18.9	334	4914.4	4930.21	-15.793	249.42	32428.79	9.8981	16.684
335	18.9	335	4914.5	4929.98	-15.519	240.84	32669.63	9.9198	16.717
336	19.0	336	4941.3	4929.64	11.6451	135.61	32805.24	9.9254	16.767

REFERENCES

Allen T. and Roberts A. (1982),"Production Operations: Well Completion, Workover and Stimulation," vol 2 3rd ed. Oil and Gas Consultants International, Inc. Tulsa

ASTM ,"Standard test method for the determination of the in situ stress in rock using the hydraulic fracturing method," Designation D 4645 – 87 (Reapproved 1997)

Antoci, J. C. and Anaya, L. A. (2001)," First Massive Hydraulic Fracturing Treatment in Argentina," SPE 69581.

Baree, R.D.,and Mukherjee, H. (1996),"Determination of Pressure Dependent Leak-off and Its Effect on Fracture Geometry," SPE 36424.

Branagan, P.T. and Holzhausen, G.R. (1994),"Applied Geomechanics Inc. Improvements in Defining the Magnitude of the Minimum In-Situ Stress Using Hydraulic Impedance Testing and Pressure Derivative Analysis," SPE 27898

Castillo, J.L. (1987),"Modified Fracture Pressure Decline Analysis Including Pressure-Dependent Leakoff," SPE 16417

Daneshy, A.A., Slusher,G.L.,Chilholm, P.T. and Magee, D.A. (1986),"In-Situ Stress Measurements During Drilling," JPT, Vol 38, No. 9.

deBree, P. and Walters, J.V. (1989),"Micro/Mini-frac Test Procedures and Interpretation for In-situ Stress Determination," international Journal of Rock Mechanics and Mining Sciences, Pergamon Press, Vol. 26 No.6.

Doe, T.W. and Korbin, G.E. (1987),"A comparison of hydraulic fracturing and hydraulic jacking stress measurements," ARMA 87-0283.

Economides, M.J. and Nolte, K.G. (2000),"Reservoir Stimulation," 3rd edition ISBN 0 471 49192 6, Schlumberger Dowell, Sugar Land, Texas.

Gu, H. and Leung, K.H. (1993),"3D Numerical Simulation of Hydraulic Fracture Closure With Application to Minifracture Analysis," SPE 20657-PA.

Haimson, B.C. (1974),"A simple method for estimating in-situ stresses at greater depths," Field Testing and Instrumentation of Rock, ASTM STP 554, American Society for Testing of Materials, pp 156-182.

Hallahan, C. and Atkinson, L.,"Introduction to using SAS EG for Statistical analysis," Paper 117-29.

Holt, R.M., Pestman, B.J. and Kenter, J. (2001),"Use of a discrete particle model to assess feasibility of core based stress determination," ISBN 90 2651 827 7.

Hubbert, M.K. and Willis, D. G. (1957)," Mechanics of Hydraulic Fracturing," Trans, AIME, Vol . No. 210.

Jackson, C.W.,"SAS Programming basics," CSQA.

Jones, J. and Britt, L. (2009)."Design and Appraisal of Hydraulic Fractures," ISBN 978-1-5563-143-7, Society of Petroleum Engineers, Richardson, TX.

Lee, M.Y. and Haimson, B.C. (1989),"Statistical Evaluation of Hydraulic Fracturing Stress Measurement Parameters," International Journal of Rock Mechanics, Min. Sci. And Geomech. Abstr., Vol. 26, No. 6 pp. 447-456.

Lin, P. and Ray, T.G. (1996),"A New Method for Direct Measurement of In-Situ Stress Directions and Formation Rock Properties" SPE 26600 – PA.

Martins, C. S., Ribiero, L. and Sousa, E. (1987),"Recent advances in the interpretation of the small flat jack method," ISRM 6CONGRESS-1987-230.

McLennan, J. D. and Roegiers, J.C. (1982),"How instantaneous are instantaneous pressures," SPE 11064.

Mohamed, I.M., Nasralla, R.A., Sayed, M.A., Marongiu-Porcu, M., and Ehlig, C.A. – Economides (2011),"Evaluation of After Closure Analysis for Tight and Shell Gas Formations," SPE 140136.

Nawrocki, P. A. (2010),"Critical Wellbore Pressures Using Different Rock Failure Criteria."

Nolte, K.G. (1988),"Application of Fracture Design Based on Pressure Analysis" SPE Production Engineering.

Nolte, K.G. amd Smith, M.B. (1981),"Interpretation of Fracturing Pressures," SPE 8297

SAS Institute Inc.,"SAS enterprise guide 4.2."

"SAS Online Doc Version 8,"
http://ciser.cornell.edu/sasdoc/saspdf/common/mainpdf.htm, Sept 2012

Smith, M.B., Holman, G.B., Fast, C.R., and Covlin, R.J. (1978),"The Azimuth of Deep, Penetrating Fractures in The Wattenberg Field ," SPE 6092 – PA

Siegfried, R. W., and Simmons, G. (1978), "Characterization of Oriented Cracks with Differential Strain Analysis," J. Geoph. Res 83.(B3), 1269-1278.

Soliman, M.Y., and Daneshy, A.A. (1991),"Determination of Fracture Volume and Closure Pressure From Pump ln/Flowback Tests," SPE 21400.

Simmons, G., and Richter, D., (1976), "Microcracks in Rocks," The Physics and Chemistry of Minerals and Rocks (R.G.J Strens, ed.), Interscience, New York, pp 105-137.

Thompson, J.W. and Church, D.C. (1993),"Design, Execution, and Evaluation of Minifracs in the Field: A Practical Approach and Case Study," SPE 26034.

Upchurch, E.R. (1993),"Determining Fracture Closure Pressure In Soft Formations Using Postclosure Pulse Testing" SPE 56723.

van Dam, D.B. and de Pater, C.J. (1996),"Roughness of Hydraulic Fractures: The Importance of In-Situ Stress and Tip Processes" SPE 56596.

van Dam, D.B., de Pater, C.J. and Romijn, R. (1998),"Analysis of Hydraulic Fracture Closure in Laboratory Experiments" SPE/ISRM 47380.

Warpinski, N. R., and Smith, M.B. (1982),"Rock Mechanics and Fracture Geometry," in Recent Advances in Hydraulic Fracturing, SPE Monograph, 12, p. 57-80.

Warpinski, N. R., Branagan, P.T. and Wilmer, R. (1983),"In-situ Stress Measurements at DOE's Multiwell Equipment Site," SPE 12142 - 58.

Warpinski, N.R., Clark, J.A., Schmidt, R.A., Huddle, C.W. (1982),"Laboratory Investigation on the Effect of In Situ Stresses on Hydraulic Fracturing Containment," SPE 9834 – PA.

Weng, X., Pandey, V., and Nolte, K.G. (2002), "Equilibrium Test – A Method for Closure Pressure Determination" SPE/ISRM 78173.

Wright, C.A., Weigers, L., and Minner, W.A. (1996),"Robust Technique For Real-Time Closure Stress Determination" SPE Production and Facilities.

VITA

Soumitra Bhaskar Nande was born in Pune, Maharashtra, India. He received his primary and secondary education in Pune, India graduating from Bharat English School and Junior College in 2006. Soumitra received a Bachelor of Engineering degree in Petroleum Engineering from Maharashtra Institute of Technology, affiliated to University of Pune in May 2010. He received a Master of Science degree in Petroleum Engineering from Missouri University of Science and Technology, Rolla, Missouri in May 2013.